Budapest University of Technology and Economics
Faculty of Civil Engineering
Department of Construction Materials and Technologies

Shear performance of concrete exposed to elevated temperatures

PhD Thesis

Naser S. Alimrani

Supervisor:
Prof. Dr. -habil György L. Balázs, PhD

Budapest, 2020

Acknowledgements

All thanks and praise go to God, Lord of the worlds, the Merciful and the Compassionate. However, as the Prophet Muhammed (PBUH) said: "He who does not thank people, does not thank God". Therefore, I gratefully would like to thank the following people, who provided me a great deal of support and assistance, in which without whom I would not have been able to complete this research.

I would first like to thank the Hungarian Government that granted me the Stipendium Hungaricum Scholarship in cooperation with the Palestinian Ministry of Higher Education. I am thankful also for Budapest University of Technology and Economics that accepted me to join them as a PhD student. In addition, I would like to thank Hungarian Research Grant NVKP_16-1-2016-0019 "Development of concrete products with improved resistance to chemical corrosion, fire or freeze-thaw".

I would like to express my sincere gratitude to my supervisor Prof. Dr. György László Balázs who truly advised me, as a father before as a supervisor, at both academic and personal levels. Your insightful thinking is deeply appreciated, and your kind personality will always be remembered.

I would also like to thank the current Head of the Department Prof. Dr. László Dunai and the former Head of the Department Dr. György Mihály Stocker. Special appreciations to the Head of the lab Dr. Salem Georges Nehme for his continuous help from the beginning to the end, and for Dr. Éva Lublóy for her valuable advices. Many thanks go to Dr. Tamás Károly Simon, Dr. Katalin Kopecskó, Dr. Rita Nemes, Dr. Olivér Fenyvesi, and Dr. Imre Péczeli. I would like to thank Ildikó and Krisztina as well. Great thanks for my colleagues, in the lab Viki, Panka, Burai, Krisz and Alina. Many thanks also for my colleagues András, Dani and Viktor, and for my nice office-mates Sándor and Ahmed. I am particularly thankful for my wonderful comrades Nabil and his wife Nada.

My deepest thanks for my family; beloved Mama and Dad, for my wonderful sisters and brothers, and for the soul of my brother Emad, you all have been always present in my heart. In addition, I would like to express deep thanks for my friends and relatives back home in Palestine as well as my new friends here in Hungary. To all of you and the ones who I could not mention their names, you have given me such a wonderful and meaningful life! I love you all.

Table of Contents

Notations

σ_{fl}	computed flexural stress at failure
b	width of beam (prism)
C_f	an aggregate effectiveness factor
d	depth of beam (prism).
$\mathcal{E}_{uk}$	characteristic strain at maximum stress
f_{cm}	the mean compressive strength
f_{st}	the tensile strength of the reinforcement
f_y	the yield strength of the reinforcement
I	the second moment of area (moment of inertia).
L	span length (prism)
M_c	bending moment of concrete
P	load
P_u	load at failure
P	load at failure
P_u	peak load
s	a coefficient depending on the strength class of cement
t	concrete age in days
T	degree of temperature
w	the crack width
$\beta_{cc}(t)$	a function to describe the strength development of concrete with time
δ	the shear displacement at the first crack
λ	thermal conductivity
c_p	specific heat
ρ_c	density of concrete
ρc_p	volumetric specific heat
μ	the tangent of the internal friction angle
ρ	the reinforcement ratio
σ	the mean normal stress
τ	the mean shear stress
τ_u	ultimate shear stress
υ_u	the ultimate longitudinal shear stress at the interface

φ	the internal friction angle
A_c	shear plane area
B	depth of the push-off specimen
D	thermal diffusivity
H	height of the push-off specimen
Hs	height of the shear plane of the push-off specimen
W	width of the push-off specimen

Abbreviations

AASHTO	American Association of State Highway and Transportation Officials
ACI	American Concrete Institute
ASCE	American Society of Civil Engineers
ASTM	American Society for Testing and Materials
CECS	China Association for Engineering Construction Standardization
CMOD	Crack Mouth Opening Displacement
COV	Coefficient of Variations
fib	International Federation for Structural Concrete
HPFRCC	High-Performance Fibre-Reinforced Cement Composites
FIER	Fibre Intrinsic Efficiency Ratio
FRC	Fibre-Reinforced Concrete
HSC	High Strength Concrete
ISO	International Organization for Standardization
ITZ	Interfacial Transition Zone
JSCE	Japan Society of Civil Engineers
LVDT	Linear Variable Differential Transformer
NSC	Normal Strength Concrete
SFRC	Steel Fibre-Reinforced Concrete
UHPFRC	Ultra-High-Performance Fibre-Reinforced Concrete

1. INTRODUCTION

Shear failure is generally considered to be among the most studied topics in reinforced concrete structures due to specific features that shear failure possesses, including little warning and brittle nature. Such kind of failures, therefore, shall be avoided at high priorities. Comprehensive understanding of the shear behaviour of concrete structures is of great importance to design against shear failure specially at high temperatures.

Several attempts have been made to generate a better understanding of the shear behaviour. These attempts were carried out using both large and small scales of experiments. Due to the complexity and high expensive costs, different experimental models and design methods have been proposed by researchers (Soetens and Matthys, 2017). *Push-off* is one of the most models that is used to test shear capacity. The push-off model is a non-standard, but widely recognized, test that has advantages of being relatively small, inexpensive, easy to perform with no need for sophisticated equipment or procedures (Echegaray-Oviedo, 2014). A wide range of dimensions were used for the push-off model, yet there are two main types of the model: (I) precracked and (II) non-precracked specimens. Initial cracks were reported in some studies to have irregular shapes due to the high stiffness before crack occurring. Therefore, several authors proposed to provide the specimens with a precrack line along the shear plane prior to the test. However, the majority of previous studies have been carried out on non-precracked specimens. Planning of experiments for present PhD study, non-precracked push-off specimens were considered.

Fibre-Reinforced Concrete (FRC) is widely used, particularly in recent years. Previous researches showed that deformation capacity and toughness of FRC are increased by the virtue of the "*bridging effect*" of the fibres, helping to resist the opening of cracks. When cracks initiate, shear force across the crack is transmitted through a mechanism that is achieved by interaction of several components: shear resistance provided by shear reinforcement or fibres known as "*dowel action*" of the reinforcement, and forces between the rough concrete faces known as "*aggregate interlock*", (*see Sections 2.1.2 and 2.1.3*).

In recent years, High Strength Concrete (HSC) is increasingly used in civil engineering practice due to its higher strength and better durability compared to Normal Strength Concrete (NSC). However, with the increasing engineering applications as well as increasing the deepening of related research activities, it was noticed that HSC can be inferior to NSC in the aspects of some mechanical properties after *elevated temperatures*. Hence, the elevated temperature as

one of the most severe environments should be considered in the design of HSC elements and structures. The properties of NSC and HSC at elevated temperatures have been widely studied. Studies show that concrete can experience mechanical and chemical changes when exposed to elevated temperature. However, a lack of knowledge is realized for shear performance especially with fibres at elevated temperatures.

The overall aim of the current study is to evaluate the shear performance of concrete using different types and amounts of fibres in the case of elevated temperatures. To fulfil the targeted aim, the following objectives were performed:

1. To evaluate the influence of fibres with different types and ratios on shear strength at different maximum levels of temperatures.
2. To evaluate the influence of fibres with different types and ratios on shear toughness at different maximum levels of temperatures.
3. To evaluate the influence of fibres with different types and ratios on shear stiffness at different maximum levels of temperatures.
4. To specify the different shear failure modes of the push-off specimens at elevated temperatures regarding FRC.

Three main parameters are investigated in the current study, namely: type and amount of fibres, maximum temperature, and age of concrete at testing. Accordingly, five concrete mixes depending on fibres content were chosen as well as five maximum temperatures. In addition, concrete is tested at two different ages; (I) 28-days and (II) one-year age. Test setup is designed to measure the deformations occurred at the shear surface plane. Two different deformations are investigated, i.e., relative displacement parallel to the load considered as "*crack slip*" and relative displacement perpendicular to the load considered as "*crack width*". Displacement values were measured by means of Linear Variable Differential Transformers (LVDTs), fixed horizontally and vertically on both faces of the specimens.

2. STATE OF THE ART

2.1 Shear failure of reinforced concrete

Shear failure is usually considered as one of the most critical structural failure modes for concrete structures. Unlike other failure modes such as flexural failure, only little warning occurs signalizing that the structure is at the onset of failing in shear. Therefore, shear failures of structural elements usually lead to catastrophic losses and have to be prevented at high priority (Yang, 2014).

2.1.1 Historical background

Shear research has been widely known by the publication of book in 1908 by Mörsch (Mörsch, 1908). In fact, a few studies have been already preceded him using steel strips as stirrup reinforcement in beams. Ritter (1899) suggested that the stirrups to be around the longitudinal bars one by one and remained open all the way to the top (*Fig.2.1 a*). It is worthy to note that both the longitudinal reinforcement and the stirrups had to be completely embedded into the concrete. That was the norm for a period (*Fig. 2.1 b*) until closed stirrups *(Fig. 2.1 c)* made of small diameters reinforcing bars (not opened or in strip form) were used till the present time (Balazs, 2010).

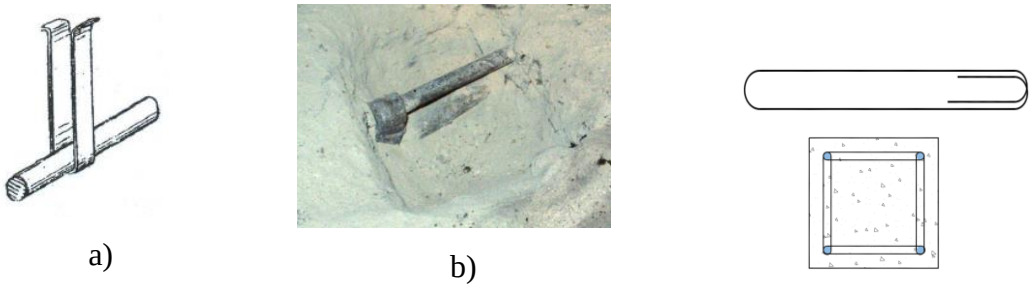

a) b) c)

Figure 2.1: Stirrup reinforcement, a) shape of stirrups at end of 19th century Ritter, b) a steel strip from 1905 at BME Library (Balazs, 2010) and c) closed stirrups as reinforcement of a beam (Mörsch, 1908)

Some important steps in shear design have been presented after Mörsch. Kupfer (1962) proposed modifications with respect to inclination of the strut. Walther (1962) developed a generalized design theory using Mohr circles (Balazs, 2010). Kani (1964) published an important paper intending to answer two questions: (a) What is the internal mechanism of the shear failure of a reinforced beam, and (b) What is the strength of this mechanism? A reinforced concrete beam, by increasing load, transforms into a comb-like structure (*Fig. 2.2 a*). In which

the flexural cracks create “vertical” concrete teeth in tensile zone, while the compressive zone represents the backbone of the concrete comb. Using the teeth model and an arch analogy, Kani explained the influence of shear slenderness ratio to the shear capacity, which is often referred as Kani’s Valley or riddle of shear failure, *(Fig. 2.2 b)* (Kani, 1964).

Fenwick and Paulay (1968) experimentally modified Kani’s model emphasizing on the role of aggregate interlock in a teeth structure whereas Taylor (1974) emphasized on the role that be played by dowel action. Further improvements were proposed by MacGregor and Walters introducing a simplified dowel action expression and shear stress distribution between cracks (MacGregor and Walters, 1967). Although both simplified relationships were not validated by experiments yet, authors showed that the development of the inclined crack is due to the bending of the concrete teeth (Yang, 2014). From another perspective, Leonhardt and Mönig (1973) published a textbook that was studied in many universities indicating the influence of the amount of stirrup reinforcement on the inclination of cracks. Results showed that for lower amount of shear reinforcement, the inclination of cracks was reduced in the shear span. In addition, positive influence of prestressing on the shear capacity was proven to be depending on the level of prestressing (Balazs, 2010). However, Hamadi and Regan (1980) modified kani`s model to clarify a reinforced concrete beam with a plain web resists shear, with particular reference to the transfer of shear forces across flexural cracks. This action is known as aggregate interlock. Results showed that vertical displacements and thus interlock forces are developed even at vertical cracks and the actions are not reliant upon the cracks being curved as has been assumed in some previous works (Hamadi & Regan, 1980).

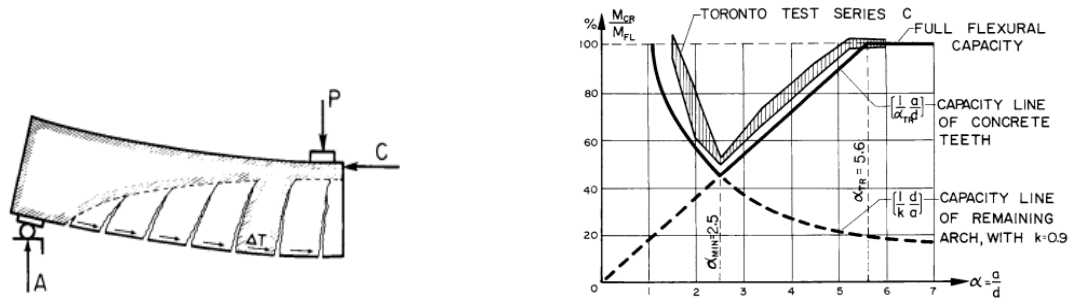

a) b)

Figure 2.2: Kani`s model: a) the function of concrete teeth and b) theoretical and results of the model (Kani, 1964)

Experimental research as well as derivation of a theoretical model was given by Walraven (1981). His study provided an insight into the mechanism of transmission of forces across

cracks whose faces are subjected to shear displacements. The mechanism is achieved by interaction of several components: axial and transverse stiffness known as dowel action (*see Section 2.1.3*) of the reinforcement and direct transfer of forces between the rough concrete crack faces, generally denoted by the term aggregate interlock (*see Section 2.1.2*). Results concluded that shear transfer across cracks cannot be simple as a relation between shear stress and shear displacement but is a more complex mechanism to involve shear stress, shear displacement, normal stress and crack width. Additionally, in cracks in plain concrete the stresses in the normal and the shear direction are mainly a function of crack width, shear displacement and concrete quality. Furthermore, theoretical and experimental formulations were developed to study the shear in prestressed concrete members (Walraven and Mercx, 1983).

Alternatively, by carrying out a series of experiments on hollow core slabs, four principal failure modes were observed, i.e., pure flexural failure, anchorage failure, shear tension failure and shear compression failure (*Fig. 2.3*). These failure modes are compatible with the primary four beam failure modes defined by ACI- ASCE Committee 426 (1973) with some differences in names descriptions. A comprehensive study investigated then modified the four failure mode equations presented by Walraven and Mecx including a new parameter as elevated temperatures (Fellinger, 2004). Finally, despite the fact that determination of a shear failure mechanism remains a challenging task, researchers often describe different shear failure mechanisms based on crack patterns (Dinh, 2009). Therefore, failure mode is depending on whether the opening of the diagonal crack results in the collapse of the beam or not (Yang, 2014).

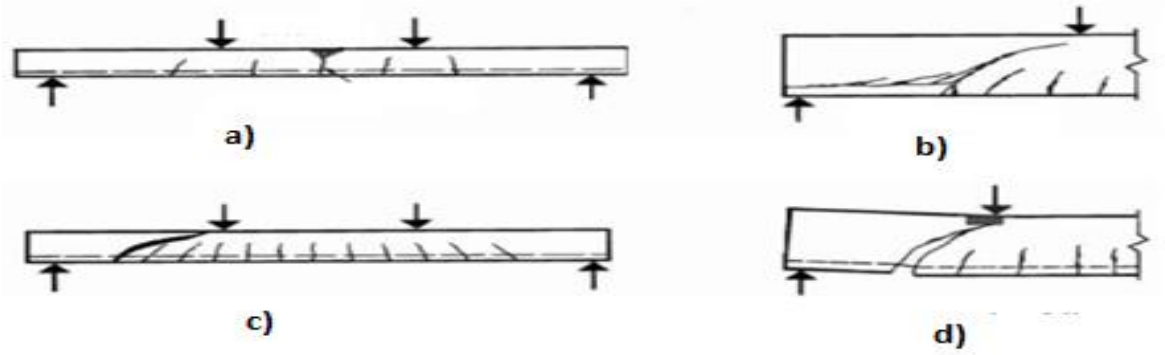

Figure 2.3: Failure modes, a) flexural, b) shear tension, c) anchor and d) shear compression (Walraven and Mercx, 1983; Fellinger, 2004)

Notwithstanding, many theories and empirical formulas have recently been proposed to estimate the shear strength of reinforced concrete members contain no transverse

reinforcement. These approaches are noticed to be different not only in the resulting design expressions, but also on the governing parameters thus, on the interpretation of the failure mechanisms and governing shear-transfer actions (Fernández et al., 2015). Basically, no general agreement on the parameters and phenomena governing shear strength is yet found in the scientific community. This lack of agreement is also reflected in codes of practice, whose provisions for shear design are often based on empirical formulas (ACI 318, 2011). In addition, no general consensus is yet available on the role that size and strain effects exhibit on the shear strength and how should they be accounted. However, results showed that size effect has an impact in mechanical properties in which larger sizes are associated to lower levels of deformation Fernández et al., 2015). Furthermore, studies have shown significant effectiveness of the arrangement of the bars and stirrups on bunching shear capacity while cages of continuous stirrups and shear studs have shown the least effective shear reinforcement (Koris et al., 2018). Moreover, it has been experimentally observed that specimens are sensitive to a strain effect (Muttoni and Fernández, 2008). Finally, some approaches investigated shear strength in beams after cracking using fibres in the cement matrix (Casanova and Rossi, 1997; Meda et al., 2005; Minelli and Plizzari, 2013).

2.1.2 Aggregate Interlock

The strength of concrete-to-concrete interfaces, subjected to longitudinal shear stresses, can be described by the *shear-friction theory*. This theory was initially proposed in 1966 by Birkeland and Birkeland (Birkeland and Birkeland, 1966), then was adopted in all design codes for reinforced concrete structures. The theory can also be used to predict the shear strength of the interface between two parts of an element generated by a crack (Santos and Julio, 2012). Aggregate interlock has a remarkable contribution in transferring the forces, as a result of its rough structure, through the cracks. The mechanism of aggregate interlock is directly related to the way in which a crack is formed in concrete. As the strength of the hardened cement paste in most concretes is lower than the strength of the aggregate particles, cracks intersect the cement paste but run along the edges of the aggregate particles. Therefore, the aggregate particles, extending from one of the crack faces, "interlock" with the opposite face and resist shear displacements (*Fig. 2.4 a and b*) (Walraven, 1980). Different methods have been developed to evaluate surface roughness of concrete (Simon, 2003). Finally, aggregate interlocking can be considered as the governing shear transfer action explaining shear strength according to the compression field theory and its derivatives (Bentz et al., 2006).

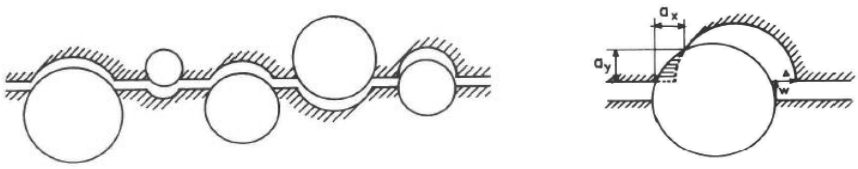

Figure 2.4: Schematic model for aggregate interlock, a) general structure of crack planes and b) development of a contact area between matrix and aggregate (Walraven, 1980)

According to Walraven (1980), the validity of the theory has been verified by a number of experiments including parameters such as concrete quality, particle sizes and external restraining stiffness against crack opening. Thus, experimental results can be adequately described by the theoretical model.

2.1.3 Dowel Action

Dowel action is defined as the capacity of reinforcing bars to transfer forces perpendicular to their axis (*Fig. 2.5 a*). When the tensile strength of the concrete is reached and a crack is formed, an adjustment in the load carrying system may be expected. After the formation of the crack, generally no redistribution of stresses is possible, resulting in failure must be expected; only if the beam is reinforced with stirrups. Then the dowel crack may be stopped, and a completely different mechanism is activated to transfer dowel forces (Walraven, 1980). The total distance between the axis of the undeformed parts of the bars on both sides of the crack is defined as the deflection of the dowel (*Fig. 2.5 b*). Total deflection is a result of the deformation of the part of the bar embedded in the concrete and the part which is free over a certain length as well. Results showed that the total transverse shear at the cracked sections of beams without stirrups is resisted by both the concrete remaining intact above the inclined crack and the longitudinal reinforcement. The magnitude of the shear resisted by the reinforcement (and the concrete below) can be appreciable (Krefeld & Thurston 1966).

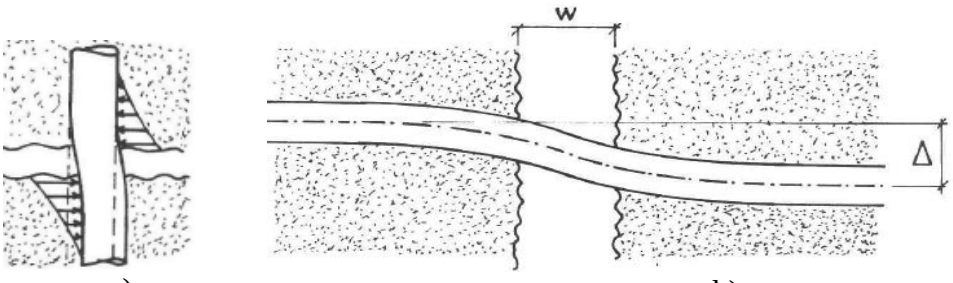

Figure 2.5: Dowel action, a) an illustration of the concept and b) deflection of a bar due to dowel force (Walraven, 1980)

Three mechanisms of shear transfer over the free length were noticed (Paulay et al, 1974). The first is the load transfer by bending which has limited capacity by the formation of plastic hinges in the bar. The second is the load transfer by pure shear and the third is the load transfer by kinking (Paulay et al, 1974). Ever since then, further developments regarding mechanisms of cracks around reinforcement bars have been carried out by numerous researches (Baumann and Rüsch, 1970; Goto, 1971; Taylor, 1971; Dulacska, 1972; Eleiott, 1974; Houde and Mirza, 1974; Stanton, 1977; Vintzeleou and Tassios, 1986; Chana, 1987 and Regan, 1993).

2.1.4 ModelCode 2010

When the crack faces are subjected to shear displacements (crack slip) with opposite signs, resisting shear stresses and normal stresses develop as a result of the roughness of the crack faces (*Fig. 2.6 a*). Thus, the mean shear stress τ and the mean normal stress σ may be calculated from the following general relations (Model Code 2010):

$$\tau = C_f \{-0.04 f_{cm} + [1.8 w^{-0.8} + (0.292 w^{-0.7} - 0.25)\, f_{cm}]\, \delta\} \qquad 2.1$$

$$\sigma = C_f \{-0.06 f_{cm} + [1.35 w^{-0.63} + (0.242 w^{-0.55} - 0.19)\, f_{cm}]\, \delta\} \qquad 2.2$$

where:

δ is the shear displacement (crack slip) in mm;
w is the crack width in mm;
f_{cm} is the mean compressive strength in MPa at the age of 28 days.

C_f is an aggregate effectiveness factor. If the aggregate does not fracture upon cracking of the concrete, the factor is 1.0. If the concrete is high strength (strong cement paste), then the factor is about 0.35, due to the high probability of particles to be broken. For more accurate values for C_f, push-off test is suggested. The crack opening path (development in shear displacement in relation to crack opening) can be constructed from diagrams as shown in *Fig. 2.6 b*.

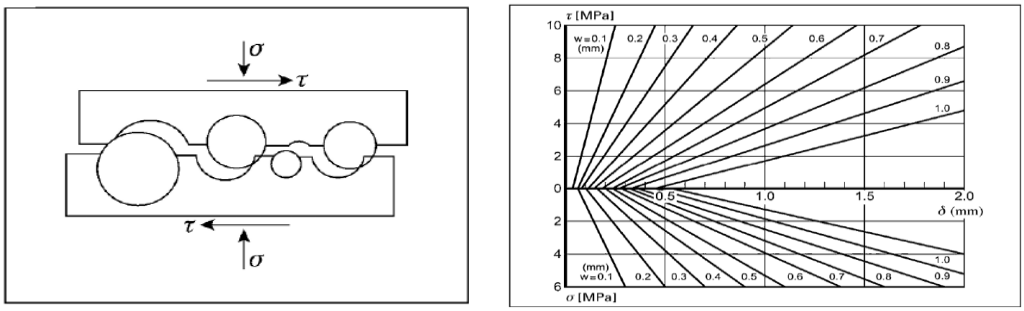

a) b)

Figure 2.6: Shear stresses and displacements, a) Principle of shear friction in concrete crack and b) Relations according to Egs. 2.1 and 2.2 for fcm = 30 MPa (ModelCode 2010)

2.1.5 Models

The ideal test method is the one that is relatively simple to conduct, requires small, easily fabricated specimens, and is capable of measuring both shear strength and shear stiffness simultaneously (Walrath and Adams, 1983). Different types of direct shear tests have been adopted to investigate the direct shear of steel fibre reinforced concrete. The following types of specimens (*Fig. 2.7*) are commonly used to investigate direct shear response of plain and reinforced concrete as well (Soetens and Matthys, 2017):

a) Push-off specimen (see more details in *Section 2.1.6)*

b) Double notched push-through specimen

c) Single notched FIP-type specimen

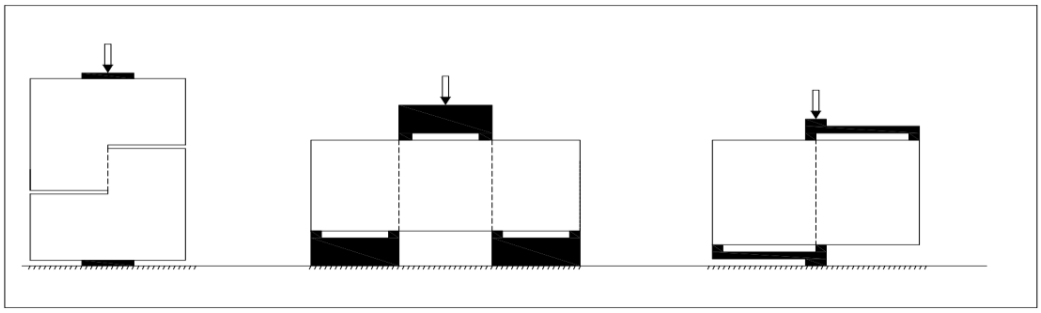

a) b) c)

Figure 2.7: Different test setups used to investigate the direct shear behaviour (a) Push-off, (b) JSCE-type and (c) shear block (Soetens and Matthys, 2017)

Each model has various names according to different researches. For instance, the first model (*Fig. 2.7 a*), which has been adopted by the current study, is widely well-known as push-off model whereas some researchers called it *Z-type* or *S-shaped model* (Naus et al., 1976), and other researchers called it *Hoffbeck-style* or *double L-shaped* specimen (Khanlou et al., 2012). On the other hand, double notched push-through specimen (*Fig. 2.7 b*) is basically developed by the Japan Society of Civil Engineers JSCE-SF6 and adopted by Japanese Standard (JSCE, 1984). Shear strength is simply determined, without toughness measurements, as load divided by cross-sectional area (Tatnall, 2006). This model was the basic model that has been adopted and developed by several researchers (Mirsayah and Banthia, 2002; Appa and Sreenivasa, 2009). Finally, compared to the push-off model, the crack measurement in JSCE model is not clear resulting in stress field on the specimen which reveals that this test is not pure direct shear test (Echegaray-Oviedo, 2014). The third model (*Fig. 2.7 c*) has been adopted in many different researches with the name *shear block* model (Ali *et al.*, 2008; Smith et al., 2011). This model is similar to the model that has been originally proposed by Nicolae Iosipescu of Bucharest,

Rumania in the early 1960's (Iosipescu, 1967). The model has been extensively studied and developed by the composite research community within the last 20 years with remarkable works by Walrath and Adams in the early eighties (Adams and Walrath, 1987). The fixture developed by Adams and Walrath, known as the 'modified Wyoming fixture', was included in an ASTM Standard (ASTM D 5379-93) and is widely used in composite research laboratories (Xavier et al., 2004).

2.1.6 Push-off Model

The push-off test is a non-standard, but widely recognized, test used to study the mechanisms of shear transfer. This test has the advantages of being relatively small, inexpensive, easy to perform, and not needing any highly specialized pieces of testing equipment (Echegaray-Oviedo, 2014). Anderson (1960) was one of the firsts to experimentally test push-off specimens. Hanson (1960) developed, based on push-off tests carried out by Anderson, expressions involving parameters of rough interfaces and properties of the reinforcements (Hanson, 1960). Birkeland and Birkeland (1966) proposed a linear expression to evaluate the ultimate longitudinal shear stress of the concrete surface (Santos and Julio, 2012). The formula was proposed as follow:

$$\upsilon_u = \rho f_y \tan \varphi = \rho f_y \mu \qquad 2.3$$

Where υ_u is the ultimate longitudinal shear stress at the interface, ρ is the reinforcement ratio, f_y is the yield strength of the reinforcement and φ is the internal friction angle. μ is the tangent of the internal friction angle, designated as coefficient of friction. From another hand, Walraven et al. (1987) proposed a non-linear function to predict the shear strength of initially cracked interfaces. Hofbeck et al. (1969) determined the influence of pre-existing crack, strength, size and arrangement of reinforcement including dowel action factor (Hofbeck et al., 1969). Over three decades, remarkable push-off tests and developments were carried out by Mattock, both individually and collectively (Santos and Julio, 2012). Rahal et al. (2016) tested normal strength, high strength and normal strength conventional concrete. Specimens of the same group are differed by the number and size of the clamping reinforcement provided (Rahal et al., 2016). Echegaray-Oviedo (2014) developed an extensive experimental program including adjusting or calibrating the design and restraint frame and evaluating the behaviour of tested material that published in the doctoral thesis (Echegaray-Oviedo, 2014).

Since the push-off test is a non-standard test, there is no limitation on the dimensions as a principle. However, most of the tests have used models with dimensions ranging from 200 mm up to 800 mm height. *Table 1* below shows some of the tests that used push-off model. *Figure 2.8* illustrates a schematic representation of 3D push-off model showing shear plane (*Fig. 2.8 b*) and different dimensions mentioned in Table 2.1 (*Fig. 2.8 a*).

Table 2.1: Different geometrical properties used for the push-off model

Name	H (mm)	B (mm)	W (mm)	Hs (mm)	Pre-crack / non crack	Ambient/ elevated
Hofbeck et al. (1969)	511.8	127	254	254	Both	Ambient
Mattock and Hawkins(1972)	546	120-150	254	250-300	Both	Ambient
Paulay (1974)	457	127	305	191	Pre-cracked	Ambient
Naus et al. (1976)	305	140	140	140	Non cracked	Elevated, in hot state
Mattock (1976)	559	127	305	254	Non cracked	Ambient
Walraven (1981)	600	120	400	300	Pre-cracked	Ambient
Valle (1993)	533	76	254	254	Non cracked	Ambient
Khaloo (1997)	520	125	300	220	Non cracked	Ambient
Barragan (2006)	260	150	150	60	Non cracked	Ambient
Al-Owaisy (2007)	440	100	200	200	Non cracked	Elevated
Mansur et al (2008)	750	150	400	300	Pre-cracked	Ambient
Cuenca (2010)	670	120	400	250	Both	Ambient
Kim (2010)	660	125	400	305	Non cracked	Ambient
Xiao et al (2014)	600	150	400	300	Pre-cracked	Elevated
Echegaray-Oviedo (2014)	670	120	400	260	Pre-cracked	Ambient
Rahal et al. (2016)	540	125	250	250	Non cracked	Ambient

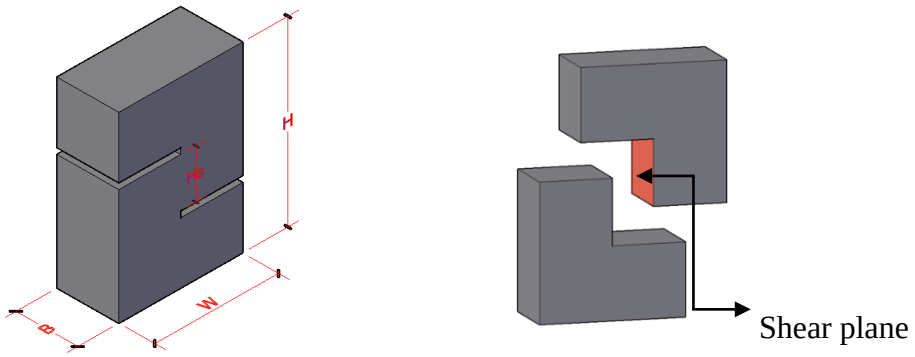

a) b)

Figure 2.8: Schematic representation of the push-off model, a) dimensions and b) shear plane

2.2 Fibre Reinforced Concrete (FRC)

Since ancient times, fibres have been used to reinforce brittle materials. First, straw was used to reinforce sun-baked bricks, then horsehair was used to reinforce masonry mortar and plaster (ACI Committee 544, 2002). Afterwards, starting with pioneer studies in the early 60`s of last century, FRC has been fully considered as a structural material (Ferrara and Mobasher, 2016). Furthermore, a wide research has been performed during the last three decades on material properties of FRC, and research was particularly developed for structural purposes in recent years (Barros, 2005; di Prisco et al., 2009; Ali et al., 2012).

2.2.1 Definition and types

FRC is a composite material characterized by a matrix, made either from concrete or mortar, and discrete or discontinuous fibres (Model Code 2010). Length and diameter of the fibres used for FRC do not generally exceed 76 mm and 1 mm, respectively (ACI Committee 544, 2002). Moreover, fibres used in concrete could be characterized in different ways (Naaman, 2003). First, according to the fibre material: natural organic such as cellulose, sisal, jute, bamboo, etc.; natural mineral such as asbestos, rock-wool, etc.; man-made such as steel, titanium, glass, carbon, polymers or synthetic, etc. Second, according to their physical/chemical properties: density, surface roughness, chemical stability, non-reactivity with the cement matrix, fire resistance or flammability, etc. Third, according to their mechanical properties such as tensile

strength, elastic modulus, stiffness, ductility, elongation to failure, surface adhesion property, etc. (Naaman, 2003).

However, two main types of fibres are commonly used in construction, steel and synthetic fibres. Steel fibres are used in a wide range of structural applications such as industrial pavements (AASTO, 1993; Sorelli et al., 2006; Belletti et al., 2008), precast structural elements (Ferrara and Meda, 2006), tunnel linings (Bernard, 2002; Gettu et al., 2006; Hansel and Guirguis, 2011; De la Fuente et al., 2012; Bakhshi and Nasri, 2016). Synthetic fibres are usually smaller than steel fibres and are most typically used in industrial pavements to reduce the cracking induced by shrinkage (Buratti et al., 2011). In some applications, as well as in the present study, steel and synthetic fibres are mixed together to obtain better performance (Sivakumar and Santhanam, 2007). Some studies evaluated a comparative investigation between the different types of the fibres that considerably vary in effectiveness and cost (Morgan, et. al, 1989; Sukontasukkul, 2004; Buratti, et al., 2011; Soutsos et al., 2012). Table 2.2 lists the common types of fibres with typical properties.

Table 2.2: Typical properties of common fibres (Bentur and Mindess, 2007)

Fibres	Diameter (μm)	Specific gravity	Modulus of elasticity (GPa)	Tensile strength (GPa)	Elongation at break (%)
Steel	5-500	7.84	200	0.5-2	0.5-3.5
Glass	9-15	2.6	70-80	2-4	2-3.5
Polypropylene	20-400	0.9-0.95	3.5-10	0.45-0.76	15-25
Armid (kevlar)	10-12	1.44	63-120	2.3-3.5	2-4.5
Carbon, high strength	8-9	1.6-1.7	230-380	2.5-4	0.5-1.5
Nylon	23-400	1.14	4.1-5.2	0.75-1	16-20
Acrylic	18	1.18	14-19.5	0.4-1	3
Polyethylene	25-1000	0.92-0.96	5	0.08-0.6	3-100
Wood fibres	-	1.5	71	0.9	-
Sisal	10-50	1.5	-	0.8	3

2.2.2 Benefits

One of the greatest benefits to be gained by using fibre reinforcement is improving long-term serviceability of the structure or product. Serviceability is the ability of a structure or an element to maintain its strength and integrity providing its designed function over its intended service life. An important aspect of serviceability that can be notably enhanced by using fibres is control of cracking (ACI Committee 544, 2002). Shortly after the formation of the first crack,

collapse is likely to occur due to the brittle nature of concrete. Yet, addition of steel fibres aids in converting the brittle characteristics to a ductile one. The principal role of fibres is to resist the formation and growth of cracks by providing pinching forces at crack tips (Lim and Oh, 1999). The mechanical properties of a cementitious matrix are modified when fibres are added. However, elastic properties and compressive strength are not significantly affected by fibres, unless a high percentage of fibres is used. Thus, depending on their composition, FRC can show hardening or softening behaviour under uniaxial tension force (*Fig. 2.9*). Hardening or softening is of great importance in terms of structural design since it is based on the post-cracking residual strength (Model Code 2010; Ismail and Hassan, 2019).

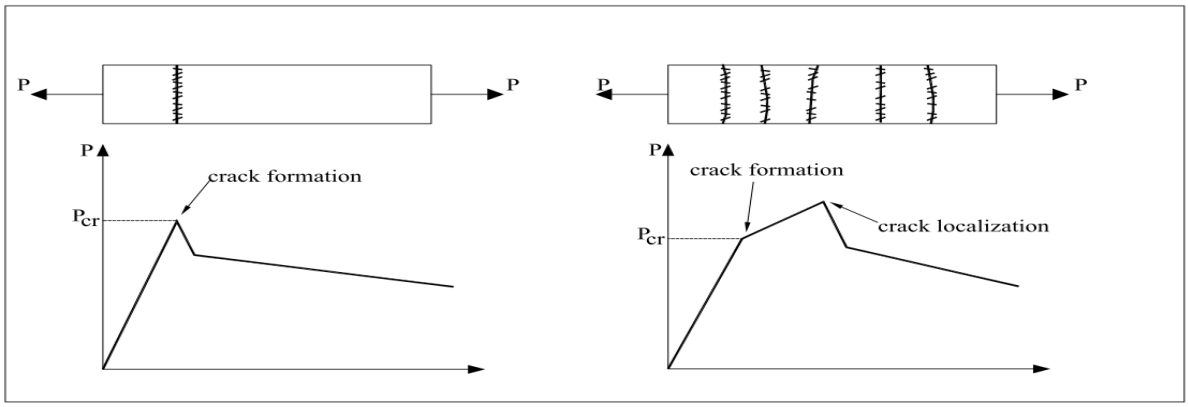

a) b)

Figure 2.9: Different behaviours in axial tension, (a) Softening and (b) hardening (Model Code 2010)

2.2.3 Codes

Several research papers, international symposia, and state-of-the-art reports facilitated the way for technical guidance to use FRC in structural elements and constructions. International Federation for Structural Concrete (*fib*) allowed in Model Code 2010 to use FRC to substitute partially and totally the conventional reinforcement (Model Code 2010), whereas some new rules in ACI 318 2008 were introduced with reference to minimum shear reinforcement (ACI 318, 2008). ACI Committee 544 published a comprehensive study as state-of-the-art report regarding FRC in 1973 (ACI Committee 544 TR-73, 1973). RILEM Committee on fibre reinforced cement composites has also published a report in 1977 (RILEM Technical Committee 19-FRC, 1977). First standard in Australia to include procedures for the design of SFRC structures was published in 2014 by the Public Comment Australian Standard (DR AS5100.5). Although it was released basically for the design of the bridges, it is considered one of the few national standards in the world to include the design of SFRC in a

comprehensive way (Foster, 2016). In China, the first guideline for FRC structures was developed in 1992 by the China Association for Engineering Construction Standardization (CECS), and was updated later in 2004 (CECS, 2004; Leung, 2016). Japan Society of Civil Engineers (JSCE) published recommendations on design, production and application of different classes of fibre-reinforced cement composites covering SFRC, ultra-high-strength fibre-reinforced concrete, and high-performance fibre-reinforced cement composites (HPFRCC) with multiple fine cracking characteristics (JSCE, 2008).

2.3 Steel Fibre-Reinforced Concrete (SFRC)

SFRC is concrete made of hydraulic cements containing fine and coarse aggregate as well as discontinuous discrete steel fibres. Steel fibres can be defined as short, discrete lengths of steel having an aspect ratio (ratio of length to diameter) from about 20 to 100, with any of several shapes of cross-sections, and that are sufficiently small to be randomly dispersed in fresh concrete mixture (ACI Committee 544, 2002). Today, the industry has about 30 major global producers of steel fibres scattered all over the world offering hundreds of types of different fibres. Therefore, SFRC became the third main concrete based structural material beside traditionally reinforced concrete (by rods and stirrups), and concrete reinforced (by steel meshes known as ferrocement) (Kovacs and Balazs, 2004; Katzer and Domski; 2012).

2.3.1 Overview

The relatively small tensile strength of concrete has raised concerns for increasing its resistance to crack growth. Cracks are initiated once the tensile strength of concrete is reached. At the crack vicinity, the steel resists the entire tension. Reinforcement is usually used to increase the resistance of concrete to crack propagation (Shah and Rangan, 1971). Using steel fibres as a substitution of the conventional reinforcement should increase the ultimate load and enhance the other mechanical properties of the concrete. Introduction of fibres into the concrete results in post-elastic property changes that range from subtle to substantial, depending upon a number of factors, including matrix strength, fibre type, fibre modulus, fibre aspect ratio, fibre strength, fibre surface bonding characteristics, fibre content, fibre orientation, and aggregate size effects (ACI Committee 544, 2002). The enhanced properties include tensile strength, compressive strength, elastic modulus, crack control, resistance to impact and abrasion, shrinkage, expansion, thermal characteristics, and fire resistance (ACI Committee 544, 2002). Moreover, fibre reinforcement found to provide a better control of the crack development to improve the

structural durability and to reduce the number of joints (Balugaru and Shah, 1992; di Prisco et al., 2004). Fibre reinforcement enhances also the fatigue resistance of concrete structures as well as reduces labour costs due to the amount of time saved in the placement of the reinforcement (Ramakrishnan et al., 1989; Lee and Barr, 2004; Sorelli et al., 2006).

a)

b)

Figure 2.10: The LKS building in Mondragon, Spain: a) SFRC pouring along with continuity rebars at LKS slab and b) view of the LKS building showing 4 levels plus roof (Destree, 2016)

Improvements in mechanical properties generally depend on the type and volume percentage of fibres present (Johnston, 1974; Anderson, 1978). Fibres that fabricated with surface deformations or improved end anchorage (hooking) are more effective than equivalent straight uniform fibres of the same length and diameter. Consequently, the amount of these fibres required to achieve a given strength and ductility is usually less (found to be 60%) than the amount of equivalent straight uniform fibres (Ramakrishnan et al., 1980). Finally, all the advantages of using steel fibres provided successfully the industry, so far, with about 15 million square meters of ground suspended slabs, and about 100 buildings including these suspended elevated slabs (Destree, 2016). *Figure 2.10* Shows the LKS office building that was constructed and successfully completed using steel fibres and structural integrity rebars in Spain in 2010. The figure shows also the building during construction phase.

2.3.2 Geometry of SFRC

ASTM A 820 provides a classification for three general types of steel fibres based upon the product used in their manufacture. The three types are Type 1: cold-drawn wire, Type 2: cut sheet and Type 3: melt-extracted (ACI Committee 544, 2002). Japanese Society of Civil Engineers (JSCE) has another type of classification based on the shape of cross-section. Accordingly, three types are addressed, i.e., square section, circular section and crescent

section (ACI Committee 544, 2002). Generally, engineered shapes have been produced as: twisted, crimped, flattened, spaded, coned, hooked, surface-textured and melt-cast steel fibres (*Fig. 2.11 a*). These steel fibres have circular, square, rectangular or irregular cross-section as well as different diameters and lengths (*Fig. 2.11 b*) (Maidl, 1995; Katzer and Domski, 2012).

Since post-cracking strength is solely dependent on the fibre reinforcing parameters and the bond, improving these parameters is a key to success for the composite mix (Naaman and Reinhardt, 1996). Most common steel fibres are round in cross-section with a diameter and length ranging from 0.4 to 0.8 and from 25 to 60, respectively. One of the ways to characterize the factor of the shape of the cross-section of the fibre is Fibre Intrinsic Efficiency Ratio *(FIER).* It can be defined as the ratio of bonded lateral surface area of the fibre, to its cross-sectional area. *Figure 2.11 b* illustrates the relative values of the *FIER* for circular, square, triangular and flat rectangular fibres. It shows that, for the same cross-sectional area, a rectangular fibre is 28% more effective than a circular fibre whereas a square fibre is more effective by only 12% (Naaman, 2003).

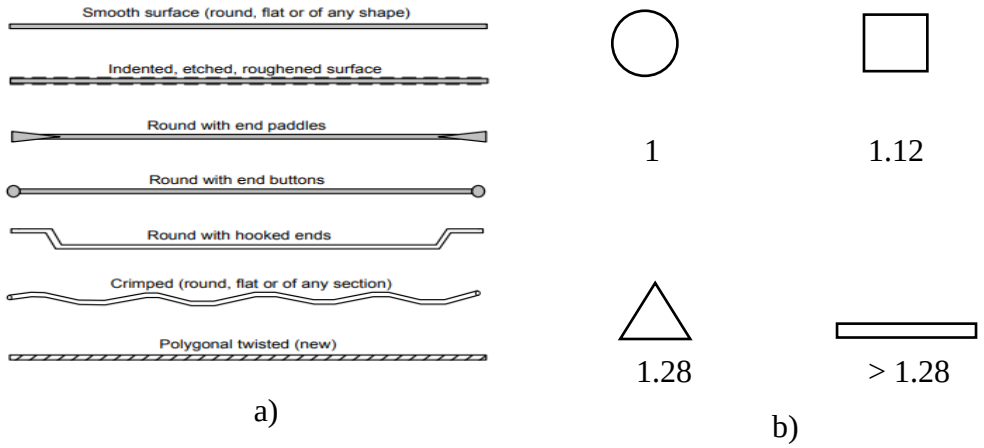

Figure 2.11: Geometric shapes, a) typical profiles of commonly used steel fibres and b) fibres sections with corresponding FIER ratio compared to the circular one (Naaman, 2003)

An increase in aspect ratio would lead to increase in mechanical properties. Moreover, when aspect ratio exceeds a certain value, the addition of steel fibres into concrete may have an effect of increasing the ductility rather than the strengths. When cracks propagate, some fibres were either broken or drawn out from the concrete mix, particularly for the fibres with the aspect ratio of 80 where most of the fibres were broken into two parts (Bayramov et al, 2004; Wang et al., 2010).

2.3.3 SFRC in compression

Generally, the ultimate strength is affected by the presence of fibres (Dixon and Mayfield, 1971; Ezeldin and Balaguru, 1992) (*Fig. 2.12 a*). Notwithstanding, a gab in knowledge is still present in terms of influence of steel fibres on compressive strength (Alani, and Aboutalebi, 2013). For instance, results from Moghadam and Izadifard (2019) found that the inclusion of steel fibres decreased the compressive strength. Casanova and Rossi (1997) indicated that the influence is negligible. However, numerous studies confirmed increases in compressive strengths (Holschemacher et al, 2010; Balendran et al., 2002). The difference between the results could be related to several factors such as the experimental conditions, the cure condition of the specimen (dry or saturated state) and the heating rate (Pliya et al., 2011).

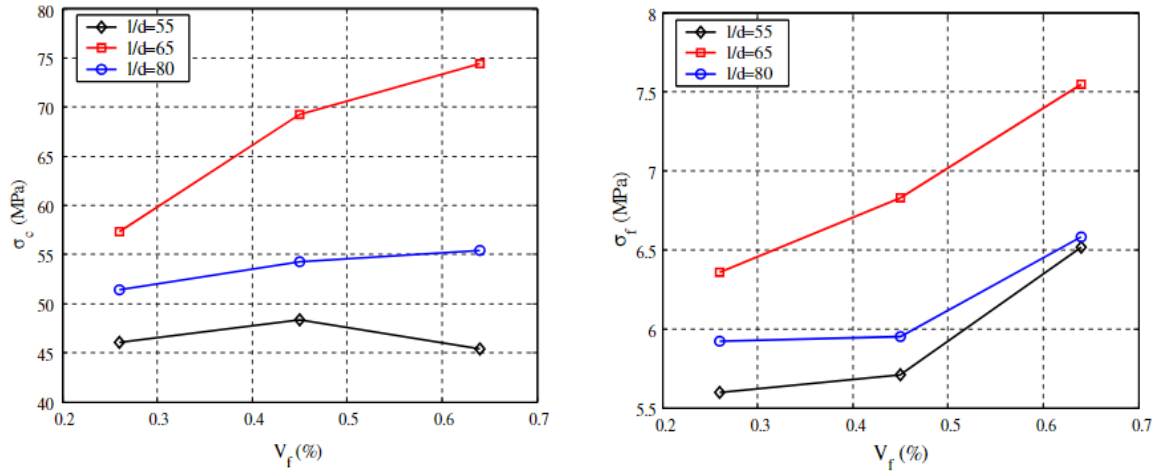

a) b)

Figure 2.12: Mechanical properties of SFRC using different aspect ratios including, a) relationship of compressive strength and volume fraction, and b) relationship of splitting tensile strength and volume fraction (Bayramov, et al., 2004; Wang et al., 2010)

2.3.4 SFRC in tension and flexure

The improvement in strength is significant in terms of tensile strength, depending on many factors such as aspect ratio or volume of the fibres (*Fig. 2.12 b*) (Bayramov et al, 2004; Wang et al., 2010). The increase in strength, in randomly distribution, can be up to reach 60% (Chanh, 2004). However, by using lower fibre volume concentrations, a significant increase in flexural strength may not be realized especially when using beam specimen tests (Snyder and Lankard, 1972; Johnston, 1989; ACI Committee 544, 2002). Finally, by increasing temperatures, flexural strength of concrete decreases (Ma et al., 2015).

2.3.5 SFRC in shear perspective

Using fibres as shear reinforcement or part of the shear reinforcement has promising applications since shear failure has brittle nature. This is of greater importance in case of HSC that has more brittle nature than conventional concrete (Barragan et al., 2006; *fib*, 2010). The first shear tests of SFRC beams were performed at the beginning of the 1970s namely by Batson et al. in (1972). The results showed that replacement of vertical stirrups by round, flat, or crimped steel fibres provided effective reinforcement against shear failure. In addition, the shear span ratio decreased with increasing fibre content (Batson et al., 1972). Generally, considerable improvement of the failure load was observed in beams without stirrup reinforcement, due to the increasing fibre content, and independently of the type of the steel fibres (Cuenca and Serna, 2010; Echegaray-Oviedo, 2014). Steel fibres in sufficient quantity, depending on the geometric shape of the fibre, can increase the shear strength of the concrete beams enough to prevent catastrophic diagonal tension (Jindal, 1984; Jindal and Sharma, 1987). On the other hand, the failure mode is changed from shear to simultaneous (shear and bending) failure for the beam containing steel fibres and no stirrup based on different compressive strength of concrete and the type of steel fibre. Meaning that the higher fibre content leads to changing of the failure mode from shear failure to bending failure (Cuenca and et al., 2015). Several works have been published concerning the prestressed precast concrete with steel fibre application (Lim et al, 1987; Narayanan and Darwish, 1987; Vecchio and Collins, 1986; Swamy et al, 1993; Meda, 2005; Minelli, 2005; Parra-Montesinos, 2006; Cuenca and Serna, 2013; Soetens and Matthys, 2013).

Lim et al (1987) proposed an analytical approach for predicting shear capacity and moment. They modified the plasticity analyses proposed by Braestrup (1974) and Thurlimann (1979) for ultimate shear capacity in beam by including the effect of fibres on shear capacity. The results suggested that fibres can replace vertical stirrups either partially or totally, so long as parity in the shear reinforcement factor is maintained (Lim et al, 1987). Similarly, Narayanan and Darwish (1987) established the inclusion of steel fibres in reinforced concrete beams resulting in a substantial increase in their shear strengths. In which for 1 percent volume fraction of fibres used, an increase of up to 170 percent in ultimate shear strength was observed. A considerable proportion of this increase was due to the improvement in dowel action and arch action of the beam resulting from the inclusion of fibres (Narayanan and Darwish, 1987). A different program consists using lightweight concrete was carried out by Swamy et al, (1993). Results reported that the addition of 1 percent by volume of crimped steel fibres to

lightweight concrete beams without conventional shear reinforcement reduced the beam deformations at all stress levels. This effect was more pronounced after cracking. In addition, the fibres enhanced the first cracking loads making the beam more ductile and showing more than one active shear crack. One percent of fibre by volume increased the ultimate shear strength varying from about 60 to 210 percent, depending on the shear span and amount of tension steel. Results were also similar to that reported by previous researchers (Swamy et al, 1993).

Over the last decade, many of remarkable studies have been conducted to provide the field with new models and approaches. This orientation shows increasing tendency towards investigating the field of SFRC in terms of shear as well as using new tools and programmes in applications. Several studies cover a wide range of related fields including, experimental investigations (Amin and Foster, 2016a; Spinella, 2013), analytical models and formulas (Maya et al., 2012; Foster, 2010; Foster et al., 2006), numerical modelling (Rossi et al., 2016; Amin and Foster, 2016b; Khomwan and Foster, 2005), applications (Foster, 2009) and prestressed concrete (Voo, et al., 2006; Voo et al., 2010; Lee et al, 2019).

2.3.6 Toughness and ductility of SFRC

A concrete structural element containing steel fibres suffers damage by gradual development of single or multiple cracks. However, a degree of structural integrity and post-crack resistance is remained, in which a similar element without steel fibres fails suddenly at a small deflection by separation into two pieces (Johnston, 1986; Ezeldin and Balaguru, 1992). Two available methods for evaluating toughness of SFRC are widely recognized. The first (*Fig. 2.13 a*) is developed and adopted by ASTM C 1018 Standard [ASTM C 1018-89 (1990)]. JSCE Method of test (*Fig. 2.13 b*) is the second one and developed for flexural strength and flexural toughness of FRC [(JSCE-SF-4 (1984)]. Both measurements of toughness obtained from ASTM and JSCE methods are derived from analysis of the load-deflection curve. Although these methods provide the designers with toughness levels appropriate to their applications and using, some studies argued about the accuracy of results of using this technique (Balaguru et al., 1992). Some other studies included the two methods to comparatively investigate the toughness of concrete mixes contain either steel fibres or synthetic fibres (Sukontasukkul, 2004). Finally, indices and factors used ASTM C 1018 are corresponding to higher end-point deflections. Therefore, the JSCE SF-4 method is often used as an alternate to design methods based on first-crack strength (Johnston, 1986; Nanni, 1991; Gopalaratnam et al., 1991; Trottier and Banthia, 1994; Nataraja, et al., 2000; ACI Committee 544, 2002).

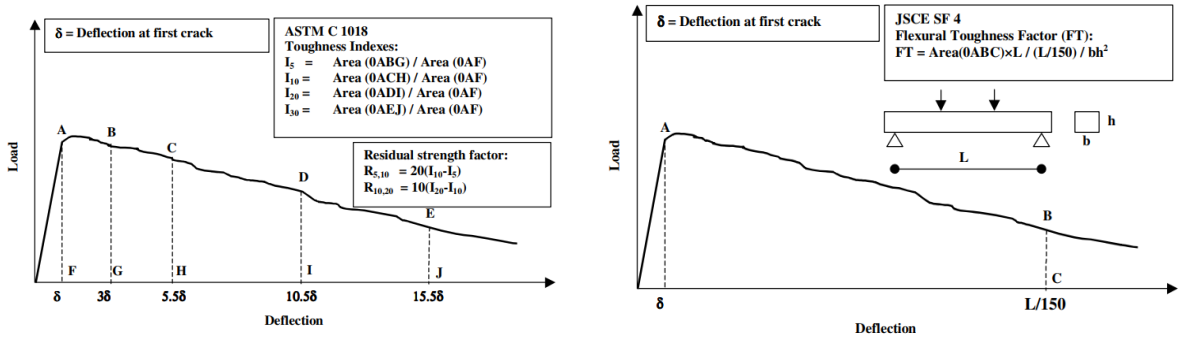

a) b)

Figure 2.13: Methods for characterizing the toughness properties of SFRC, a) ASTM C 1018 Standard test method, and b) JSCE SF-4 Method (Kovács and Balázs, 2004)

ASTM Method depends on deformation (mm) at the first crack, identified as δ (*Fig. 2.13 a*). Results showed that shear toughness values, indicated by toughness indexes such as I_5, are generally increased when the concrete mix contains fibres regardless the type of fibres (Gopalaratnam et al. 1991). However, several studies recommended to use indexes higher than I_5, for instance I_{100}, to obtain more accurate of the toughness values since I_5 or I_{10} do not provide a good indication of deflection in the curves (Balaguru et al., 1992). From another hand, calculations to obtain the first crack depend on approximate evaluations from the curves, in which the first deformation or changing in stiffness is considered as the first crack. Therefore, inaccuracies in measuring deflection at first crack are expected (Gopalaratnam et al. 1991).

Model Code 2010 defines ductility as: plastic deformation capacity characterized by irreversible deformations and energy dissipation, usually referred to quantitatively as the ratio between plastic deformation and the limit of the elastic behaviour (*Model Code 2010*). Ductility is generally addressed implicitly in codes and is expressed mostly for beams in flexural investigations. However, from design perspective, four ductility classes are defined according to the characteristic value of the ratio $(f_t/f_y)_k$. This ratio corresponds to the 5% of the relation between actual tensile strength and actual yield strength. The four classes are defined by minimum specified values for the characteristic value of the ratio f_t/f_y and the characteristic strain at maximum stress $\mathcal{E}_{uk}$ as follows:

Class A: $(f_t/f_y)_k \geq 1.05$ and $\mathcal{E}_{uk} \geq 2.5\%$;
Class B: $(f_t/f_y)_k \geq 1.08$ and $\mathcal{E}_{uk} \geq 5\%$;
Class C: $(f_t/f_y)_k \geq 1.15$ and ≤ 1.35 and $\mathcal{E}_{uk} \geq 7.5\%$;
Class D: $(f_t/f_y)_k \geq 1.25$ and ≤ 1.45 and $\mathcal{E}_{uk} \geq 8\%$.

Noting that ductility classes C and D should be used where high ductility of the structure is required (*Model Code 2010*).

2.3.7 Durability of SFRC

Air void characteristics of SFRC and non-fibrous concrete are similar in nature, thus for freezing and thawing resistance, SFRC must be air entrained (Balaguru and Ramakrishnan, 1986). In general, literature shows the superior durability of un-cracked SFRC exposed to chlorides relative to conventional reinforcement. Nevertheless, the durability of cracked SFRC is still under discussion (Victor et al., 2016). Once the surface fibres corrode, there does not seem to be a propagation of the corrosion much more than 0.10 in. (2.5 mm) below the surface (Schupack, 1986). Since the fibres are short, discontinuous, and rarely touch each other, there is no continuous conductive path for stray or induced currents or currents from electromotive potential between different areas of the concrete (ACI Committee 544, 2002).

If concrete mix does not reach critical strain (micro crack width), damages would eventually have self-healing (Homma et al., 2009; Solgaard, 2010; Mobasher, 2016). Crack width up to 0.1 mm has no adverse effect in corrosion but, once the tensile capacity of the concrete is reached, cracks occur and bond is then "activated" (Granju and Balouch, 2005). The strain damages the interfacial transition zone (ITZ). The extent of this damage is directly related to the strain and the shape of the fibres causing corrosion damage of the hook (Nemegeer et al., 2000). The damaged ITZ would provide a preferential path for diffusion of chlorides, metal ions and oxygen, promoting corrosion at the areas with greater damage (Victor et al., 2016). In case of excessive damages and the tensile capacity of the steel is lower that the fibre-matrix bond strength, the failure mode of the SFRC would change from fibre pull-out to fibre yield (Bernard, 2004; Nordström, 2005; Homma et al., 2009). Finally, to reduce the potential for corrosion at cracks or surface staining, the use of alloyed carbon steel fibres, stainless steel fibres, or galvanized carbon steel fibres are possible alternative, taking into considerations the precautions for using the galvanized steels (ACI Committee 544, 2002).

2.4 Synthetic fibres

Synthetic fibres have become more attractive in recent years as reinforcements for cementitious materials. They can provide effective, relatively inexpensive reinforcement for concrete and are alternatives to asbestos, steel and glass fibres (Zheng and Feldman, 1995). Synthetic fibres are man-made fibres resulting from research and development in the petrochemical and textile industries. Synthetic fibres utilize fibres derived from organic polymers which are available in a variety of formulations (ACI Committee 544, 2002).

There are many types of synthetic fibres i.e. acrylic, aramid, carbon, nylon, polyester, polyethylene and polypropylene. Each type has specific properties as summarized in Table 2.

2.4.1 Background

Historically, first synthetic fibres that used as a component of construction materials were reported in 1965 by Goldfein (1965). Williamson (1966) investigated 72 explosive loading tests on fibrous-reinforced concrete slabs using various synthetic and steel fibres to develop a concrete that would resist explosive loadings. The project tested fibres to be used in blast resistant structures for the U.S. Army Corps of Engineers Research and Development Section. However, it needed another fifteen years before large scale development activities began with synthetic fibres showing better distribute cracking, reduce crack size, and improve other properties of concrete (Yang, 1993; Zheng and Feldman, 1995). Nowadays, several applications intend to use polymeric fibres mainly to control plastic shrinkage (Serdar et al., 2015), bonding properties (Tighiouart et al., 1998; Yuan et al., 2018) and improve fire resistance (Bisby, 2003).

2.4.2 Properties of synthetic fibres

Generally synthetic fibres have some unique properties that make them suitable for incorporation into concrete matrices. They are chemically inert and very stable in the alkaline environment of concrete. They have a relatively high melting point with low cost raw materials. Additionally, polymer has a hydrophobic surface so that it does not absorb water. Disadvantages include poor fire resistance, sensitivity to sunlight and oxygen, a low modulus of elasticity, and a poor bond with the concrete matrix. However, these disadvantages are not necessarily critical. Embedment in the matrix provides a protective cover, helping to minimize sensitivity to fire and other aggressive environmental effects (Zheng and Feldman, 1995).

To increase the strength of their composites, fibres must have a modulus of elasticity greater than that of the matrix. This is difficult to meet in case of cementitious materials, where the modulus of elasticity ranges from about 15 to 30 GPa. Therefore, attempts have been made to develop fibres with a very high modulus of elasticity for cement reinforcement. Considerable improvements were observed with respect to the strain capacity, toughness, impact resistance and crack control of the fibre-reinforced concrete composites even with fibres that have low modulus of elasticity (Zheng and Feldman, 1995; Bentur and Mindess, 2007). Most of the current applications with FRC involve the use of fibres ranging around 1% by volume with respect to concrete. It is usually assumed that the fibres do not influence the tensile strength of

the matrix, and that only after the matrix has cracked do the fibres contribute by bridging the crack (Shah, 1991). Further properties including durability, chemical compatibility and different mechanical properties of fibres are individually determined and summarized for each type in the following sub-sections.

Acrylic

Acrylic fibres contain at least 85 percent by weight of acrylonitrile (AN) units (ACI Committee 544, 2002). Fibres with AN in a predominant amount remain as white powders up to a temperature of 250°C at which point they become darker due to the beginning of degradation. These polymers have a low thermal plasticity and cannot be used as a plastic material (Zheng and Feldman, 1995). *Table 2.2* summaries some of the properties that Acrylic fibres have. Additionally, acrylic fibres exhibit, besides high tensile strength and elastic modulus, very good resistance to acids and alkalis and are low in cost as well as improving toughness (Accion et al., 1990; Raheel, 1993).

Aramid

Aramid (aromatic polyamide) is a high-modulus, manmade polymeric material that was first discovered in 1965. By the early 1970s they were produced for commercial applications, then was incorporated into concrete as a form of reinforcement by the late 1970s (ACI Committee 544, 2002). *Table 2.2* summaries some of the properties obtained by Aramid fibre content in concrete. Properties showed that Aramid fibres have relatively high tensile strength and a high tensile modulus. Aramid fibres are two and a half times as strong as E-glass fibre and five times as strong as steel fibres per unit weight (ACI Committee 544, 2002). Furthermore, Aramid fibres are reasonably resistant to high temperatures when compared to many other synthetic fibres because of its stable chain structure. At temperatures above 300 °C, the fibre may lose most of its strength (Bentur and Mindess, 2007). Further studies are available in (Gale et al., 1986; Nanni, 1991; Li, et al, 1992).

Carbon

Carbon fibres were primarily developed for their high strength and stiffness properties for applications within the aerospace industry. Although laboratory research has been increasingly developed, carbon fibres has limited commercial development. This drawback is attributed to the fact that carbon fibres have high cost compared to other types of fibres (ACI Committee 544, 2002). Furthermore, carbon fibres are inert in aggressive environments, abrasion-resistant and stable at high temperatures, medically safe, as strong as steel fibres and more chemically

stable than glass fibres in alkaline environments. Carbon fibres are also low in density, especially when compared to steel fibres. Their strength to density ratio is one of the highest among all fibre types (Zheng and Feldman, 1995). *Table 2.2* summarises properties of carbon fibres. Additional studies and results can be found by (Toutanji, 1993; Garcés et al., 2005).

Nylon

Nylon is a generic name that identifies a family of polymers characterized by the presence of the amide functional group - CONH (*The Condensed Chemical Dictionary*, 1981). Nylon fibres are spun from nylon polymer. The polymer is transformed through extrusion, stretching, and heating to form an oriented, crystalline, fibre structure. For concrete applications, high tensile strength, heat and light stable yarn is spun and subsequently cut into shorter lengths (ACI Committee 544, 2002). Nylon is a relatively inert material, resistant to a wide variety of organic and inorganic materials including strong alkalis and exhibit good tenacity, toughness, and excellent elastic recovery (Cook, 1984). Further tests and results are available (Ozger et al, 2013; Yap et al., 2013).

Polyester

Polyesters are defined as polymers containing -CO-O- groups in the main chain (Zheng and Feldman, 1995). Polyester fibres available to the concrete industry belong to the thermoplastic polyester subgrouping. This type of polyester exhibits physical and chemical characteristics that depend on manufacturing techniques (ACI Committee 544, 2002). Previous studies indicate that polyester fibres provide a higher modulus of rupture at the beginning of aging, but the values slightly decrease or remain the same with accelerated aging (Khajuria et al., 1991). Furthermore, studies showed that addition of polyester fibre has increasing impacts on split tensile strength, flexural strength and compressive strength. Yet, there was no change in modulus of elasticity and shear strength (Patel et a1., 1989). All thermoplastics are temperature sensitive in which fibre characteristics are altered at temperatures above normal temperatures. Temperatures above 280 °C would cause molecular breakdown (Cook, 1984). Polyester fibres are somewhat hydrophobic (do not absorb much water) and have been shown not to affect the hydration of the Portland cement concrete (Golding, 1959). Finally, bonding of polyester fibres within the cement matrix is mechanical. There is no consensus on the long-term durability of polyester fibres in Portland cement concrete (ACI Committee 544, 2002).

Polyethylene

Polyethylene, as concrete reinforcement, has been produced in monofilament form with wart-like surface deformations along the length of the fibre (Kobayash, 1983). One of the advantages of polyethylene fibre is that it can be produced with a relatively high modulus of elasticity even under long-term exposure to aggressive environments such as seawater, alkalis and acids. Additionally, these fibres also have reasonable thermal stability, retaining a significant percentage of their room temperature properties at elevated temperatures near 80°C (Zheng and Feldman, 1995). It has also reported that the shear strength of polyethylene FRC is increased by using the fibres (Li et al., 1992).

Polypropylene

Refractory product manufacturers use polypropylene fibres for early strength enhancement and because they disappear at high temperatures, providing a system of "relief channels" for use in controlling thermal and moisture changes (ACI Committee 544, 2002) since the melting point and elastic modulus are low relative to many other fibre types (Mai et al., 1980). Polypropylene is hydrophobic and not expected to bond chemically in a concrete matrix, but bonding has been shown to occur by mechanical interaction (Rice et al., 1988). Several studies indicated that existence of the fibre has no significant change for compressive strength but flexural, split tensile and shear strength improves greatly, when compared to the plain concrete (Patel, et al., 2012). Disadvantages of polypropylene include poor fire resistance, sensitivity to sunlight and oxygen, a low modulus of elasticity, and a poor bond with the concrete matrix (Zheng and Feldman, 1995). *Table 2.2* shows some of the properties of polypropylene fibres.

Concrix

Concrix is a bi-component macrofibre serving as a structural concrete reinforcement. The main component of concrix is Polypropylene. Concrix (*Fig. 2.14 a*) is the brand name of polyolefin-based and macro-synthetic bi-component fibres. Concrix is used in several applications such as tunnelling (shotcrete) (*Fig. 2.14 c*), prefabrication applications, slabs and concrete walls, industrial floors, outside standings, for concrete repair works, concrete piles, special foundation works and many different special applications (Contec Fibre AG, 2017). Generally, applications using macro-synthetic polymer fibres have grown significantly worldwide since their introduction in the late 1990s. While the steel fibres are used at relatively short length (30–35 mm) to reduce lime blockage, the more flexible macro-synthetic polymer fibres can

typically be used with larger length (40–60 mm) without significantly reducing the pumpability and sprayability of the mixture (Dufour et al., 2006; Kaufmann et al., 2013).

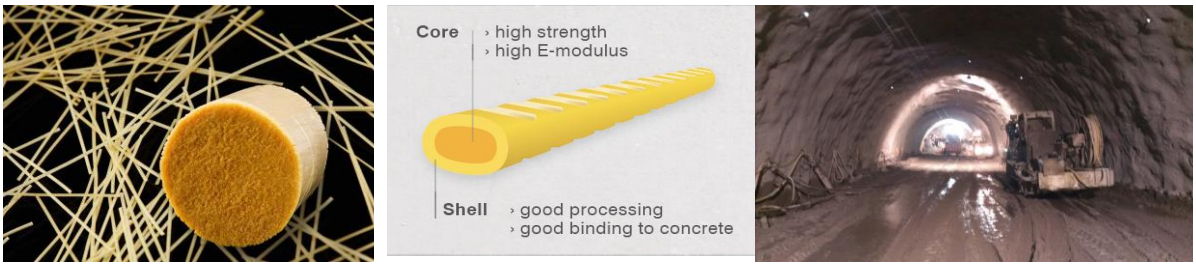

a) b) c)

Figure 2.14: bi-component polymer fibres, Concrix a) The final product, b) The core element and c) shotcrete for tunnelling (Contec Fibre AG, 2018)

The core polymer may be optimized by designing a high tensile strength and a low elongation at break. Concrix, with a modulus of elasticity of more than 11 GPa, is suitable for the highest requirements in the static range. Resistance to aggressive waters and the successfully passed creeping test lasting more than 4 years makes concrix the optimal fibre for superior precast elements and tunnel construction. Furthermore, the high E-modulus of the core of the fibre guarantees the highest strength, while the special, structured shell ensures excellent binding to the concrete (*2.14 b*) (Contec Fibre AG, 2018). Finally, concrix ES fulfils the standard EN 14889-2 according to system 1 and therefore guarantees a consistently high quality.

2.5 Influences of elevated temperatures on concrete

Historically, the fire performance of concrete has often been taken for granted considering its non-combustible nature and ability to function as a thermal barrier, preventing heat and fire spread (Fletcher et al., 2007). Notwithstanding, when concrete is subjected to heat, a number of changes and reactions occur (Schneider et al., 1981; Bazant et al., 1982). Changes with temperature occur also in the thermal hydra mechanical properties depending upon the heating rate, initial moisture condition, boundary conditions, geometry and size of the heated member, type of constituents, chemical physical interactions etc. (fib, 2007). Although decades of research on the effect of fire on concrete have been produced, there still remain areas need further investigations and clarifications (Khoury, 2008). This could be due to the fact that many of the reported test results are hard to interpret (Schneider, 1988). Possible causes of the differences in interpretations could be due to differences in the tested types, equipment,

procedures and conditions of concretes as well as incompleteness of descriptions of the tests (fib, 2007).

2.5.1 Basic behaviour

Water inside concrete begins to majorly vaporise when the temperature exceeds 100 °C, causing usually a build-up of pressure within the concrete. When the temperature reaches about 400 °C, the calcium hydroxide in the cement will begin to dehydrate, causing significant reduction in the strength of the material (Khoury, 2000; Carvel, 2005; Fletcher et al., 2007). At temperature 550–600 °C, a marked increase in the basic creep of Portland cement paste and concrete is reported. This temperature is considered to be critical, above which concrete is not structurally useful (Khoury et al., 1986; Khoury, 2000).

Table 2.3: A brief description of some phase changes in heated concrete (Khoury, 1992; fib, 2007)

Temperature (°C)	Transformation
20-80	Increase in hydration, slow capillary water loss and reduction in cohesive forces as water expands
100	Marked increase in water permeability
80-200	Increase in the rate of loss of capillary water and then physically bound water
150	Peak for the first stage of decomposition of calcium silicate hydrate (CSH)
300+	Marked increase in porosity and micro-cracking
350	Break-up of some river gravel aggregates
374	Critical point of water when no free water is possible
400-600	Dissociation of Ca (OH)2 into CaO and water
573	α-β transformation of quartz in aggregates and sands
550-600+	Marked increase in thermal effects
700+	Decarbonation of CaCO3 into CaO and CO2 (in paste and carbonate aggregates)
720	Second peak of CSH decomposition into β-C_2S and β--CS
800	Start of ceramic binding which replaces hydraulic binding
1060	Start of melting of some constituents

For this level of temperatures, there is decomposition of the portlandite in which it explains the significant reduction in strength [$Ca(OH)_2 \rightarrow CaO + H_2O$] (Quon, 1980; Naus, 2005). Between 600 °C and 900 °C the limestone begins to undergo decarbonation [$CaCO_3 \rightarrow CaO + CO_2$]. Above 1200 °C, some components of the concrete begin to melt. Above 1300 °C to 1400 °C concrete exists in the form of a melt (Muir, 1977; Chu, 1978; Naus, 2005). *Table 2.3* summarizes some phase changes of concrete due to elevated temperatures. Worth to mention that the melting points of aggregates vary greatly, in which at 1060 °C basalt is at the lower

limit of all types of rock, with quartzite not melting below 1700 °C (Schneider et al., 1981). Finally, the ability of reconstruction for some fire-damaged buildings or improvement of fire resistance may be applicable (Lublóy et al., 2016; Czoboly et al., 2017).

2.5.2 Thermal properties

Thermal analysis is important for design calculations and fire assessment. It is also required for both simplified and complex calculations as well as for separating or load-bearing function. Thus, it should be carefully analysed in order to obtain accurate and reliable results. Thermal properties used in computation are thermal conductivity (λ) and volumetric specific heat (ρc_p). The latter is a function of the density and specific heat. These properties are required to be determined experimentally or from standards (*fib, 2007*).

(I) Thermal diffusivity

Measurement of the rate of heat flow under transient thermal conditions is given by the concept of the thermal diffusivity. It is described as follow:

$D = \lambda / \rho c_p$ (m^2/s)

λ = thermal conductivity (W/mK)
c_p = specific heat J/kgK
ρ_c = density of concrete (kg/m^3)
ρc_p = volumetric specific heat J/m^3K

Noting that thermal diffusivity of concrete is much easier to measure experimentally than the measuring the three components separately. However, the problematic part is that λ and ρc_p are required to be input separately into the calculations (*fib,* 2007).

(II) Thermal conductivity

Thermal conductivity is defined as the ratio of the heat flux to temperature gradient. Since transient diffusivity is easy to measure, thermal conductivity is sometimes calculated indirectly from transient diffusivity (*fib, 2007*). Direct thermal conductivity measurements are carried out at steady-state, not at transient temperature. Additionally, physical-hydra-chemical transformations would be completed at the test temperature. Thus, it is not uncommon to obtain various conductivity measurements on "identical" specimens (Collet, 1975). These various measurements are also affected by the method used (Neville, 1995).

Previous studies confirmed that with the increase of steel fibre volume fraction, the thermal conductivity and thermal diffusivity increase gradually (Li et al, 2019). This increase is

significantly greater for copper fibres than steel as would be expected (Cook and Uher, 1974). From another hand, thermal conductivity is largely determined by the type of aggregate used since aggregate constitute 60-80% by volume of concrete. Moisture content is also an important factor that affect thermal conductivity since water, although low, is much higher than that of air (*fib, 2007*) (*Table 2.4*). Therefore, a rich mix has a lower thermal conductivity than a lean one. The reverse is true for lightweight aggregate concrete. Finally, increasing the w/c increases the concrete porosity and correspondingly reduces the thermal conductivity (Neville, 1995; *fib,* 2007).

Table 2.4: Thermal conductivities at ambient temperature (Khoury, 1983)

Material	Thermal conductivity (W/m°C)
Aggregate	0.7-4.2
Saturated concretes	1.0-3.6
Saturated hardened cement paste	1.1-1.6
Water	0.515
Air	0.0034

(III) Density

Changes in density of concrete are related to weight changes, thermal dilation and changes in porosity. In unsealed condition, these factors reflect the influences of the physical-chemical transformations. Transformations include water dilation up to about 80 °C, loss of free, and physically bound water at 100-200 °C. Degree of influence is depending on the heating zone and heating rate (*fib,* 2007).

2.5.3 Shear properties at high temperatures

(I) Testing of push-off specimens

Although most of shear tests were implemented at room temperature, many of other papers were concerned about the influence of elevated temperatures. Al-Owaisy (2007) showed that shear transfer strength is significantly affected when exposed to elevated temperatures. The results also showed that shear transfer strength of higher amount shear reinforcement specimens was higher than those of lower shear reinforcement ones, both before heating and after exposure to each particular temperature. Xiao et al (2014) studied the influence of compressive strength of concrete in transferring shear across a crack using five LVDTs to record crack displacements, both width and slip. Results showed that a higher compressive strength HSC results in more brittle shear failure, irrespective of the elevated temperature (Xiao

et al., 2014). Although most of the studies have been conducted to measure the residual strength, at the cold state, due to complexity and expensive cost, a few researchers have carried out some tests in the hot-state (Naus et al., 1976).

(II) Using different models or elements

Although most of the studies use push-off model to investigate the shear, several studies have been carried out to investigate shear performance at elevated temperatures using different models such as shear block, or different elements such as hollow core slab (Acker, 2003; Fellinger, 2004; Smith et al., 2011; Yang, 2016; Kodur and Shakya, 2017).

2.5.4 FRC at high temperatures

In general, SFRC exhibits at elevated temperatures mechanical properties that are more beneficial to fire resistance than those of plain concrete. The compressive strength at elevated temperatures of FRC is higher than that of plain concrete. The presence of steel fibres increases the ultimate strain and improves the ductility of a fibre-reinforced concrete member (Lie and Kodur, 1995; Novák and Kohoutková, 2017). Additionally, decrease in flexural strength can be less significant at elevated temperatures by the presence of steel fibres compared to plain concrete (Khaliq and Kodur, 2011). Results showed also that shear strength values in HSFRC still high at high temperatures by the addition of steel fibres (Ahmed and Abdullah, 2019). Some studies indicated that improvement in fire resistance can be reached if small diameter fibres with relatively short lengths are used (Balazs and Lubloy, 2012). Although using SFRC has steadily increased in recent years (Kodur et al, 2003; Hugo et al, 2019), a comprehensive design approach in case of fire is still, so far, missing (Dehn and Herrmann, 2016).

The temperature at which polymeric fibres are converted from a solid to a glassy or liquid state is called the melting point (ACI Committee 544, 2002). Polypropylene fibres have negative effect on the residual mechanical properties of FRC after high-temperature exposure, in which elevated temperature significantly decreases the residual compressive strength, elastic modulus and tensile strength in PFRC compared to plain concert (Novák and Kohoutková, 2017). However, concrete mixes that contain polymeric fibres have been proved to considerably reduce the probability of spalling (Wille and Schneider, 2002; Dehn and Wille, 2004; Wahter et al., 2005; Dehn and Werther, 2006). Moreover, studies indicated that advantages of influence of polymeric fibres is mainly available for the thin fibres not for thicker fibres (Balazs and Lubloy, 2016).

Using of steel fibre simultaneously with polypropylene fibre (cocktail) can provide some benefits to structures including tensile strength (improved up to 10 %) (Yermak et al, 2017), good toughness of a concrete and spalling resistance (Serrano et al., 2016; Novák and Kohoutková, 2017). First, the prevention of spalling phenomena by the virtue of polypropylene fibre and avoids the steel reinforcement to be directly exposed to fire thus reaching very high temperatures with a consequent mechanical decay (Colombo et al., 2009).

2.6 Age Factor

Compressive strength of concrete at 20 °C and curing in accordance with ISO 1920-3 at various ages $f_{cm}(t)$ may be estimated from (Model Code 2010):

$$f_{cm}(t) = \beta_{cc}(t) \cdot f_{cm} \qquad 2.4$$

with:

$$\beta_{cc}(t) = \exp\left\{ s \cdot \left[1 - \left(\frac{28}{t}\right)^{0.5}\right] \right\} \qquad 2.5$$

where:

$f_{cm}(t)$ is the mean compressive strength in MPa at an age t in days;
f_{cm} is the mean compressive strength in MPa at an age of 28 days;
$\beta_{cc}(t)$ is a function to describe the strength development with time:
t is the concrete age in days adjusted.
It is a function of the number of days and the mean temperatures, given as an equation 5.1-85 in Model Code 2010.
s is a coefficient depending on the strength class of cement, given as follow in Table 2.5.

Table 2.5: Coefficient (s) depending on the strength class of cement (Model Code 2010)

f_{cm} (MPa)	Strength class of cement	s
≤ 60	32.5 N	0.38
	32.5 R, 42.5 N	0.25
	42.5 R, 52.5 N, 52.5 R	0.20
> 60	all classes	0.20

Furthermore, the tensile strength of concrete primarily depends on those parameters which also influence the compressive strength of the concrete. However, tensile and compressive strength are not proportional to each other. It is recommended to carry out experiments for tensile strength considering conditions and dimensions of the structural member. Additionally, for the high strength concrete the increase in compressive strength leads only to a small increase of the tensile strength (Model Code 2010).

3. Experimental program

The current chapter is presented to cover three main headlines, i.e., experimental outline, materials and test methods. Experimental program is usually designed to identify motivation, limitations and test parameters regarding all phases of the overall test program. Moreover, all mix ingredients are presented beside the mix design. Finally, a comprehensive analysis of the test procedures including equipment, model, measurements and test types that carried out are presented as well.

3.1 Experimental outline

3.1.1 Motivation

Current study aims to investigate the effect of adding different types and amounts of fibres on the behaviour of concrete in terms of shear failure at elevated temperatures. Significance of the study is clear since several studies have investigated the shear at ambient temperatures, yet there was a lack of knowledge in literature regarding elevated temperatures. Additionally, elevated temperatures may cause serious deterioration to concrete structures. However, fibres content is found to provide concrete with significant enhancements specially in a view of ductile behaviour. Thus, the possibility of enhancing shear performance, which is identified as a brittle failure, by addition different types and amounts of fibres are of great importance.

3.1.2 Limitations

Different types of fibres including different amounts are presented herein. However, further studies are required regarding wider range of amounts as well as more different types of fibres that are not investigated in this study. Particular attention should be considered in future studies for the length and type of the steel fibres in relation to the shear plane dimensions. Additionally, due to the non-standard push-off test method and the fact that was observed by some researchers in the literature that model size has effects on results, different sizes are required in further studies as well. Finally, programming and modelling of the tests are not mainly included in the thesis, therefore it is recommended for any further studies in the future.

3.1.3 Study parameters

Three main parameters were investigated in the current study, namely; maximum temperature, concrete mix and age of concrete. Five maximum temperatures were chosen, and five concrete mixes, depending on fibres content, are chosen as well. Concrete is tested also in two different

ages. Table 3.1 lists all parameters including descriptions and the values being investigated in this research.

Table 3.1 Summary of primary parameters in present study including descriptions and values

Parameter	Description	Value
Max. temperature, °C	Indicates the maximum temperature that the specimens were exposed to for a specified period of time	20 150 300 500 700
Concrete mix, kg/m^3	Indicates the influences of fibres type and the amount of used fibres.	0 - Zero fibres 40 (steel fibres) 80 (steel fibres) 4 (polymeric fibres) 40+2 (cocktail of steel and polymeric fibres)
Age of concrete, at the start of testing time	Indicates the influences of the water content obtained by the age of the specimens	28-day One-year old

For the maximum temperature, maximum degrees are chosen to be covering the different changes occurring during the heating period, particularly the significant deterioration interval from 550 to 600 °C. Moreover, fibres content was chosen within the range that has significant influences in concrete properties, in which steel fibres content below 20 kg/m^3 was found to have no significant influence on concrete whereas a concrete mix containing above 150 kg/m^3 of steel fibres was found to reduce the workability for usual steel fibres. Therefore, two amounts between the abovementioned limits of steel fibres are chosen herein. Additionally, synthetic fibres as well as cocktail fibres are also chosen to be within the suggested or preferred by the producers and researchers as stated in the literature.

Water content plays an important role that affects the properties of concrete. Although testing concrete samples at the age of 28-days is widely accepted, testing concrete after one-year of storing in lab conditions is of great importance. This is clear by representing the actual concrete structures in the real life as well as the significance of the water content at elevated temperatures in terms of spalling.

3.1.4 Test series

In order to easily identify all mixes by ID, specific code has been adopted for each series. The first digit for each “ID code” starts with an abbreviation referring to the type of the fibres used followed by the amount of the fibres. The third digit is refereeing to the temperature level then

the last digit is either 28 or 365 to represent the age. Thus, coding could be illustrated by the simple formula (Type of fibres-amount of fibres-level of temperature-age of concrete). Each mix has three samples coded as a, b and c. For instance, the series (SFRC-80-150-28 a) means that the mixture, contains steel fibres with an amount of 80 kg/m^3, exposed to max temperature 150 °C, tested at the age of 28-day, and this is the first sample. A total of 50 different series of mixtures are designed. Table 3.2 describes the complete list of the specimens ID`s.

Table 3.2 Details of test specimens

Series ID	Fibre type	Fibres amount (kg/m^3)	Age of the specimen	Sample number	Temperatures (°C)
SFRC-0	-	0	28-days 365-days	a, b, c	20, 150, 300, 500, or 700
SFRC-40	steel (5D Dramix)	40	28-days 365-days	a, b, c	20, 150, 300, 500, or 700
SFRC-80	steel (5D Dramix)	80	28-days 365-days	a, b, c	20, 150, 300, 500, or 700
P4	concrix EX	4	28-days 365-days	a, b, c	20, 150, 300, 500, or 700
SP	steel + concrix	40 + 2	28-days 365-days	a, b, c	20, 150, 300, 500, or 700

3.2 Materials

3.2.1 Basic cementitious material

One type of ordinary Portland cement was used (CEM I 52.5 N) for all mixes. Natural sand was used as fine aggregate with maximum size of 4 mm *(Fig. 3.1 a)***.** Coarse aggregate (Danube quartz gravel) with size range 4 to 8 mm was used *(Fig. 3.1 b)*. MasterGlenium 300, a second generation of polycarboxylic ether polymers was also used as superplasticizer.

3.2.2 Steel fibres

Dramix 5D (5D 65/60BG) was used as steel fibres with length 60 mm, diameter 0.9 mm and aspect ratio 65. Tensile strength for the steel fibres is 2300 MPa and Young`s modulus is 200000 MPa. Aspect ratio of the steel fibres is defined as the ratio of the length to the diameter and it is 65. Finally, strain at ultimate strength is 6%, *(Fig. 3.1 c).*

3.2.3 Synthetic fibres

Concrix ES is used with standard lengths of 50 mm. Generally, the recommended dosage for concrix ES as a structural reinforcement is 2.0 to 7.5 kg/m^3 of concrete. Thus, 4 kg/m^3 was chosen to be the percentage in polymeric mixes and 2 kg/m^3 was as the percentage of the cocktail one. Tensile strength is 590 N/mm^2 and modulus of elasticity > 11 GPa *(Fig. 3.1 d).*

a) b) C) d)

Figure 3.1: Material a) fine aggregate, b) coarse aggregate, c) steel fibres and d) concrix

3.3 Mix design

3.3.1 Approach

Concrete mixtures are designed using volumetric approach in which fine aggregate constitutes of 45% of the total volume of the mix whereas coarse aggregate constitutes of 55%. Cement mass is fixed as 400 kg/m^3. Water to cement ratio is also fixed as 38% or 152 kg/m^3 in terms of weight. As for the fibres content, the weight of the fibres is fixed for each series. Fibres content is included in the overall volumetric mix; thus, volume of the aggregate will be slightly reduced by the presence of the fibres as shown in Table 3.3.

Table 3.3 Mix proportions

Series	Short ID	Fibres amount (kg/m^3)	Fine aggregate (kg/m^3)	Coarse aggregate (kg/m^3)	Cement (kg/m^3)	Water (kg/m^3)	Super-plasticizer (kg/m^3)
Reference	SFRC-0	0	829	1013	400	152	3.33
Steel fibres (40)	SFRC-40	40	823	1006	400	152	3.33
Steel fibres (80)	SFRC-80	80	817	999	400	152	3.33
Synthetic fibres	P4	4	824	1008	400	152	3.33
Cocktail fibres	SP	40+2	821	1003	400	152	3.33

3.3.2 Procedures

All concrete mixes were cast in a 60-litre mixer (*Fig. 3.2 a*) according to the proportions obtained from the mix design calculations. Th mixer has 4 rotating blades to assure uniform distribution of the ingredients. Then fresh concrete was formed in a rectangular metal mould (*Fig. 3.2 b*). Compaction phase followed the casting using an electrical table vibrator (*Fig. 3.2 b*). Twenty-four hours after casting, specimens were cured in natural water for seven days. After that, specimens were removed from water containers and stored in laboratory conditions.

a) b) c)

Figure 3.2: Phases of sample preparations, a) mixing ingredients, b) metal mold and table of vibration and c) fixed drill-in machine for thermocouples

a) b)

Figure 3.3: preparations of push-off specifications, a) saw cut-off machine for notches and b) final output of push-off specimen

After 7-days of water treatment, notches were cut (*Fig. 3.3 a*) as mentioned in section 3.4.1. Two thermocouples were used to record temperatures at two points in addition to the oven temperature itself. One of the thermocouples was fixed at the surface of the specimen whereas

the other one was installed in 50 mm inside and at 50 mm distance from both edges. A fixed-machine driller was used to drill inside the specimen (*Fig. 3.2 c*). Half of the specimens were heated and tested after 28days whereas the other half of the specimens were stored in the laboratory conditions for one year. The final output of the specimens is, then, ready to be heated then load-testing, as shown in *Figure 3.3 b.*

3.4 Test method

3.4.1 Push-off specimen

As the push-off specimen is a non-standard model, several dimensions have been used by previous researchers. However, chosen dimensions in the current study should fit dimensions of the available oven in the laboratory as well as other requirements such as saw-cut machine and LVDTs domains. Thus, the height of the uncracked push-off model is chosen to be 260 mm, and both width and depth are 150 mm. All adopted dimensions are shown in more details, for both front and side views, in *Figure 3.4*. Concerning the notches that form the shear plane, some previous researchers (Xiao, 2014) used preformed notches instead of cut. In such a way, the preformation could cause a non-uniform fibres distribution near the notches due to wall effects in their experiment (Bao et al, 2019). Therefore, in present experimental study notches, 4 mm width by 75 mm length, were cut after two weeks of casting perpendicular to the axis of the specimen using saw cut-off machine. *Figure 3.5 a* is a 3-D illustration for the push-off specimen and *Figure 3.5 b* shows a schematic illustration for the shear plane.

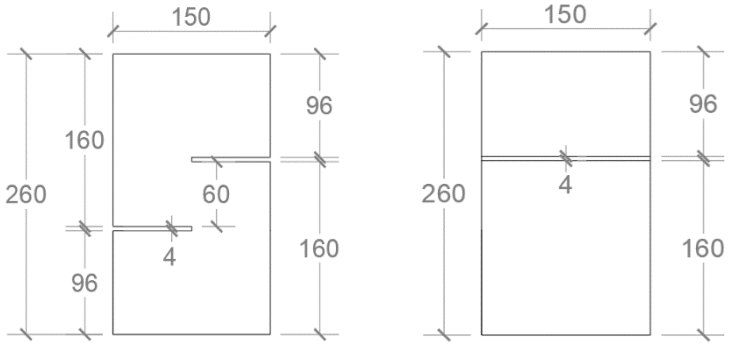

a) b)

Figure 3.4: Schematic illustration for the dimensions adopted, a) dimensions of the front view, and b) dimensions of the side view

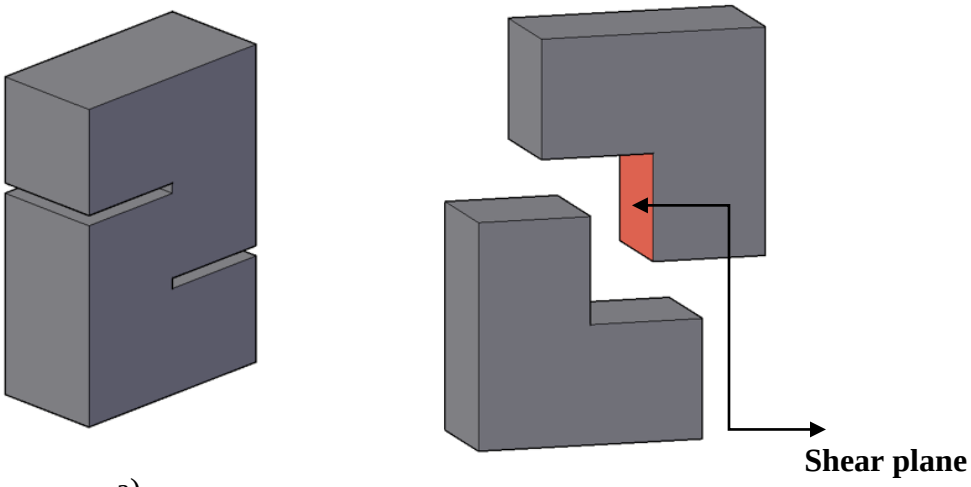

a) b)

Figure 3.5: A 3-D illustration for the push-off model, a) general view, and b) a view showing the shear plane of the specimen

3.4.2 Elevated temperatures

After 7-days of curing, specimens were stored at laboratory conditions until 28 days before loading tests. Specimens were exposed to heating regime using an electric oven (*Fig. 3.6 a*). Five maximum degrees of temperature are chosen. Once the oven temperature reaches the target max temperature, this temperature is kept the same for two hours. Afterward, specimen is taken out to be air cooled for 24-48 hours (*Fig. 3.7*), before loading test using INSTRON. The specimens were heated slowly according to the ISO-834 Standard fire curve (*Fig. 3.6 b*). Two thermocouples were installed in the specimen surface and 50 mm deep, respectively. Readings of thermocouples should be taken manually each 5 minutes. Specimens were kept in a steel cage during heating to protect the oven from explosive spalling (*Fig. 3.6 a*).

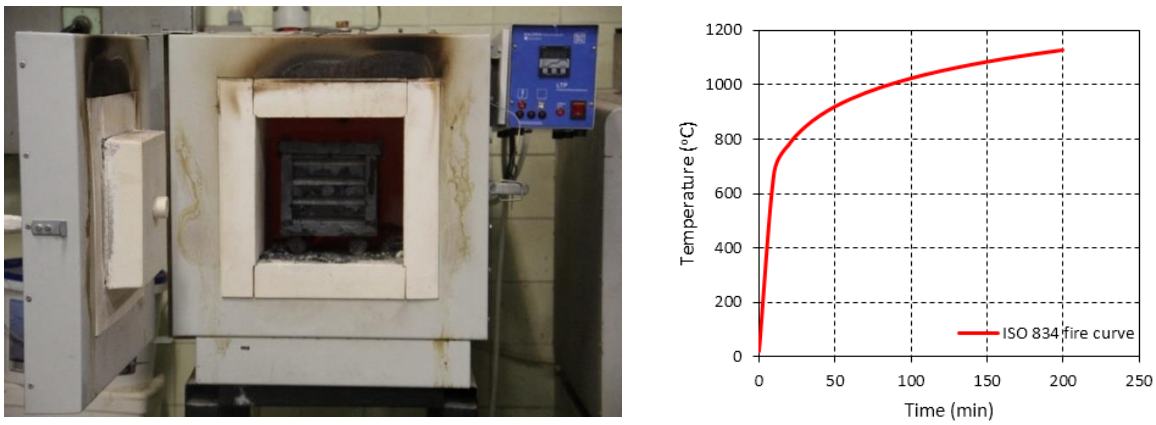

a) b)

Figure 3.6: Heating procedures, a) an electric oven showing the specimen covered by steel cage and two thermocouples and b) ISO-834 Standard fire curve

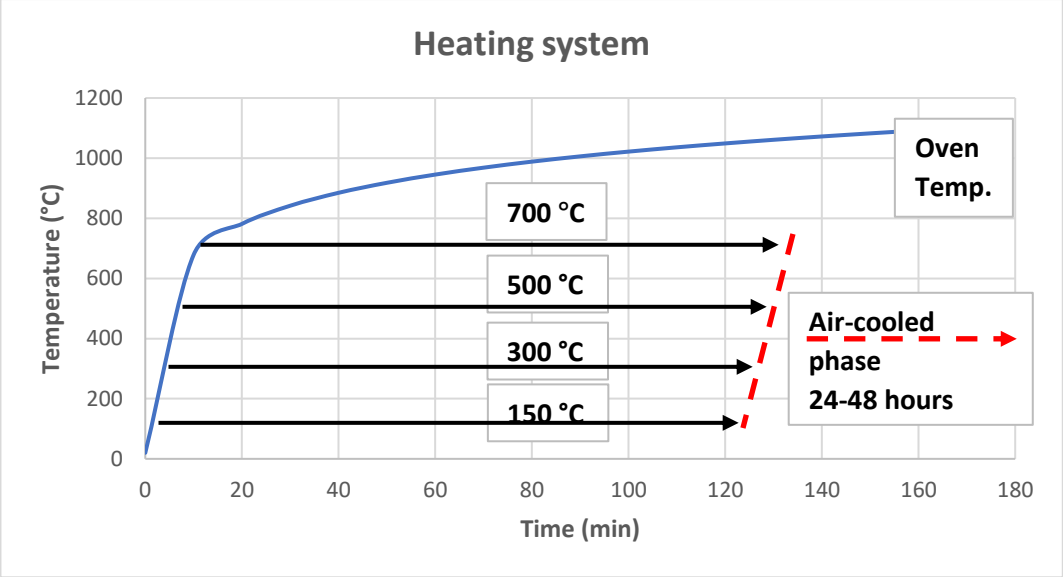

Figure 3.7: Heating regime for all levels of elevated temperatures

3.4.3 Deformations (crack slip, crack width)

Generally speaking, addition of steel fibres is found to improve the cracking behaviour. The inclusion of steel fibres decreases both the deformations of cracks at both directions, in which a greater reduction of the values of crack deformations has been noticed if steel fibres with a higher aspect ratio are used (Vandewalle, 2000).

The push-off specimens were tested in a displacement-controlled compression testing machine. Tests were carried out at the cold state 24-48 hours after heating exposure. Tests are carried out for both series; 28-day and one-year old specimens. The push-off test was carried out using INSTRON testing machine with a capacity of 600 kN. The specimens were loaded in their vertical axis with a rate of 0.06 mm/min. Test setup is designed to measure the deformations occurred at the shear surface plane. Two different deformations are investigated, i.e., parallel to load, considered as "**crack slip**" and perpendicular to load, considered as **"crack width".** Displacement values were measured by means of Linear Variable Differential Transformers (LVDTs) (*Fig. 3.8*), fixed horizontally and vertically on both faces of the specimen. Three LVDTs were used with a 10 mm of capacity of measurement. Two vertical LVDTs (*Fig. 3.8 a*) give displacement of the crack slip whereas one horizontal LVDT (*Fig. 3.8 b*) gives the dilatation of the crack width during the loading. At the 28-days specimen tests, LVDTs were fixed to the surface using metal pipe-holder and glue, but for the one-year specimens, LVDTs were fixed to the surface using special-made equipment made from metal (*Fig. 3.8*). The metal equipment is tightened by screws to fit the LVDT whereas hot melt glue rods are used to glue the metals on the concrete surface. All measurements were automatically recorded each half a second using software.

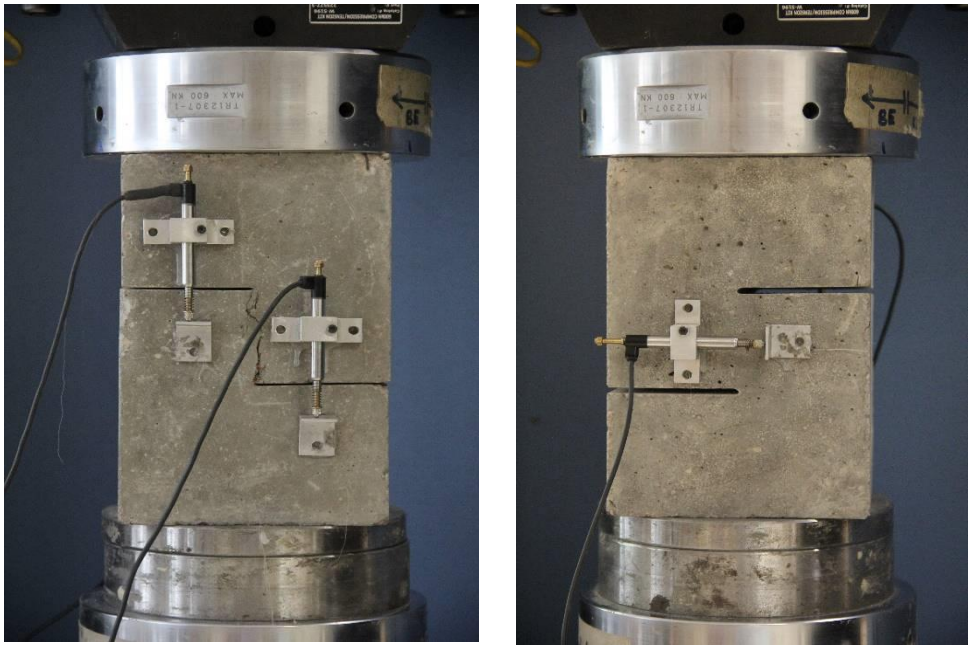

a) b)

Figure 3.8: Push-off loading illustrating a) LVDTs, vertically fixed (crack slip) and b) LVDT, horizontally fixed in middle of specimens (crack width)

3.4.4 Compressive and flexural strengths

In order to obtain a comprehensive understanding thus reasonably interpreting the results, compressive and flexural strength tests are required. Prisms of dimensions 70 x 70 x 250 mm^3 were cast and tested for each series of the mixtures. Each series has three samples. Prisms are designed to provide the results with the flexural strength as well as the compressive strength after exposed to elevated temperatures for all series of the tests. After flexural test (*Fig. 3.9 a*), a compressive test is carried out using the remained parts of the prism (*Fig. 3.9 b*).

a) b)

Figure 3.9: Preparations for compressive and flexural strength tests, a) flexural test and b) compressive strength

4. Results and Discussions

4.1 Physical properties

Concrete is frequently exposed to elevated temperatures either by direct fire or when it is near to furnaces and reactors. The mechanical properties such as strength, modulus of elasticity and volume stability of concrete are significantly affected during these different exposures. Furthermore, numerous changes are considerably occurred by increasing temperatures regarding other properties including chemical compositions or changes on physical structure level of the concrete. Thermal responses, mass losses and spalling are considered herein to be among the physical changes. Further details, results and discussions are addressed at the following sections.

4.1.1 Thermal response

One of the first important steps in design phases, thus protection of the structures, is the prediction of the temperature distribution. Reliable prediction requires sufficient knowledge of the thermal properties of the member or element of the structure. Important thermal properties are usually considered to be thermal conductivity and thermal diffusivity (*See Chapter 2*). Although previous studies confirmed that thermal conductivity of steels is much higher than that of plain concrete or FRP composites (Naser, 2019), no significant effect of steel or polypropylene fibres on thermal conductivity of HPCs in a 20–800 °C temperature range has been reported by other studies (Khaliq and Kodur, 2011b).

Since the equations of abovementioned properties are difficult, if not an intractable task to be solved (*fib*, 2007), it is much easier to experimentally measure than analytically solve. Therefore, the following results are direct measurements for the temperatures in a function of time at two different locations in addition to the oven temperature. Thermocouples were used to measure temperature during heating on two locations: at the surface of the specimen and at 50 mm depth form the surface. Thermocouples indicated the temperature on screen and recorded manually. *Figure 4.1* shows the temperature measurements for the synthetic as well as for the cocktail mixtures for the duration of 180 minutes. The figure shows a slight increase in temperatures in the cocktail mixes compared to polymeric mixes that could be attributed to the fact that cocktail mixes contains steel fibres (which provide conductive behaviour). Previous studies confirmed that with the increase of steel fibre volume fraction, the thermal conductivity and thermal diffusivity increase gradually (Li et al, 2019).

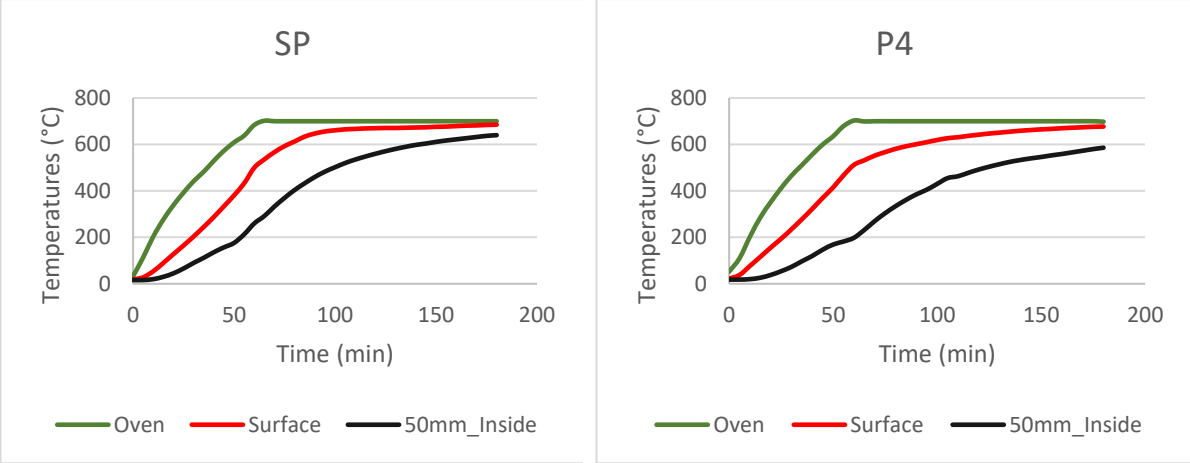

Figure 4.1: Temperatures of different categories of the 28-days push-off specimens in three different places i.e. oven, surface and in-50 mm inside up to 200 minutes

Furthermore, calculations of the area under the temperature-time curve known as fire severity (Serrano et al., 2016) are 91097.5 and 68895 (°C . min) for cocktail mixture and 90097.5 and 60235 (°C . min) for the polymer synthetic mixture, for both measurements, at surface and 50-mm inside, respectively. Previous results show that specimens containing steel fibres have suffered the fire action more intensely than the specimens that do not contain steel fibres. Moreover, presence of fibres was found to increase concrete porosity specially at the case of presence of polypropylene fibres, leading to decrease the pressure in the pores in the deeper concrete areas, and contributing to the confinement of dehydrated paste (Alonso, et al., 2010; Pliya et al., 2011; Ding et al., 2016). Thus, concrix fibres, that have low softening point equals approximately 150 °C, create a series of channels in the concrete mass allowing water vapor to evacuate, then gradually reducing the temperature, and decreasing the cracks in the cooling phase (Toropovs et al., 2005; Serrano et al., 2016).

4.1.2 Mass losses

Mass of the specimen was measured before and after heating. Losses of mass are measured in both ordinary concrete and FRC by increasing temperatures (*EN 1994-1-2:2005*). The mass loss is mainly due to two reasons. The first reason is the evaporation of free water during heating and the second reason is spalling by losing parts or the entire of the concrete surface. Losses of free water as well as physically bound water mainly depend on section size and heating rates. Above the temperature 100 °C, loss of chemically bound water is initiated. The dissociation of calcium hydroxide is followed at about 400-500 °C, and de-carbonation after temperatures reach 600 °C (*fib*, 2007). In general, the mass loss of FRC is more than that of normal concrete at elevated temperatures except for carbonate aggregate concrete (Li et al.,

2019). This result may be due to the larger amount of the free water in the FRC compared to the ordinary concrete. Thus, much more mass loss could be caused by the evaporation of free water. In addition, the melting of the low-melting point fibres in FRC is another reason for the larger mass loss than that of concrete (Li et al., 2019).

At the following sections mass losses, induced by heating and expressed in weight loss and rate of weight loss, are stated in more detail for both results of 28-days and one-year old specimens.

(i) *Results of 28-days specimens*

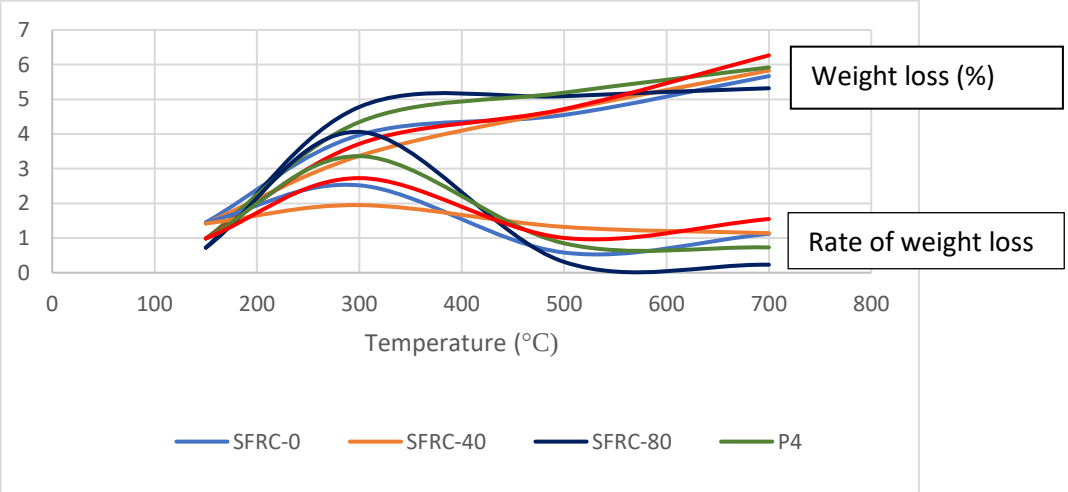

Figure 4.2: Losses in mass of the 28-days old push-off specimens

Generally speaking, maximum rate of weight losses is between 200-400 °C for all mixes. Similar results were reported in previous studies (Memon et al, 2019). Since water to cement ratio was the same for all mixes, i.e., 38 %, there was no significant differences between categories except for the mix SFRC-40. Furthermore, amount of mass losses for the specimens that contain synthetic fibres is above than mass losses occurred in cocktail specimens up to 600 °C. Content of synthetic fibres with high ratio increase the loss of mass due to its low melting point then evaporating at relatively high temperatures. Same results were confirmed by studies (Li et al., 2019). Above 600 °C the specimens with fibre cocktail start to lose masses more than synthetic ones. This could be due to small pieces of concrete that were spalled from the surface. *Figure 4.2* shows the accumulative percentages of losses in masses as well as rate of weight for all push-off specimens before and after exposed to different levels of temperatures.

(ii) *Results of one-year specimens*

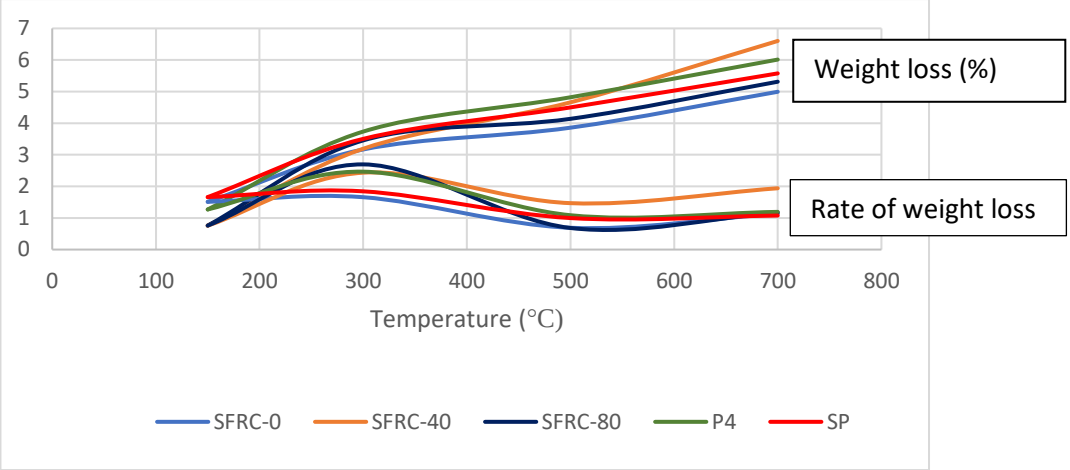

Figure 4.3: Losses in mass of the one-year old push-off specimens

Similarly, losses in mass of the one-year old concrete specimens increase with increasing temperatures. Maximum rate of weight loss is also noticed to be between 20 and 400 °C (*Fig. 4.3*), as noticed in 28-days old specimens. Yet, the losses of the one-year old specimens are lower than counterparts of the 28-days specimens. This is clear since the water content is largely evaporated by time (Neville and Brooks, 2010). For temperatures more than 400 °C, weight loss still continuously increasing due to the decomposition of chemically bounded water from C-S-H gel and Ca $(OH)_2$ (Khoury, 2008).

4.1.3 Visual inspection

(i) Changes of the colour

One of the first, simple and reliable inspections for concrete is colour changes due to high temperatures. Generally, variations in the colour patterns are attributed to the gradual dehydration of the cement paste in addition to transformations occurring to the aggregate (Hager, 2013). By increasing temperatures, the colour of concrete starts to change correspond to specific temperature ranges. Therefore, it is possible to develop the use of colour to determine what maximum temperature a specific element of concrete has been exposed to (Lau and Anson, 2006). *Figure 4.4* shows that concrete shows grey colour for the temperatures below 300 °C. For temperatures above 300 °C, the colour starts to be yellowish grey, whereas for temperatures above 500 °C, concrete colour turns reddish pink.

T 20 °C T 150 °C T 300 °C T 500 °C T 700 °C

Figure 4.4: Surface visualization of heated concrete, including colour changes and surface cracks

(ii) Crack analysis

Generally, there is no significant changes have been observed in terms of surface cracks between plain concrete and FRC. However, insignificant networks of hairline cracks were observed on plain concrete at temperatures below 500 °C whereas hairline cracks were not observed before temperature 500 °C for FRC (Lau and Anson, 2006). This observation could lead to report that presence of steel fibres may delay the spread of cracking. For a maximum temperature of 500 °C, a considerable number of hairline cracks were observed in both plain concrete and FRC, and for a maximum temperature of 700 °C, severe cracking occurs on concrete specimen surfaces for both mixes as well (*See Figure 4.4*).

A possible interpretation is that cracking is initially occurred due to the normal thermal expansion of cement paste causing local breakdowns in bond between the cement and the aggregate. By increasing maximum temperature levels, drying shrinkage eventually becomes much greater than thermal expansion as water is driven off. These two opposing actions progressively producing cracks in concrete (Lea, 1960).

4.1.4 Spalling

High temperatures, in general, cause deterioration in properties such as compressive strength, flexural strength, modulus of elasticity, bond with reinforcement and spalling. Special types of concrete such as HSC or HPC have a tendency towards explosive spalling at high temperatures more than NSC. It is probable that the dense hardened cement paste prevents free water from escaping, causing considerable internal vapor pressure that resulting finally in spalling (Lau and Anson, 2006). Numerous studies indicated that addition of steel fibres in HSC slightly contributes in pore pressure reduction in heated concrete, leading to reduce the possibility of spalling (Kodur, 1998; Mugume and Horiguchi, 2012; Ozawa and Morimoto, 2014). However,

other results of previous studies showed that addition of fibres did not help to reduce the risk of spalling. The explosions were not hindered by adding steel fibres but may delayed to higher temperatures (Hertz, 1992; Hannant, 1978). This conflicting picture may be attributed to the fact that the mechanism of spalling is not yet well understood (Jansson, 2013).

The specimen size also has an influence on the extent of spalling. A review of literature shows that the risk of explosive thermal spalling increases with increasing the specimen size. This is due to the fact that the specimen size is directly related to the length-scales of heat and moisture transport through the structure (prototype), as well as the capacity of larger structures to store more energy. Therefore, careful consideration must be given to the size of the specimens in evaluating spalling performance given that fire tests are often conducted on scaled specimens (Kodur, 2000; Liu et al., 2018).

(i) *Results of 28-days specimens*

SFRC-80-500 (a)

SFRC-80-700 (b)

SFRC-80-700 (c)

Figure 4.5: Total spalling: (a) spalling for SFRC-80-500, (b) spalling for SFRC-80-700, and (c) spalling for prisms of SFRC-80-700

Two push-off specimens were totally spalled at the current study due to elevated temperatures. Both of them were in SFRC-80-28 where the amount of fibres is the highest and the water content is high compared to one-year specimens. One of them was spalled at 500 ºC (*Fig. 4.5 a*), whereas the other one was spalled at 700 ºC (*Fig. 4.5 b*). Furthermore, the three prisms of SFRC-80 were totally spalled at 700 ºC as well (*Fig. 3.4 c*). A possible interpretation for the spalling could be attributed to the ununiform randomly distribution of the fibres in which excessive amounts are combined together, parallel to the surface of concrete forming what is

called “haystack” (*Fig. 4.5*). Thus, these excessive amounts could decrease the cross-section layers of the concrete surfaces leading to decrease the tensile strength of the concrete.

Figure 4.6: Partial spalling for some of the cocktail specimens (28-days old) at 700 ºC.

Results also showed that no explosive spalling has been observed in mixtures contain concrix or cocktail fibres. Same results were confirmed regarding polymeric fibres (Kodur and Lie, 1997; Bilodeau et al., 1998) and cocktail fibres (Dong, 2008). However, considerable surface cracks or partial spalling were observed on some specimens (*Fig. 4.6*). The possible reason for this finding is by the fact that polymeric fibres are usually melted at a relatively low temperature of approximately 150°C, creating “channels” for the steam pressure in concrete to escape, and thus prevent spalling of the concrete (Kodur, 2000). However, shortcomings of polypropylene fibres are inevitable (Jansson, 2013). After fire, an extra porosity equal to the volume of the added fibres is present where the fibres have been combusted. There is hence a risk that the long-term durability is reduced after relatively small fires when the fibres melt away (Hannant, 1978). This is an issue which has still not been resolved (Jansson, 2013).

(ii) *<u>One-year old results</u>*

Regarding one-year old specimens, where water content is less compared to 28-days specimens, only partial spalling was observed (*Fig. 4.7*). This observation is in accordance with the moisture content influence. In which the higher the moisture content, the greater is the spalling risk, especially when the moisture content exceeds a threshold limit (Mindeguia et al., 2009; Liu et al., 2018). Finally, the partial spalled specimens were found to be only from mixes that contain steel fibres and exposed to 700 °C.

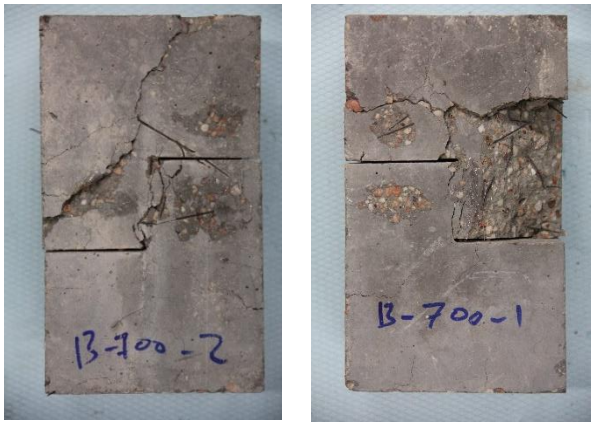

Figure 4.7: Partial spalling for one-year old specimens

4.2 Mechanical properties

Strength of concrete is commonly considered to be its most valuable property. It usually gives an overall picture of the quality of concrete since it is directly related to the structure of cement paste (Neville, 1995). Several mechanical properties are investigated at the current study. Yet, the main mechanical property that is widely and thoroughly investigated is the shear strength test. In addition to that, compressive and flexural-tensile strengths tests are investigated. All processes and phases of the tests were carried out at the Laboratory of Department of Construction Materials and Technologies at BME Budapest, Hungary. The following sections conclude the results of the abovementioned tests.

4.2.1 Compressive strength

As mentioned in the literature (*See Chapter 2*), a gab in knowledge is still present in terms of influence of steel fibres on compressive strength since different results were confirmed (Casanova and Rossi, 1997; Balendran et al., 2002; Holschemacher et al, 2010; Alani, and Aboutalebi, 2013; Moghadam and Izadifard, 2019). The difference between the results can be related to several factors such as the experimental conditions, the cure condition of the specimen (dry or saturated state) and the heating rate (Pliya et al., 2011). Similarly, results regarding polypropylene fibres are also contradictory. Several studies confirmed a decrease of residual strength due to expansion channels and porosity induced by low melting point of the fibres (Noumowe, 2005; Suhaendi and Horiguchi, 2006). Yet, other studies reported the improvement of the residual strength (Xiao and Falkner, 2006; Behnood and Ghandehari, 2009).

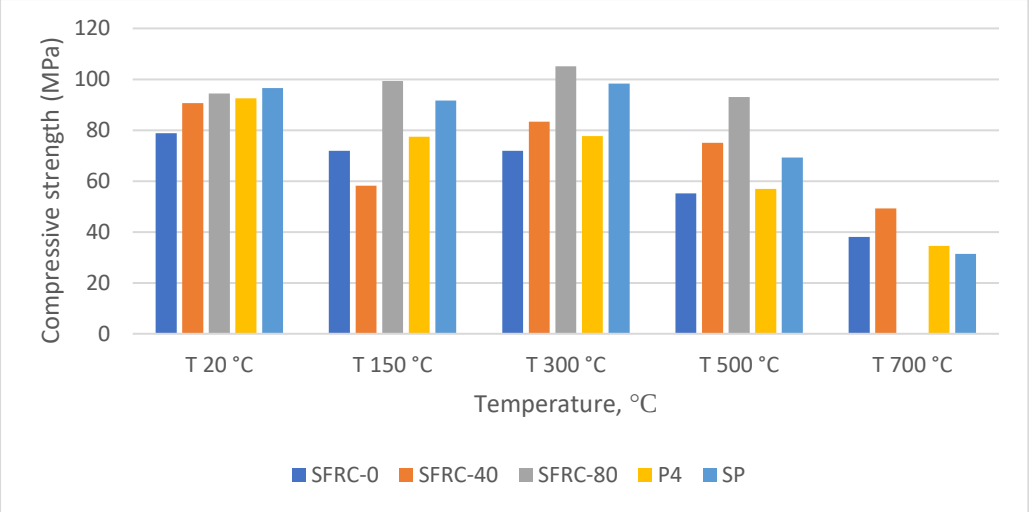

Figure 4.8: Average values of the compressive strength test at 28-days

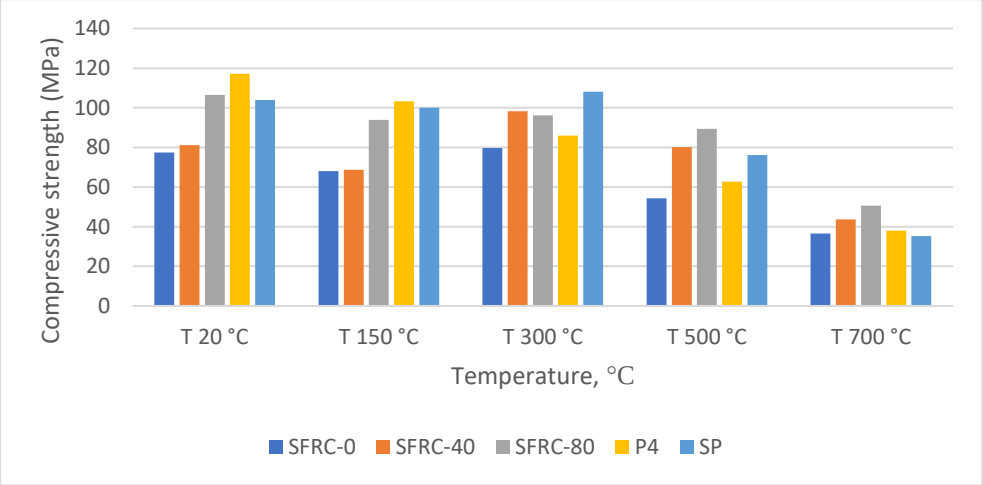

Figure 4.9: Average values of the compressive strength tests at one year old

At the current experiments, compressive strength values were obtained by testing cubes obtained from the remained parts of the prisms 70 x 70 x 150 mm sides, using compressive testing machine. Results are considered as the average of three samples. Generally, presence of fibres enhances the compression capacity of the mix regardless the type of the fibres yet, presence of steel fibre has more influence than the pp fibres. By increasing the level of temperature, the compressive strength values generally decrease (*Fig. 4.8 and 4.9*). The loss in strength is attributed to the decomposition of calcium hydroxide. A further drop in strength was observed by increasing temperatures due to calcination of limestone aggregates and total deterioration of the concrete (Chan et al., 1999; Rasiah, 2012). Some mixes showed a slight increase at temperature 300 °C due to the un-hydrated cement (Moghadam and Izadifard, 2019). The reason for the increase of strength could be attributed to the stiffening of the cement gel and the increase of surface forces between cement gel layers which is a result of the removal

of water from concrete and cement layers contraction (Moghadam and Izadifard, 2019). Finally, the effect of temperature on decreasing the strength is less significant in case of SFRC than for plain concrete.

4.2.2 Flexural strength

Generally, flexural strength is proportionally developed by fibre content (Kovacs and Balazs, 2004). Improvements are more obvious in case of steel fibres than pp fibres (Dong et al., 2008). Similar to the compressive strength reviewed in the previous section, flexural strength of concrete decreases with increasing temperatures (Ma et al., 2015). However, this decrease is less significant in case of steel fibres than for pp fibres (Lau and Anson, 2006).

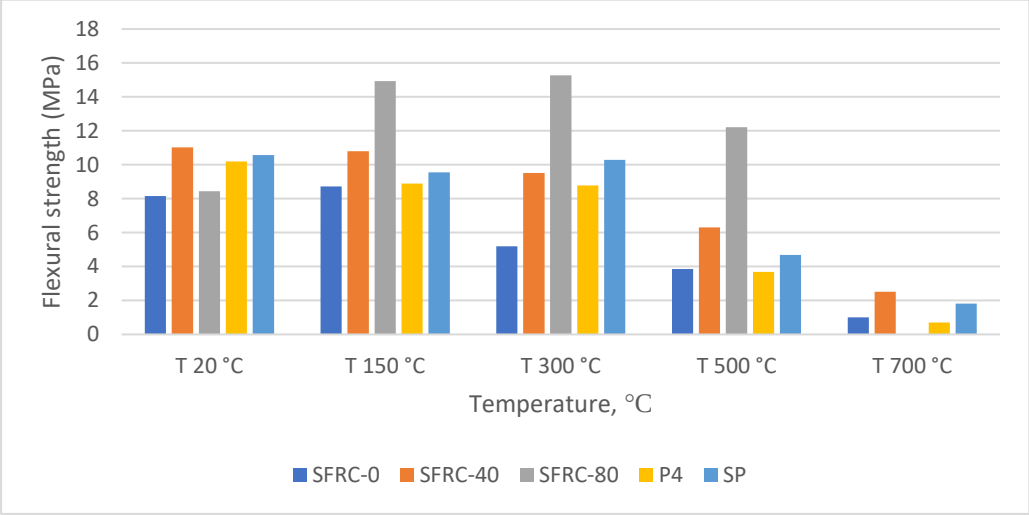

Figure 4.10: Average values of the flexural strength tests at 28-days

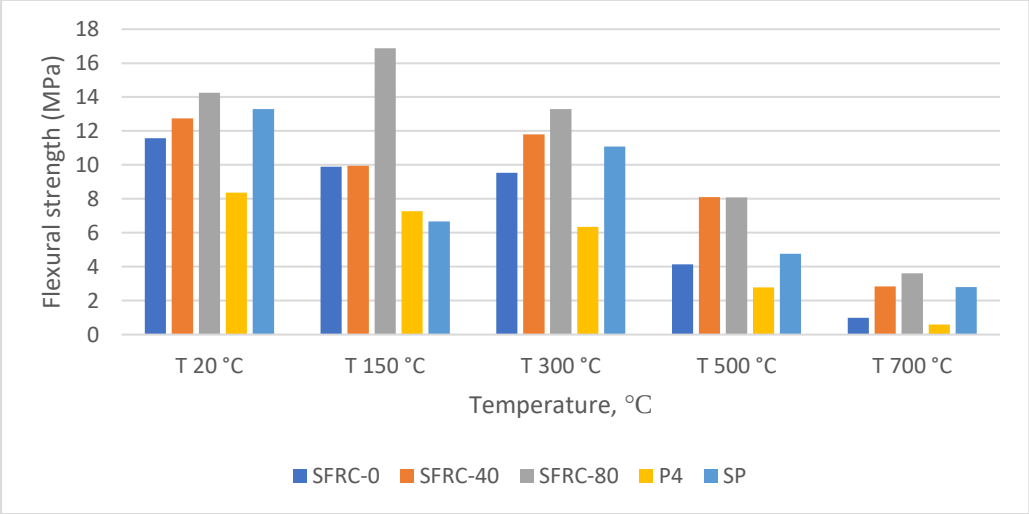

Figure 4.11: Average values of the flexural strength tests at one year old

At the current study, flexural strength is measured by a derivation of the beam equation $\sigma = Mc/I$. Where $\sigma_{fl} = \frac{3PL}{2bd^2}$

In which σ_{fl} = computed flexural stress at failure in MPa. *P* is load at failure (in N). *L* is span length (mm). *b* is width of beam (mm). *d* is depth of beam (mm). Results showed an increase in strength by increasing the fibres content at ambient temperature. Yet, by increasing the temperatures the strengths start to decline for all mixes. This decrease is more significant in case of plain concrete (*Fig. 4.10 and 4.11*), as reported by previous studies mentioned above. The plain concrete kept residual strength values higher than concrete containing the pp fibres after exposed to elevated temperatures. This result is clear by understanding the low melting point of the fibres causing high porosity volume. Another observation from the results is that flexural strength values of P4 (contains only pp fibres) for one-year old specimens are lower than the values of the counterparts for 28-days. This notice could be attributed to the decay or degradation behaviour for the polypropylene fibres (Joseph et al., 2002).

4.2.3 Shear strength

Several studies confirmed significant improvements in shear strength obtained by using FRC at ambient temperatures (Casanova, et al., 1997; Lim and Oh; 1999; Choi KK, et al., 2007; Cuenca and Serna, 2013). Although a few numbers of studies have been carried out at elevated temperatures regarding shear, results confirmed that improvements are gained using fibres as well (Savva, et al., 2005; Qasim and Ahmed, 2019). By increasing temperatures, the mechanical capacities of concrete including shear are significantly decreased, yet less significantly for specimens including steel fibres (Pliya, et al., 2011; Ding, et al., 2012).

At the current study, nominal shear strength has been calculated from the equation $\tau_u = P_u / A_c$ using INSTRON testing machine. P_u is the peak load and A_c is the shear plane area. Shear planes have two dimensions, the horizontal one with fixed 150 mm and the vertical one (*See Figures 3.4 and 3.5*). The vertical ones were varied from 55 to 65 mm due to the manual cutting control, thus it has been taken into consideration during calculations. For specimens that contain fibres, each specimen has been also cut across the shear plane after test, and all fibres that appear on the surface of the shear plane were counted (*Figures 4.16 and 4.18*). This is important for understanding if the scattering in values of the residual strength is governed by fibres distribution in the shear cross-section area or not. Some studies have used the same technique to interpret the data using suitable statistical means (Soroushian and Lee, 1990;

Colombo et al, 2010). Finally, ratio of steel fibres is calculated from the number of steel fibres divided by the related shear area.

Results for 28-days specimens

Shear strength values are generally inversely proportional to the temperatures (*Table 4.1*). However, the strength, particularly in plain concrete, increases when the temperatures are increased from 20 to both 150 and 300 ºC (*Fig. 4.12*). That does not occur in the case of FRC. The interpretation can be explained as in concrete which has no fibres, the strength is totally based on concrete properties. Consequently, a slight increase in temperatures would activate the un-hydrate cement (Lankard et al, 1971). Whereas in concrete contains fibres, contribution of concrete is less thus, existence of fibres plays an important role in the strength. From another hand, higher temperatures (above 500 °C herein) significantly decrease the shear strength of the concrete, yet less significantly for specimens including fibres. Similar results are reported (Pliya, et al., 2011; Ding, et al., 2012). Further details and discussions are presented in the section of Summary (Page 68).

Table 4.1 Average values of shear strength tests

Specimen's ID	Results of 28-days tests	
	Peak load, P_u (KN)	Shear strength, τ_u (MPa)
SFRC-0-20	51.5	6.0
SFRC-0-150	84.2	10.2
SFRC-0-300	72.1	8.7
SFRC-0-500	43.3	5.3
SFRC-0-700	20.6	3.8
SFRC-40-20	114.9	13.9
SFRC-40-150	75.9	9.2
SFRC-40-300	69.2	8.4
SFRC-40-500	72.1	8.7
SFRC-40-700	26.9	3.2
SFRC-80-20	113.7	13.8
SFRC-80-150	96.1	11.7
SFRC-80-300	78.6	9.5

SFRC-80-500	71.4	8.7
SFRC-80-700	57.6	5.8
P4-20	66.1	7.4
P4-150	40.5	4.6
P4-300	49.9	5.7
P4-500	31.4	3.5
P4-700	18.9	2.1
SP-20	89.7	10.3
SP-150	82.6	9.9
SP-300	106.7	12.2
SP-500	76.6	8.7
SP-700	36.9	4.4

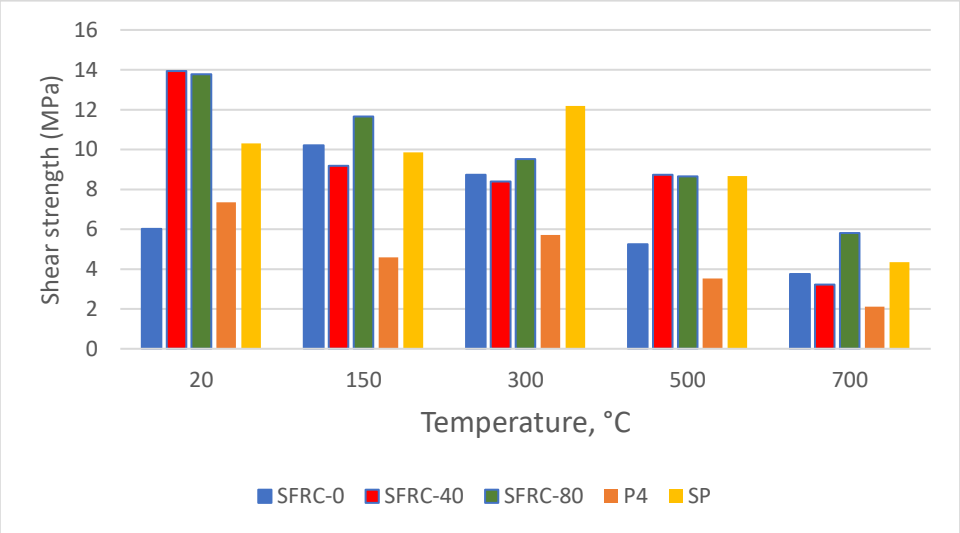

Figure 4.12: Shear strength test results at 28-days

Results for one-year old specimens

I. Concrete with no-fibres

Table 4.2 and *Figure 4.14* show the load peak and the shear strength for each specimen of the plain concrete mixture. The results showed that shear strength is developed by about 6% when specimen is exposed to 150 °C, reported similarly in case of HSC by previous studies (Xiao et al., 2014). However, by increasing temperatures, the shear strengths start to sharply decrease.

Reductions of strength for specimens that exposed to temperatures 300, 500 and 700 °C, are 44.6, 51.3 and 65.9%, respectively. No significant changes are observed in terms of inter-changes in the shear surface plane (*Fig. 4.13*).

Table 4.2 Detailed data of shear property for SFRC-0-365

Specimen	Load peak kN	Shear area mm^2	Shear strength MPa	Number of steel fibres	Ratio of steel fibres (%)	Average shear strength MPa
SFRC-0-20 -1 SFRC-0-20 -2 SFRC-0-20 -3	62.4 92.5 93.5	9000 8700 8700	6.9 10.6 10.7	---	---	9.4
SFRC-0-150 -1 SFRC-0-150 -2 SFRC-0-150 -3	89.4 113.9 61.6	9000 9000 8250	9.9 12.7 7.5	---	---	10.0
SFRC-0-300 -1 SFRC-0-300 -2 SFRC-0-300 -3	51.4 30.9 59.0	9000 9000 9000	5.7 3.4 6.6	---	---	5.2
SFRC-0-500 -1 SFRC-0-500 -2	21.9 56.0	8250 8550	2.7 6.6	---	---	4.6
SFRC-0-700 -1 SFRC-0-700 -2	32.4 23.9	8550 9000	3.8 2.7	---	---	3.2

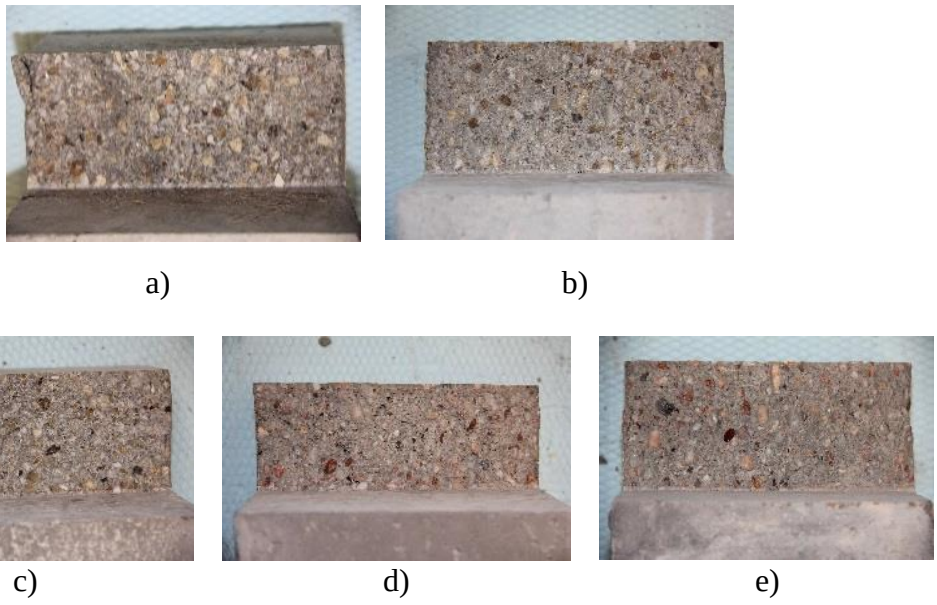

Figure 4.13: Shear plane surface for SFRC-0-365 at temperatures a) 20, b) 150, c) 300, d) 500 and e) 700 °C

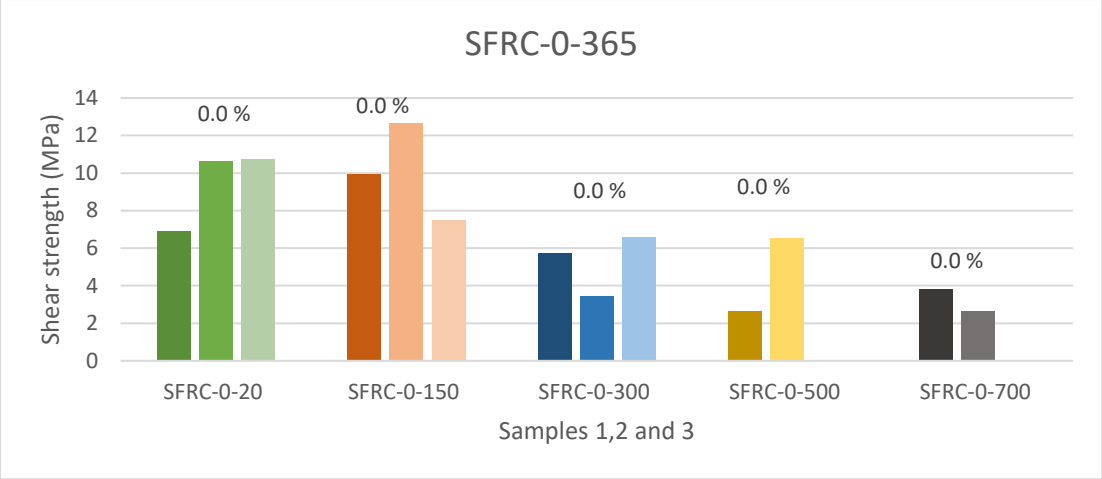

Figure 4.14: Shear strength values for the three plain concrete samples at different levels of temperatures indicating ratio of the steel fibres (top of the bar) across each shear plane

II. Concrete with 40 kg/m^3 fibres

Table 4.3 and *Figure 4.16* show the load peak and the shear strength for each specimen of the SFRC with 40 kg/m^3 of steel fibres. Results showed that adding fibres generally increases the shear strength compared to the plain concrete by about 31, 56, 86, 92 and 81% at temperatures 20, 150, 300, 500 and 700 °C, respectively. This is clear observation to indicate the significant influence of the steel fibres in improving shear capacity at high temperatures. The results also showed that the shear strength is developed at temperature 150 °C to reach about 26% compared to strength at ambient temperature. However, by increasing temperature more than 150 °C, a reduction of shear strength is noticed to be about 21.4, 28.5 and 53% for temperatures 300, 500 and 700 °C, respectively. No significant changes are observed in terms of inter-changes in the shear surface plane, except changing the colour (*Fig. 4.15*) (*See Section 4.1.3*).

Table 4.3 Detailed data of shear property for SFRC-40-365

Specimen	Load peak kN	Shear area mm^2	Shear strength MPa	Number of steel fibres	Ratio of steel fibres (%)	Average shear strength MPa
SFRC-40-20 -1	86.5	8700	9.9	33	0.4	12.4
SFRC-40-20 -2	103.8	9000	11.5	38	0.4	
SFRC-40-20 -3	119.1	9000	13.2	35	0.4	
SFRC-40-150 -1	155.0	9000	17.2	31	0.3	15.6
SFRC-40-150 -2	173.6	9000	19.3	40	0.4	
SFRC-40-150 -3	98.3	9450	10.4	33	0.4	
SFRC-40-300 -1	55.7	9450	5.9	32	0.3	9.7
SFRC-40-300 -2	120.4	8400	14.3	42	0.5	
SFRC-40-300 -3	75.6	8400	9.0	40	0.5	

SFRC-40-500 -1 SFRC-40-500 -2 SFRC-40-500 -3	129.9 43.4 48.2	8250 8400 8550	15.7 5.2 5.6	52 31 33	0.6 0.4 0.4	8.9
SFRC-40-700 -1 SFRC-40-700 -2 SFRC-40-700 -3	33.3 78.4 37.9	7800 9000 8400	4.3 8.7 4.5	30 44 35	0.4 0.5 0.4	5.8

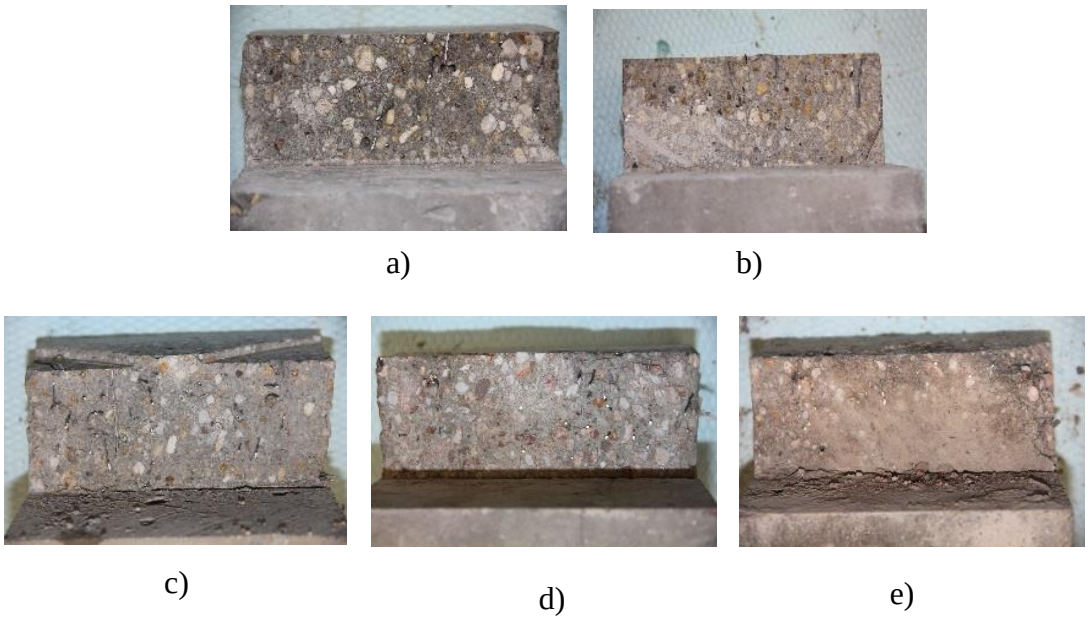

Figure 4.15: Shear plane surface for SFRC-40-365 at temperatures a) 20, b) 150, c) 300, d) 500 and e) 700 °C

In addition, the ratio of the steel fibres has a significant influence on the shear strength values as shown in *Fig. 4.16.* Since the distribution of the fibres was random, the number of the steel fibres in the same-amount mixes is not fixed. However, most of the samples showed relatively close ratio of the steel fibres distributed over shear area planes. Statistically, the standard deviation of the distribution is 5.8 N/mm^2 while the mean is 36.6 N/mm^2 (COV = 16%). The contribution of steel fibres in increasing the shear strength is obtained by the virtue of bonding behaviour of the steel fibres and bridging the cracks openings as well (Echegaray Oviedo, 2014; Cuenca et al., 2015).

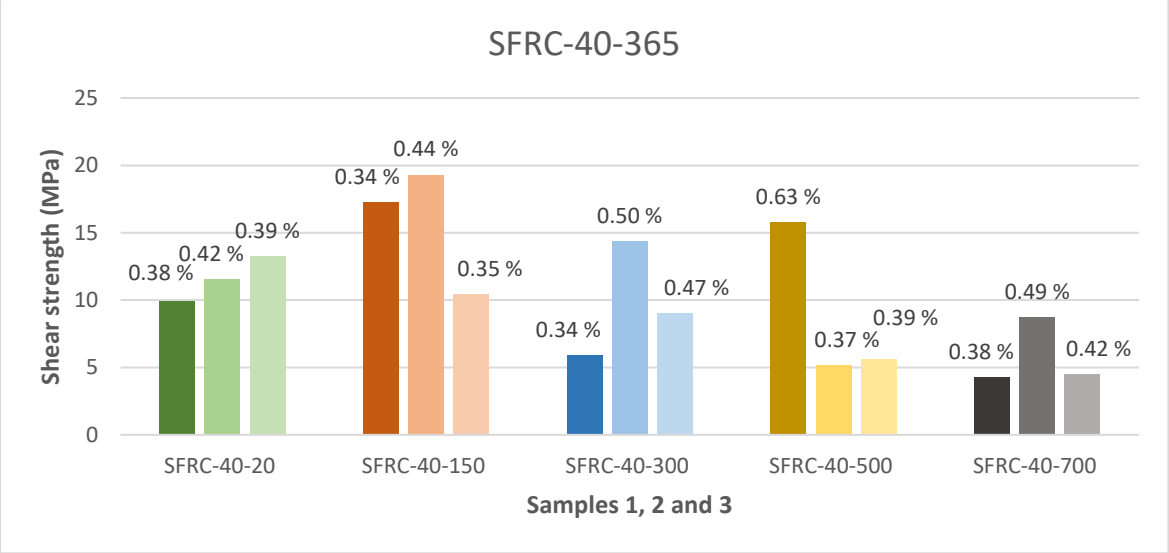

Figure 4.16: Shear strength values for the three concrete samples (40 kg/m^3) at different levels of temperatures indicating ratio of the steel fibres (top of the bar) across each shear plane

III. Concrete with 80 kg/m^3 fibres

Table 4.4 and *Figure 4.18* show the load peak and the shear strength for each specimen of the SFRC with 80 kg/m^3 of steel fibres. Results showed that adding fibres generally increases the shear strength compared to the plain concrete by about 54.4, 29, 141.7, 110 and 78 %, at temperatures 20, 150, 300, 500 and 700 °C, respectively. The results showed that shear strength has slight development at temperature 150 °C, similarly to both mixes, i.e., plain concrete and SFRC with 40 kg/m^3, yet the highest shear strength value is related to the ambient temperature rather than at 150 °C. This could be attributed to the influence of steel fibres content in which for a relatively high content of fibres, the strength is more governed by fibres than by concrete.

Table 4.4 Detailed data of shear property for SFRC-80-365

Specimen	Load peak kN	Shear area mm^2	Shear strength MPa	Number of steel fibres	Ratio of steel fibres (%)	Average shear strength MPa
SFRC-80-20 -1	124.1	8550	14.5	73	0.9	14.6
SFRC-80-20 -2	133.3	9000	14.8	79	0.9	
SFRC-80-20 -3	129.4	9000	14.4	61	0.7	
SFRC-80-150 -1	121.6	8700	13.9	73	0.8	12.9
SFRC-80-150 -2	131.5	9000	14.6	66	0.7	
SFRC-80-150 -3	84.0	8250	10.2	65	0.8	
SFRC-80-300 -1	149.1	9000	16.6	71	0.8	12.6
SFRC-80-300 -2	142.2	9000	15.8	67	0.7	
SFRC-80-300 -3	50.0	9000	5.6	35	0.4	

SFRC-80-500 -1 SFRC-80-500 -2 SFRC-80-500 -3	101.1 54.2 89.1	8700 8700 7950	11.6 6.2 11.2	69 54 64	0.8 0.6 0.8	9.7
SFRC-80-700 -1 SFRC-80-700 -2 SFRC-80-700 -3	48.1 65.2 38.5	8700 9000 8700	5.5 7.2 4.4	55 70 56	0.6 0.8 0.6	5.7

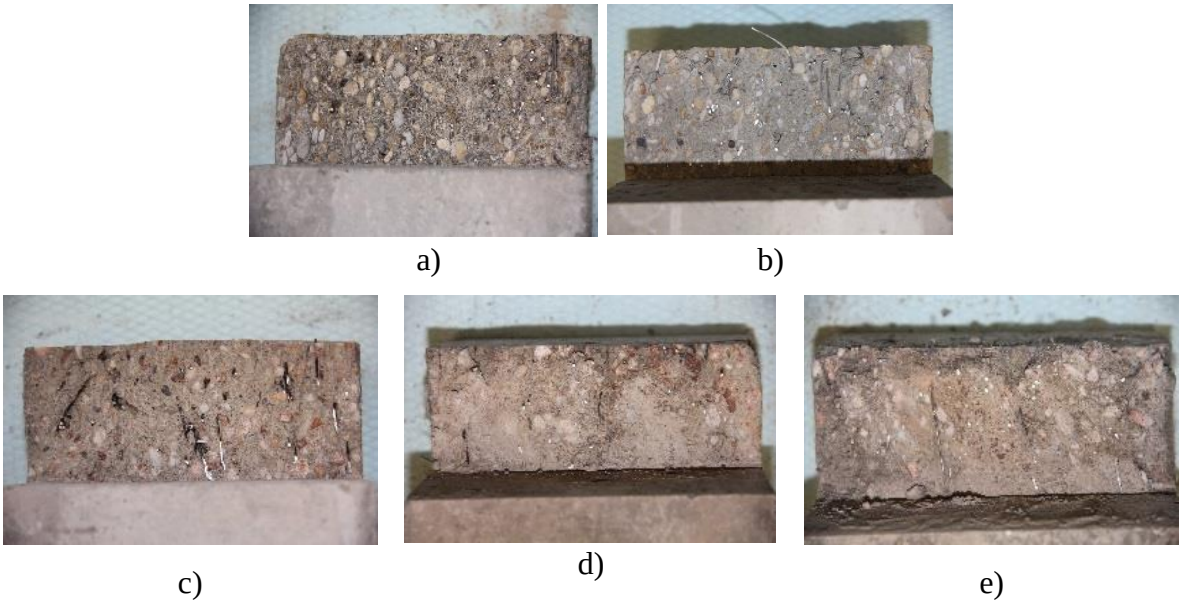

Figure 4.17: Shear plane surface for SFRC-80-365 at temperatures a) 20, b) 150, c) 300, d) 500 and e) 700 °C

By increasing temperature, a reduction of the shear strength is noticed to be about 11, 13, 33.5 and 60.6% for temperatures 150, 300, 500 and 700 °C, respectively. No significant changes are observed in terms of inter-changes in the shear surface plane, except changing the colour (*Fig. 4.17*) (*See Section 4.1.3*). Ratio of the steel fibres has significant influence on shear strength values as shown in *Fig. 4.18*. Since the distribution of the fibres was random distribution, number of the steel fibres in the same-amount mixes is not fixed. For instance, SFRC-80-300 has 79 and 74% of fibres ratio for the first two samples whereas for the third sample the ratio is 39% (almost the half) resulting in a sharp decrease in strength. Statistically, the standard deviation of the distribution is 10.3 while the mean is 63.9 (COV = 16%). However, most of the samples showed relatively close ratios of the steel fibres distributed across shear area planes (*Fig. 4.18*).

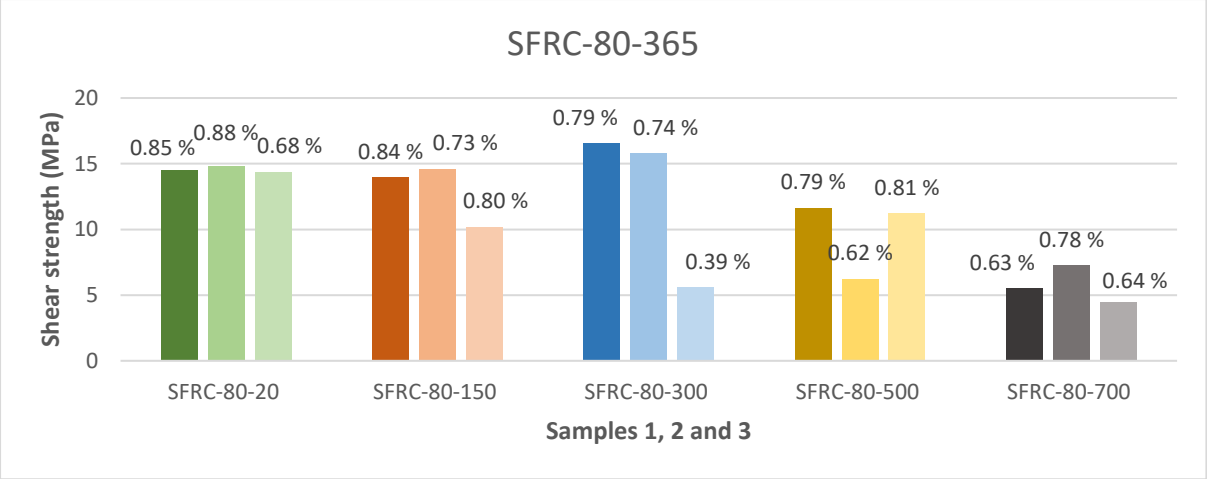

Figure 4.18: Shear strength values for the three concrete samples (80 kg/m^3) at different levels of temperatures indicating ratio of the steel fibres (top of the bar) across each shear plane

IV. Concrete with 4 kg/m^3 synthetic fibres as well as cocktail fibre concrete

Unlike the specimens that contain steel fibres, it is hard for the specimens containing pp fibres to visually count the fibres, especially after exposed to elevated temperatures when fibres are totally melted, as shown in *Fig. 4.20*. Therefore, the last two series that contain pp fibres, i.e., P4 and SP are separately presented herein, yet as averages of three samples as well.

Table 4.5 Average values of one-year old shear strength tests of pp and cocktail fibre mixes

Specimen	Load peak kN	Shear area mm^2	Average shear strength, MPa
P4_20	80.75	8500	9.5
P4_150	77.9	9400	8.2
P4_300	69.3	8950	7.7
P4_500	34.6	9050	3.8
P4_700	19.8	9000	2.2
SP_20	146.2	9750	15.0
SP _150	86.3	9300	9.3
SP _300	90.4	9000	10.0
SP _500	82.1	11625	7.1
SP _700	36.12	8850	4.1

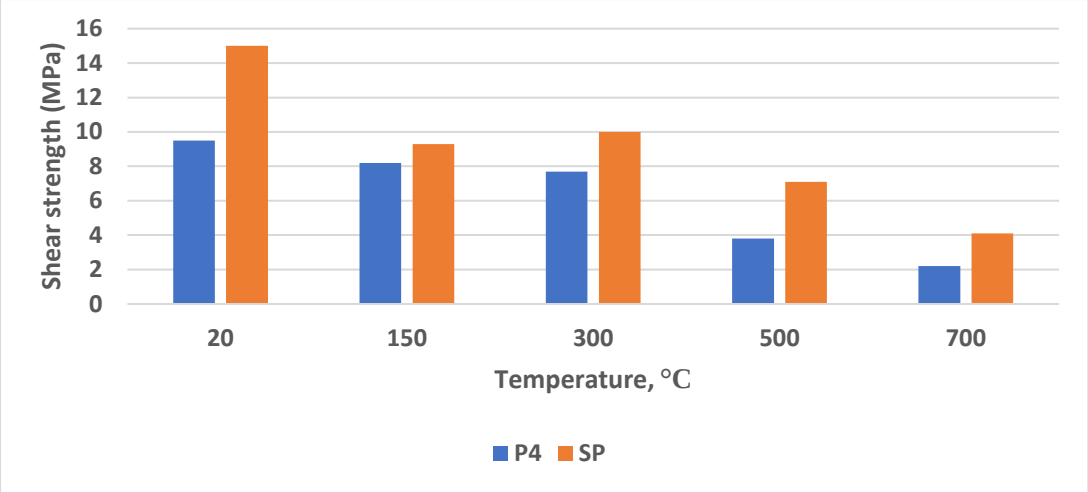

Figure 4.19: Shear strength values for the one-year old specimens of P4 and SP mixes

Table 4.5 and Figure 4.19 show averages of the shear strength values for the one-year old specimens of the P4 and SP. The results showed that shear, at ambient temperature, is significantly influenced by the fibres type. In which the specimens containing cocktail fibres show higher values than specimens containing only pp fibres. The increase is measured to be about 57.9% in shear strength at temperature 20 °C. However, this ratio is significantly increased at high temperatures to reach 85.5% at temperature 700 °C. The last notice could be clear evidence of the negative impact induced by the presence of pp fibres only on the shear strength of concrete at high temperatures which was reported by several studies as mentioned before in the literature.

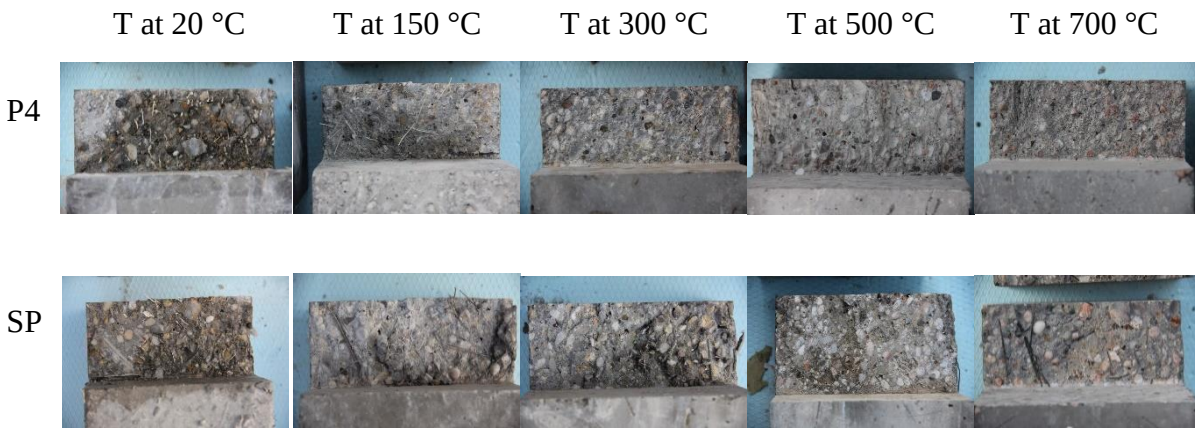

Figure 4.20: Shear plane surface for P4 and SP one-year specimens at different max temperatures

Summary of the results for all mixes

Figure 4.21 summarizes the average values of the shear strength tests for all mixes. Generally, presence of the fibres develops the capacity of concrete mixes in terms of shear investigations. Increasing temperatures, particularly above 300 °C, significantly decrease the shear capacity of the concrete. Mixes that contain fibres, especially steel fibres, have less decline in shear capacity when temperatures are elevated. This general note is valid for both 28-days and one-year old mixes. However, specimens tested at the age of one-year have generally higher shear strength values than those that tested at 28-days. A few numbers of specimens do not follow the latter notice (*Fig. 4.21*).

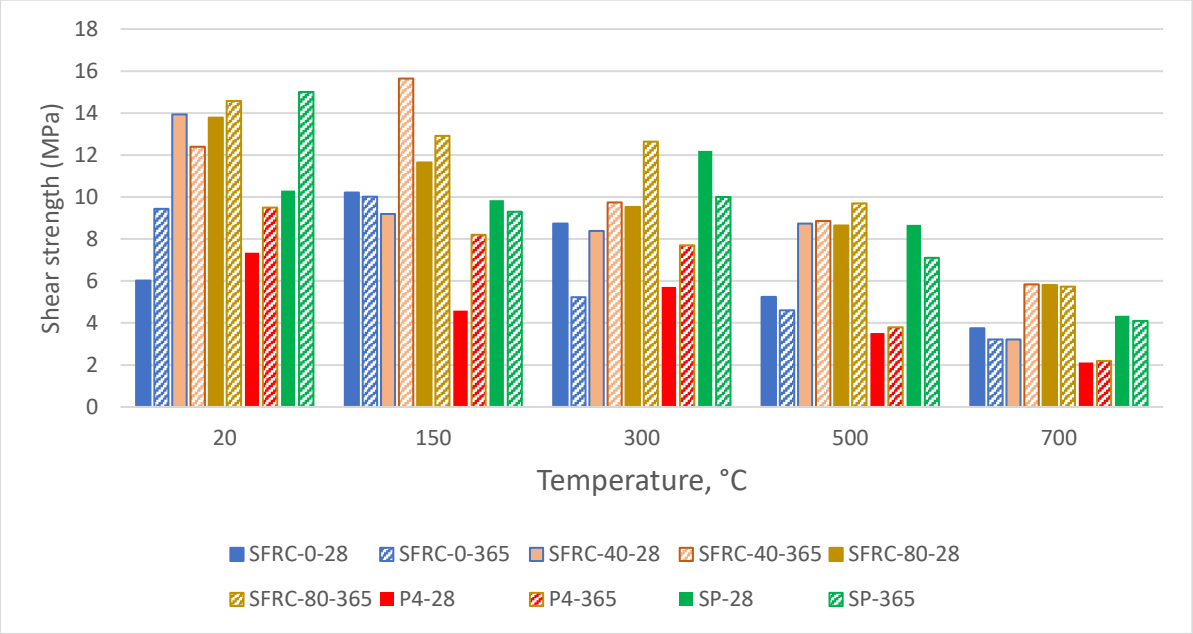

Figure 4.21: A complete summary of the average values of the shear strength tests

Regarding specimens of 28-days, results showed that shear strength is significantly developed using fibres at ambient temperature by about 131.4, 128.9, 22.4 and 71.6% for mixes SFRC-40, SFRC-80, P4 and SP, respectively (*See Figure 4.22*). This is showing the significant impact of steel fibre particularly compared to the pp fibres. Although presence of pp fibres contributes to increase the shear strength at ambient temperature (about 22 %), still much lower than the impact of using the steel fibres (about 130%). Additionally, there is almost no difference in improvement between 40 kg/m^3 and 80 kg/m^3 at ambient temperature. As the temperatures increase, significant decrease is noticed. At temperature 700 °C, a reduction in the relative residual shear strength is calculated to be about 37.7, 76.9, 57.8, 71.5 and 57.7 % for mixes SFRC-0, SFRC-40, SFRC-80, P4 and SP compared to the counterpart mixes at ambient temperature, respectively (*See Figure 4.22*). This is showing that at high temperatures, using

40 kg/m^3 has been more influenced (decreased) than using 80 kg/m3, unlike the case of ambient temperatures. Additionally, adding pp fibres to the steel fibres (producing hybrid or cocktail fibres) provide more enhancement at elevated temperatures compared to mixes with pp only.

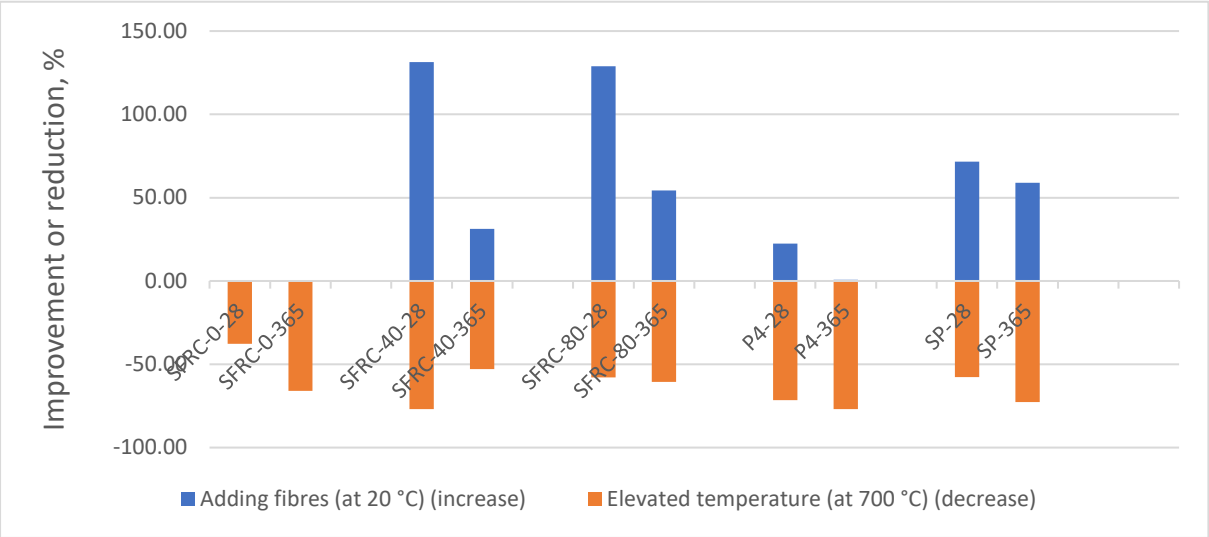

Figure 4.22: Summary of the improvements obtained by adding fibres and reductions obtained by elevated temperatures

On the other hand, results of one-year old specimens showed that shear strength is significantly developed using fibres at ambient temperature except for pp fibres where the influence was negligible. The increase obtained by adding fibres at ambient temperature is approximately 0.6, 58.9, 31.3, and 54.3 % for mixes P4, SP, SFRC-40 and SFRC-80, respectively (*See Figure 4.22*). As the temperatures increase, significant decrease is noticed. At temperature 700 °C, a reduction in the relative residual shear strength is calculated to be about 65.9, 53.0, 60.7, 76.8 and 72.6% for mixes SFRC-0, SFRC-40, SFRC-80, P4 and SP compared to the counterpart mixes at ambient temperature, respectively (*See Figure 4.22*). The previous results showed that mixes containing only pp fibres have the least advantages of all one-year old mixes, in which it has negligible increase at ambient temperature and the highest decrease at elevated temperatures. Mixes containing cocktail fibres have significant increase at ambient temperatures yet significant decrease at elevated temperatures as well. This could be attributed to the disadvantage of the presence of the pp fibres.

4.2.4 Shear stress - crack deformations curves

The stress shear-crack slip and crack width curves are presented herein. Crack deformations are relative movement that shear faces in both directions; parallel to the load and perpendicular to the load. parallel deformation is considered as *crack slip* whereas the horizontal dilation of

the crack is considered as *crack width*. As described in Chapter 3, two vertical LVDTs were used to measure the crack slip and one horizontal LVDT for the crack width. Thus, for all the following figures, the average of the two vertical values of LVDTs is considered. Worth to note that this section contains only curves that are tested at the age of one year.

(I) Results of SFRC-0

Figure 4.23 shows the shear stress – crack deformations curves over five different maximum temperatures. For convenience, measurements of the LVDTs for the same specimen are separately expressed as a function of shear stress values in a form of curve. Thus, three curves are illustrated for each category as there are three samples for each one. Although some scattering for each group exhibits in terms of the peak load, the trends are generally in good agreement with each other in terms of general behaviour and tendency.

The curves also show that ductility is weak in the reference mix which is attributed to the fact that steel fibres content is zero. Based on post-cracking residual strengths, most of the peaks of curves are sharply declined after reaching the peak meaning indicating the softening behaviour. This is also confirmed in mixes have no content of fibres (Model Code 2010). However, this sharpness occurred at the peaks is less when temperatures are increased up to 700 °C (*Fig. 4.23*). Finally, by comparing crack slip with crack width for each category, generally both have similar results as reported by previous studies (Barragan et al, 2006). However, crack width has generally more stiffness than crack slip for the same specimen. This is attributed to the natural weakness of the concrete in tension specially when no conventional reinforcement or fibres are exist, whereas in crack slip the concept of aggregate interlock as well as inter-frictional influence due to the roughness of the surface have effects reducing the stiff behaviour. Yet, stiffness is decreased for both crack slip and crack width by increasing the temperatures up to 700 °C (*Fig. 4.23*).

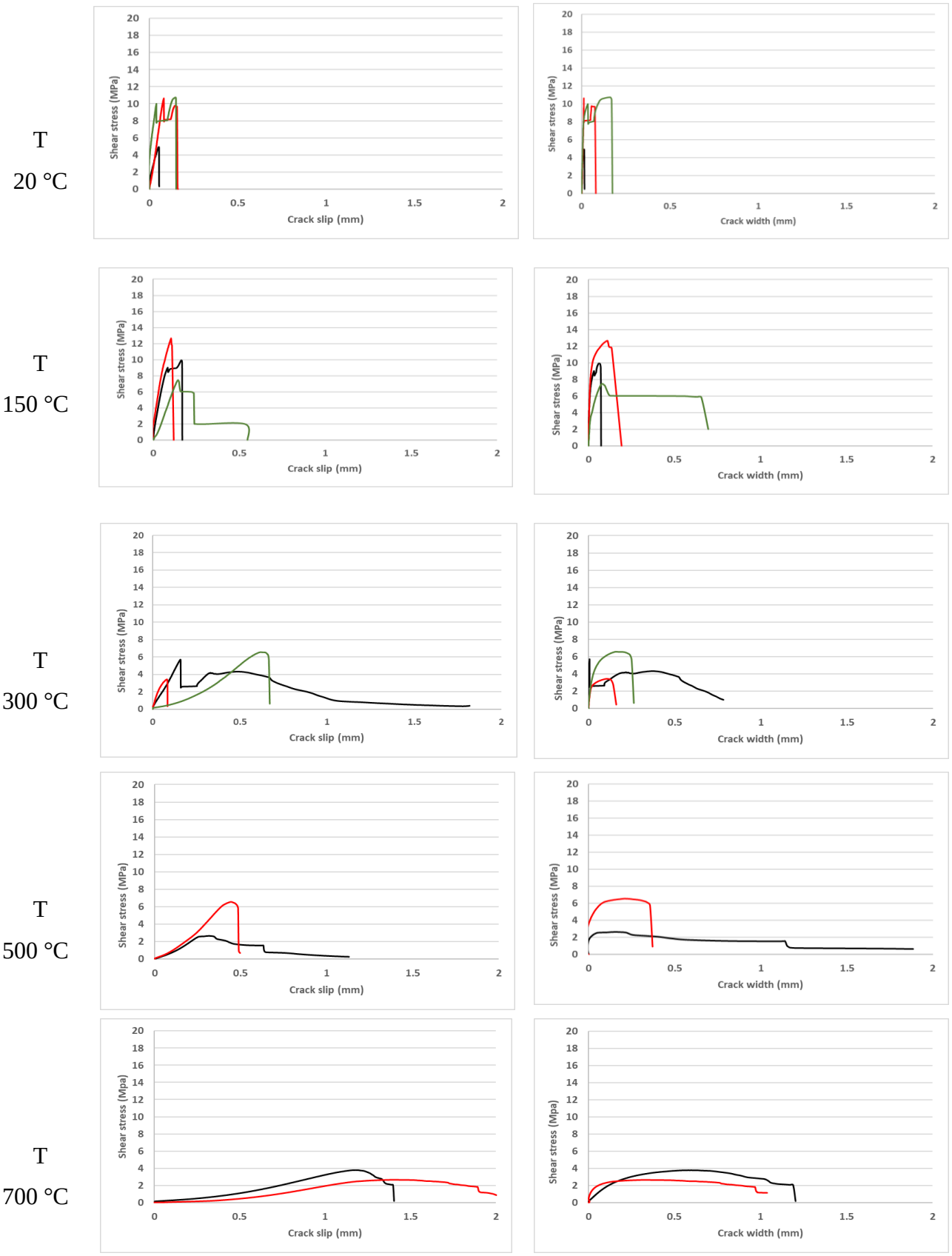

Figure 4.23: Shear stress-crack slip and crack width curves at different levels of elevated temperatures for SFRC-0

Table 4.6 lists the average values of the stiffness for the plain concrete mixes after exposure to different levels of temperatures. The results of stiffness shown in the table were considered at one third (1/3) of the peak stress. The 1/3 approach is adopted from previous researchers as well (Poon et al, 2004; Guo et al., 2014). The results presented in the table below show that values of stiffness for the shear width are higher than values of stiffness for the shear slip at ambient temperature as well as elevated temperatures. By increasing temperatures, the difference is even more. Notwithstanding, by increasing temperatures, shear stiffness in both deformations are decreased. Degradation of concrete stiffness implies that elevated temperature has a significant damage on the stiffness of the concrete in terms of shear.

Table 4.6 Results of crack openings and stiffness of SFRC-0

Results at peaks	Shear strength (MPa)	Slip opening (mm)	Width opening (mm)	Slip at $\frac{1}{3}$Strength (mm)	Width at $\frac{1}{3}$Strength (mm)	Stiffness at slip (MPa)	Stiffness at width (MPa)
SFRC-0-20	9.44	0.093	0.062	0.012	0.004	243.6	674.6
SFRC-0-150	10.02	0.137	0.084	0.031	0.005	106.6	715.8
SFRC-0-300	5.23	0.287	0.092	0.123	0.005	14.1	327.0
SFRC-0-500	4.60	0.380	0.186	0.154	0.012	10.0	133.4
SFRC-0-700	3.22	1.294	0.463	0.619	0.035	1.7	31.1

(II) Results of SFRC-40

Figure 4.24 shows the shear stress – crack deformations curves for the mix SFRC-40 over different elevated temperatures. Scattering for each group is attributed to the ratio of the fibres. For instance, SFRC-40-1 has ratio 63% whereas the other two samples from the same mix, i.e., SFRC-40-2 and SFRC-40-3 have ratio of steel fibres 37 and 39%, respectively (*See Fig. 4.16*). Notwithstanding, scattering is acceptable, and the trends are generally in good agreement with each other in terms of general behaviour and tendency. From another hand, curves show slightly more ductile behaviour compared to the plain concrete. This slight increase is limited to the relatively low amount of fibres content. Similarly, to SFRC-0, by comparing crack slip with crack width for each category, crack width has generally more stiffness than crack slip for the same specimen. This is clear by observing the shifting of the load-peak in accordance with crack width and crack slip. Yet, stiffness is decreased for both crack slip and crack width by increasing the temperatures up to 700 °C (*Fig. 4.24*).

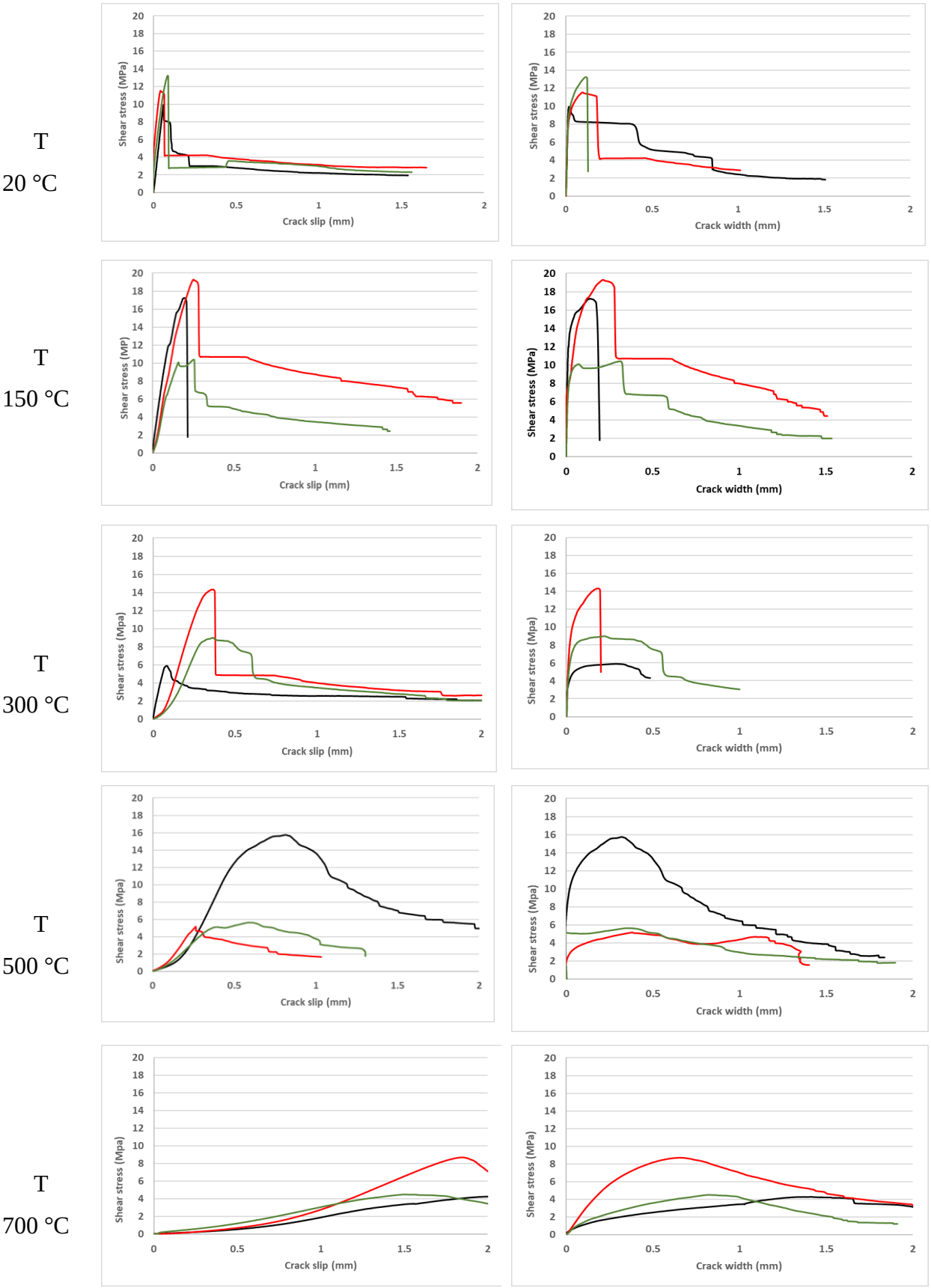

Figure 4.24: Shear stress-crack slip and crack width curves at different levels of elevated temperatures for SFRC-40

Sample 1 ——— Sample 2 ——— Sample 3 ———

Table 4.7 lists the average values of stiffness of the SFRC-40 after exposure to different temperatures. The results of stiffness shown in the table were considered also at one third of the stress peak. The results show that the stiffness of the shear width is higher than stiffness of the shear slip at both ambient and elevated temperatures. Yet, by increasing temperatures, the difference is significantly increased indicating that temperatures affect both stiffness of crack slip and crack width but more significant for the crack slip.

Table 4.7 Results of crack openings and stiffness of SFRC-40

Results at peaks	Shear strength (MPa)	Slip opening (mm)	Width opening (mm)	Slip at $\frac{1}{3}$Strength (mm)	Width at $\frac{1}{3}$Strength (mm)	Stiffness at slip (MPa)	Stiffness at width (MPa)
SFRC-40-20	12.39	0.063	0.078	0.011	0.007	361.6	525.9
SFRC-40-150	15.53	0.202	0.142	0.052	0.004	99.6	1411.9
SFRC-40-300	9.74	0.271	0.233	0.103	0.005	31.4	608.8
SFRC-40-500	8.85	0.555	0.350	0.195	0.003	15.1	983.4
SFRC-40-700	5.82	1.780	0.949	0.821	0.124	2.4	15.7

(III) Results of SFRC-80

Figure 4.25 shows the shear stress – crack deformations curves for the mix SFRC-80 over different levels of elevated temperatures. Scattering for all groups is the least among the three mixes. This is attributed to the uniformed distribution of the fibres on the shear surface planes of the specimens (*See Fig. 4.18).* Moreover, curves show more ductile behaviour compared to the other two mixes, i.e., SFRC-0 and SFRC-40. The general pattern herein is that at the peak load, a crack occurs resulting in limited sharp decline of the curve then, by the virtue of the fibres, residual shear strength keeps values relatively high. Similar to both SFRC-0 and SFRC-40, by comparing crack slip with crack width for each category, values of crack width have generally higher stiffness than the values of crack slip for the same specimens. This is clear by observing the shifting of the load-peak in accordance with crack width and crack slip. Yet, stiffness is decreased for both crack slip and crack width by increasing the temperatures up to 700 °C (*Fig. 4.25).*

T
20 °C

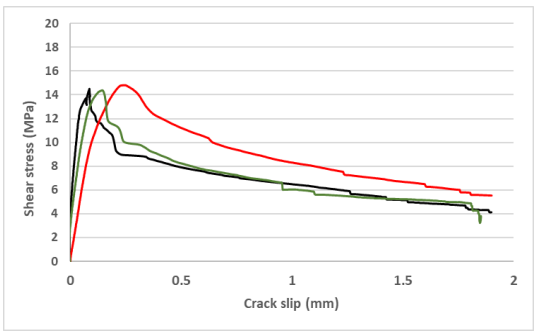

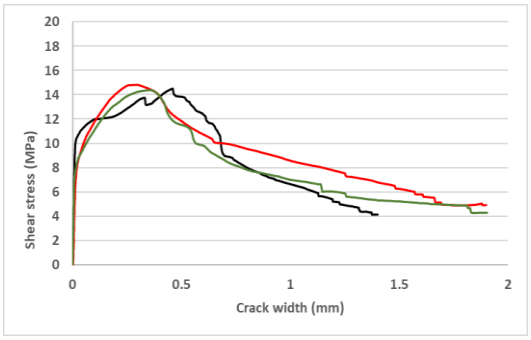

T
150 °C

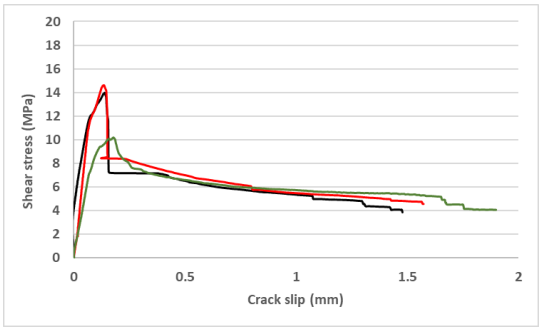

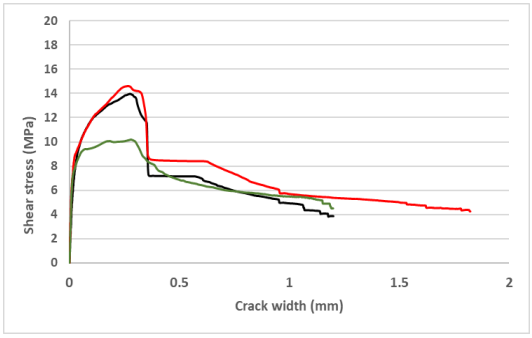

T
300 °C

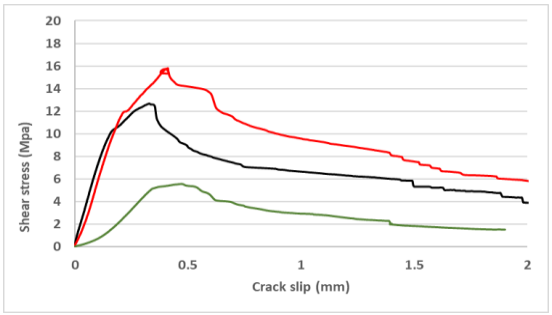

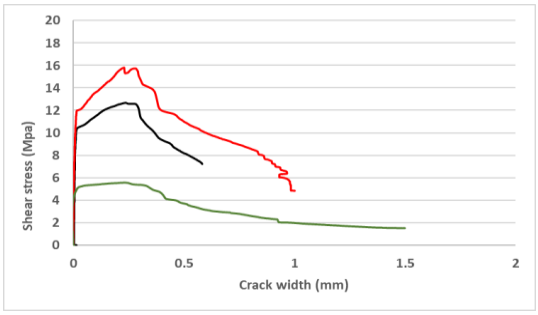

T
500 °C

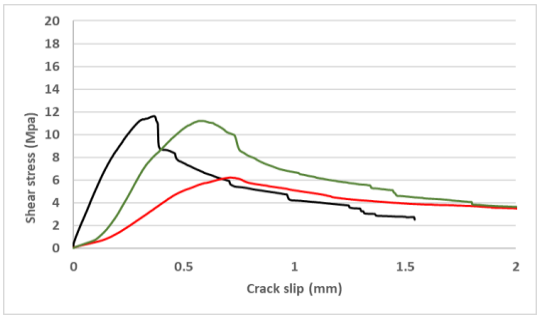

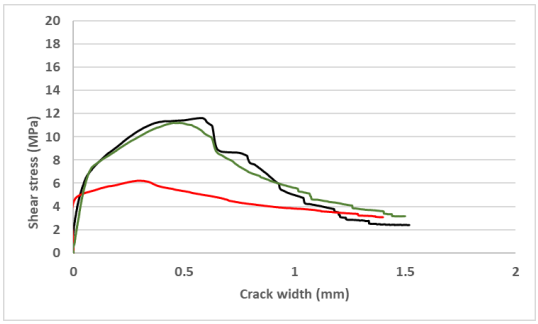

T
700 °C

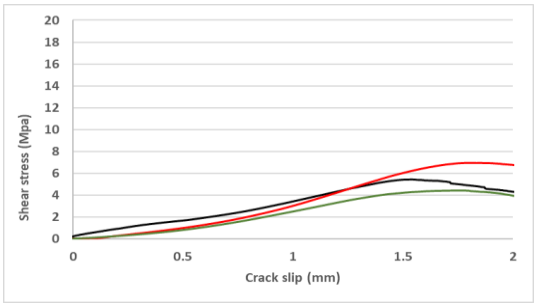

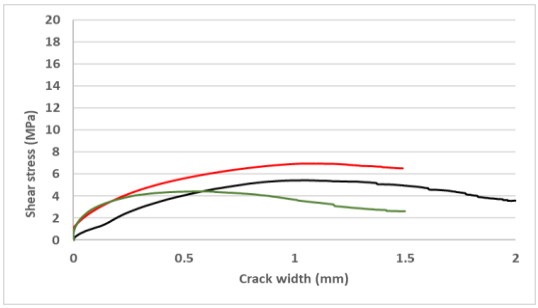

Figure 4.25: Shear stress-crack slip and crack width curves at different levels of elevated temperatures for SFRC-80

Sample 1 Sample 2 Sample 3

Table 4.8 lists the average values of stiffness of the SFRC-80 after exposure to different temperatures. The results of stiffness shown in the table were considered also at one-third of the stress peak. The results show that the shear stiffness of the crack width is larger than stiffness of the crack slip at both ambient and elevated temperature. However, increasing temperatures significantly decreases the shear stiffness in both directions but more significant degradation is noticed in the case of crack slip compared to crack width.

Table 4.8 Results of crack openings and stiffness of SFRC-80

Results at peaks	Shear strength (MPa)	Slip opening (mm)	Width opening (mm)	Slip at $\frac{1}{3}$Strength (mm)	Width at $\frac{1}{3}$Strength (mm)	Stiffness at slip (MPa)	Stiffness at width (MPa)
SFRC-80-20	14.57	0.158	0.369	0.019	0.007	260.2	693.7
SFRC-80-150	12.92	0.151	0.273	0.023	0.008	190.0	538.5
SFRC-80-300	12.64	0.400	0.250	0.109	0.004	34.6	1029.4
SFRC-80-500	9.69	0.547	0.441	0.186	0.017	17.4	189.9
SFRC-80-700	5.70	1.700	0.898	0.713	0.086	2.6	21.7

(IV) Results of P4 and SP

Figure 4.26 illustrates the results of shear stress-crack slip and crack width for two mixes, i.e., polymeric fibres and cocktail fibres exposed to the five levels of maximum temperatures. Results show that before cracking, the elastic stress–strain relation is linear for all levels of maximum temperature except higher ones, i.e., 700 °C. The ratio of the shear stress value to the compressive strength value, when the first crack is initiated, is approximately 10% as shown in *Table 4.9* and *Figure 4.26*. This approximate was similarly reported by previous studies (Jongvivatsakul et al., 2016) whereas other studies reported higher ratio up to 50% (Xiao et al., 2014). After cracking, shear capacity mainly depends on the fibre amount. As a result, the peak shear stress depends on the volume fraction of fibres that are randomly distributed over shear plane. Thus, the crack deformations (crack slip and crack width) induce a tensile stress in the fibres. Creating consequently a clamping force in the concrete across the crack. This concept is similar to that concrete that contains embedded steel bars (Hofbeck et al., 1969). The yield strength of the fibres also decreases after elevated temperatures. When the reinforcement across the crack yields, the limit state is reached, and the shear strength is obtained (Mansur et al., 2008). As a result, the resistance against the deformation of the shear plane decreases after elevated temperatures. Furthermore, at high temperatures the crack deformation occurred

earlier meaning that the initial stiffness degrades. When the temperature exceeds 300 °C, the ultimate shear stress decreases with increasing corresponding crack deformations as well as leads to a more ductile behaviour of the FRC. This is most likely due to the strength degradation resulted from the elevated temperature (Xiao et al., 2014). Similar results were obtained in the literature (Balazs and Lubloy, 2012; Khanlou et al., 2012). Differences between the two series have many impacts in which presence of cocktail fibres increases the ultimate shear stress more than synthetic fibres do. Moreover, cocktail fibres show more ductility than synthetic fibres expressed in the decline part of the curves after peaks. However, this tendency is less significant when temperature is high to be 700 °C. In addition, it is noticed that a few specimens, i.e., at temperature 150 °C showed different behaviours than the counterparts with respect to toughness (*Fig. 4.26)*. The curve showed relatively more toughness (hardening pattern) than other results. This difference could be due to the drawbacks of using random distributions in which excessive amount of fibres could be found across the shear plane. In such technique, congestion of fibres along shear plane that has the chance to be different than shear planes of other samples from the same category, may significantly affect results. More details regarding toughness will be discussed in the next section.

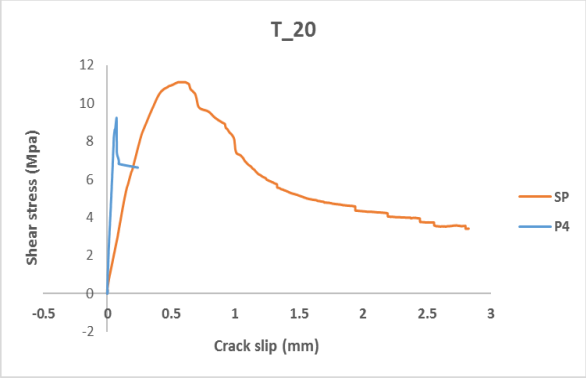

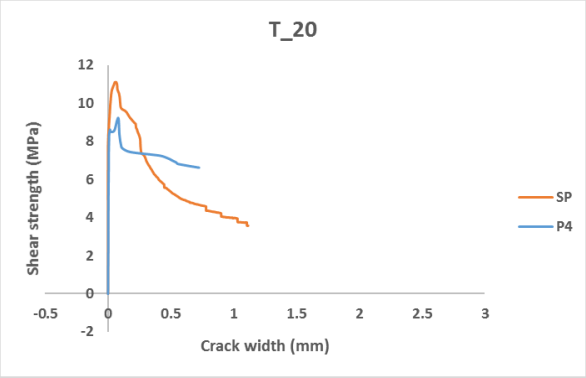

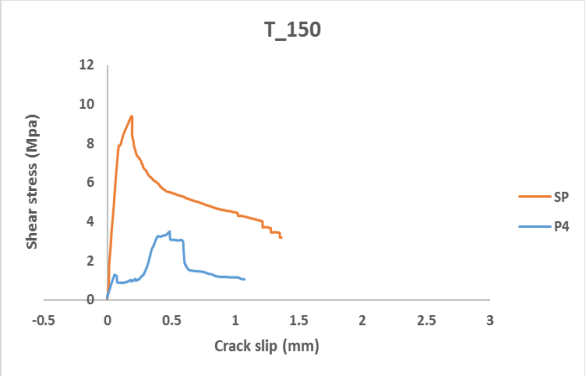

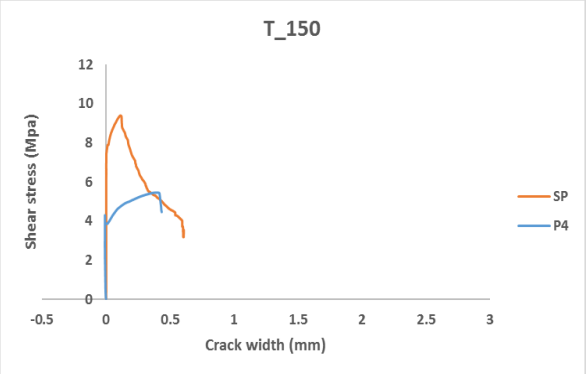

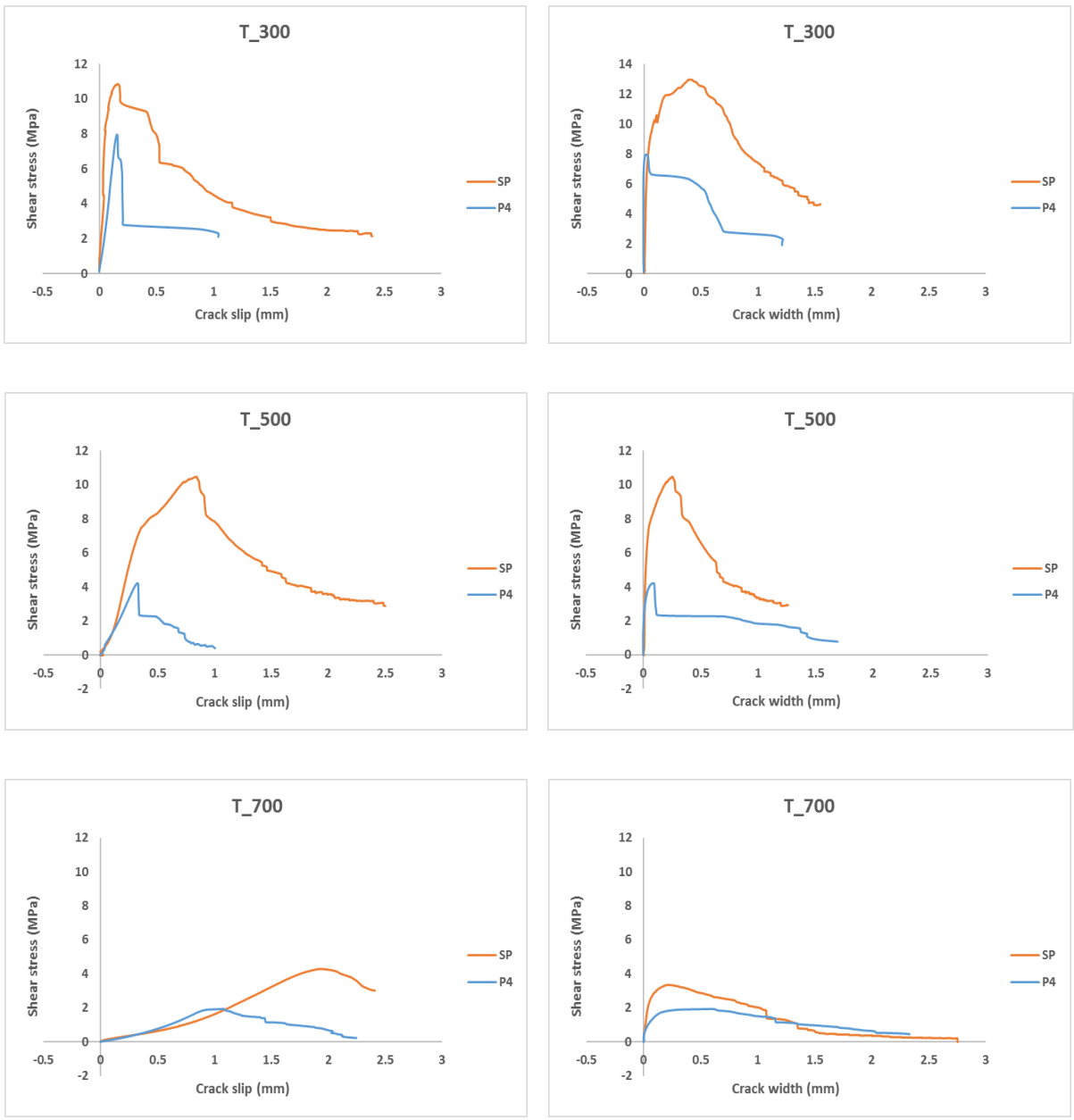

Figure 4.26: Shear stress-crack width and crack slip curves of P4 and SP at different levels of elevated temperatures

In general, results show that for both series values of crack width are nearly zero before first crack initiates whereas values of crack slip are slightly more than zero indicating that stiffness of width is higher than stiffness of slip (Hofbeck et al., 1969; Mattock and Hawkins, 1972). Furthermore, development of the crack width is more sensitive to that of the crack slip. In which, once the cracks occur, the crack width curves will immediately develop with less slopes. Yet, at high maximum temperatures, i.e., 500 or 700 °C, crack width has values higher than zero and crack slip has much higher for both mixes but for SP more obvious. *Table 4.9* lists the average values of stiffness for the P4 and SP mixes after exposure to different temperatures.

Although *Figure 4.26* showed that shear stress-crack deformations curves have approximately linear ascending parts even after elevated temperatures, stiffness magnitudes are still lower. Therefore, stiffness values shown in *Table 4.9* were obtained within one-third approach as well.

Table 4.9 Results of crack openings and stiffness of P4 and SP

Results at peaks	Shear strength (MPa)	Slip opening (mm)	Width opening (mm)	Slip at $\frac{1}{3}$Strength (mm)	Width at $\frac{1}{3}$Strength (mm)	Stiffness at slip (MPa)	Stiffness at width (MPa)
P4-20	7.347	0.148	0.031	0.018	0.002	132.5	1627.1
P4-150	4.591	0.664	0.325	0.165	0.054	9.3	28.6
P4-300	5.707	0.562	0.143	0.122	0.003	15.6	599.8
P4-500	3.515	0.558	0.147	0.169	0.003	6.9	373.2
P4-700	2.109	1.341	0.480	0.475	0.027	1.5	26.5
SP-20	10.307	0.287	0.152	0.036	0.010	96.6	344.2
SP-150	9.013	0.132	0.257	0.020	0.002	153.6	1556.3
SP-300	12.186	0.236	0.321	0.059	0.007	68.6	572.2
SP-500	8.672	0.591	0.435	0.216	0.052	13.4	55.2
SP-700	4.344	1.997	0.499	0.789	0.093	1.8	15.6

Summary of the stiffness results

Results show that crack width is nearly zero before first crack initiates whereas crack slip is slightly more than zero indicating that the shear stiffness of perpendicular-to-load direction is higher than parallel-to-load direction. This observation was confirmed for all types of mixes at all levels of elevated temperatures. Moreover, ratios of the increase of the shear stiffness related to the crack width, to shear stiffness related to the crack slip at ambient temperature were 177, 45, 167, 1128 and 256% for the mixes SFRC-0, SFRC-40, SFRC-80, P4 and SP, respectively.

From another hand, shear stiffness is significantly decreased by increasing temperatures. This notice is valid for all mixes at both crack deformations as well. The relative residual stiffness is calculated through dividing the stiffness value at 700 °C by the stiffness value at 20 °C. The results of the relative residual stiffness for all mixes at both directions are illustrated in Figure 4.27. The figure shows significant decline of the shear stiffness at both directions by increasing temperatures, in which the decreases are higher than 95% for all mixes. Results show also that

the residual shear stiffness for the cocktail fibres mixes has the highest values compared to other mixes. Finally, ratios of the increase of the shear stiffness related to the crack width, to shear stiffness related to the crack slip at elevated temperatures, i.e., 700 °C were 917, 554, 734, 1666 and 766% for the mixes SFRC-0, SFRC-40, SFRC-80, P4 and SP, respectively.

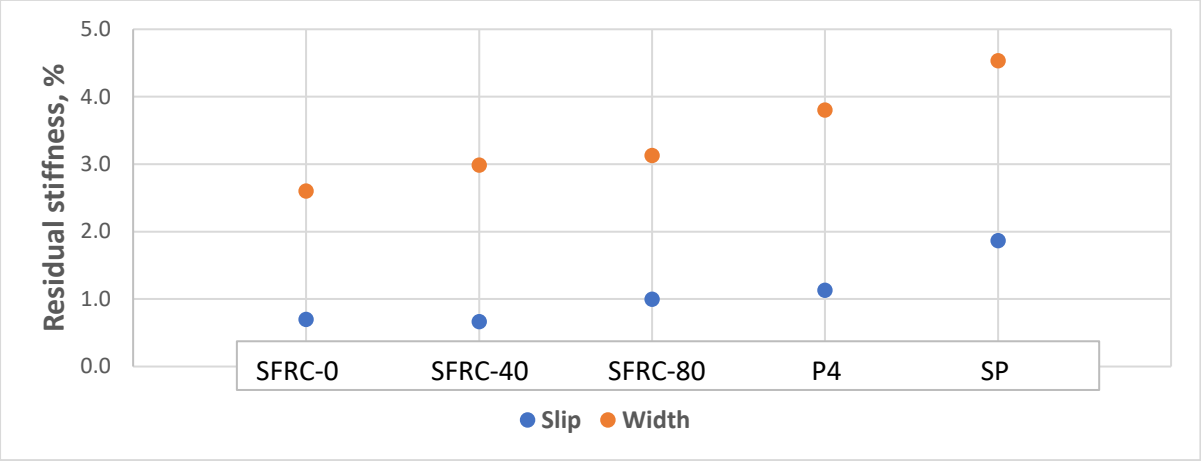

Figure 4.27: Relative residual stiffness of the mixes after exposed to 700 °C

4.2.5 Toughness measurements

Although toughness is generally accepted as a measure of energy absorption capacity of a material, there is still a debate on how it should be measured, interpreted, and used. The method used at the current study is adopted by the *ASTM C 1018*. Further discussions are presented in the state of the art. The method uses levels of deflections presented by toughness indexes, i.e., I_5, I_{10} or I_{30}. These indexes are supposed to (a) provide an indication of the relative toughness at these deflections, and (b) provide information on the approximate shape of the post-cracking load-deflection response (Gopalaratnam, et al., 1991). Moreover, several studies recommended to use indexes higher than I_5, for instance I_{100}, to obtain more accurate of the toughness values since I_5 or I_{10} do not provide a good indication of deflection in the curves, whereas some other researchers argued about the accuracy of results of using this technique (Balaguru et al., 1992). At the current study, toughness index I_5 is calculated as ratio of the area of the load-deflection curve up to deflection of 3 times the first-crack deflection divided by the area of the load-deflection curve up to the first-crack deflection (first-crack toughness), as follow (*See Fig. 2.13*):

$$I_5 = \frac{\text{Area under load}-\text{deflection curve up to } 3\delta}{\text{Area under load}-\text{deflection curve up to } \delta}$$

Where δ is the deformation (mm) at the first crack. Calculations to obtain the first crack depend on approximate evaluations from the curves, in which the first drop in load or reduction of

stiffness (slope) is considered as the first crack. This measurement of the first crack is also adopted by (Balaguru, et al., 1992). Inaccuracies in measuring deflection at first crack results in directly proportional errors in evaluating first-crack toughness, thus different methods are proposed to measure the deflection at the first crack that affect the accuracy of the results (Gopalaratnam et al. 1991). Finally, some studies developed a new method to measure the toughness without using the first crack (Banthia and Trottier, 1995).

Table 4.10 Results of shear toughness indexes at elevated temperatures

Specimens	**Slip-Toughness I_5**	**Width-Toughness I_5**
SFRC-0-20	3.50	3.84
SFRC-0-150	3.18	3.42
SFRC-0-300	3.26	3.02
SFRC-0-500	3.09	3.25
SFRC-0-700	3.04	3.30
SFRC-40-20	3.61	4.42
SFRC-40-150	3.89	4.25
SFRC-40-300	3.65	4.59
SFRC-40-500	3.60	4.29
SFRC-40-700	3.00	3.35
SFRC-80-20	4.31	5.08
SFRC-80-150	4.00	4.01
SFRC-80-300	4.15	4.15
SFRC-80-500	3.49	3.69
SFRC-80-700	3.02	3.17
P4-20	4.09	4.99
P4-150	4.53	4.88
P4-300	3.64	4.68
P4-500	3.24	4.09
P4-700	3.24	4.0
SP-20	4.00	5.02
SP-150	4.75	5.11
SP-300	4.69	5.38

SP-500	3.64	4.10
SP-700	3.57	4.05

At ambient temperature, the results shown in *Table 4.10* show that shear toughness values, indicated by toughness Index I5, is generally increased when the concrete mix contains fibres regardless the type of fibres (Minelli et al., 2014). The relative increases of the shear toughness related to the crack slip due to existence of fibres at the ambient temperatures are 3.1, 23.1, 16.9 and 14.3 % for the mixes SFRC-0, SFRC-40, SFRC-80, P4 and SP, respectively. Whereas relative increases of the shear toughness related to the crack width due to existence of fibres at the ambient temperatures are found to be 15.1, 32.3, 29.9 and 30.7 % for the mixes SFRC-0, SFRC-40, SFRC-80, P4 and SP, respectively. Previous results are shown in *Figure 4.28.*

Figure 4.28: Shear toughness at 20 °C for both directions

Figures 4.29 and *4.30* show the relative shear toughness indexes of the mixes in accordance with the different levels of maximum temperatures. The relative toughness index is calculated by dividing each mix of the FRC by the counterpart mix of the plain concrete at each level of maximum temperature. *Figure 4.29* illustrates the relative shear toughness of the parallel deflection (slip) of the push-off specimens whereas *Figure 4.30* illustrates the relative shear toughness of the perpendicular deflection (width) of the push-off specimens.

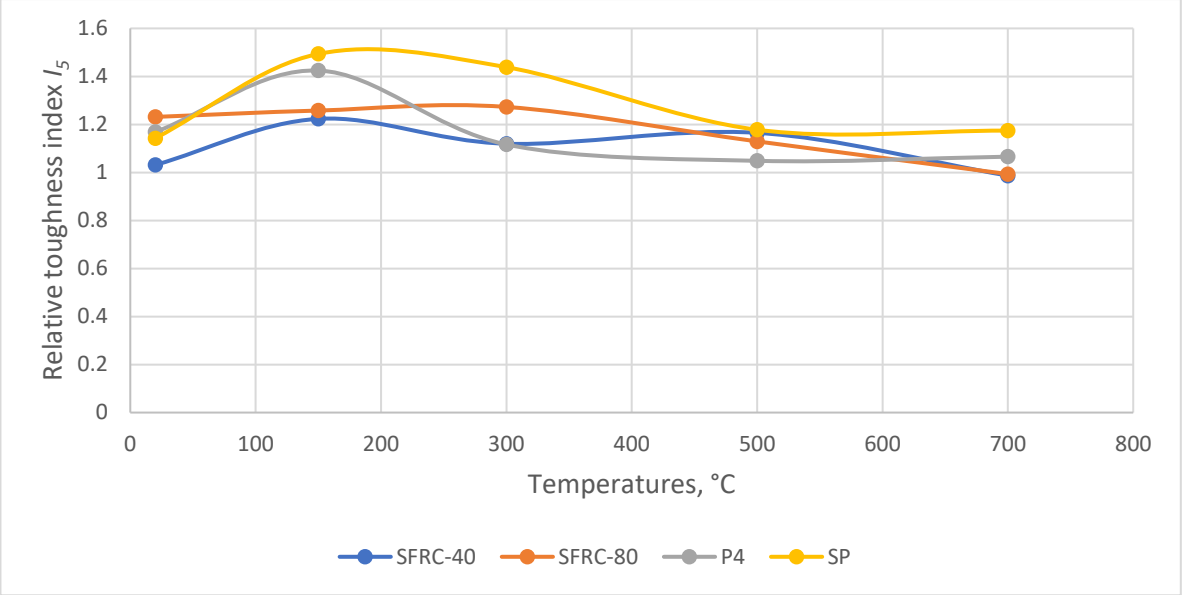

Figure 4.29: Relative shear toughness indexes (I_5) at parallel direction (slip) for mixes at maximum levels of elevated temperatures

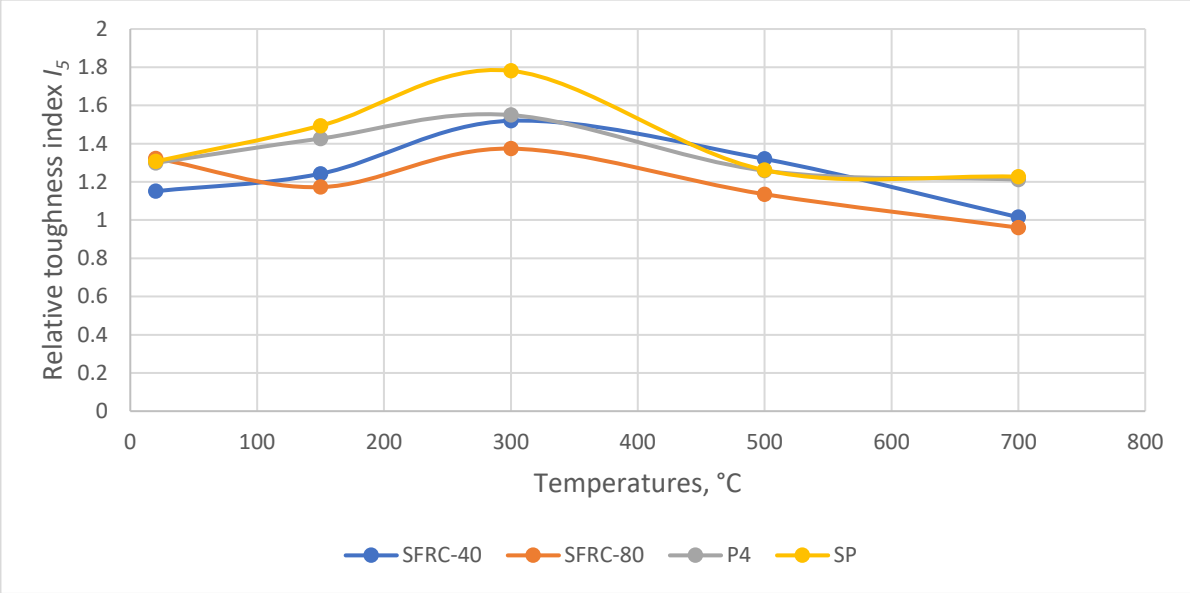

Figure 4.30: Relative shear toughness indexes (I_5) at perpendicular direction (width) for mixes at maximum levels of elevated temperatures

Most of the studies carried out the tests in terms of flexural toughness loading tests using crack mouth opening displacement (CMOD) measurements. A limited number of the studies have directed the tests regarding shear toughness measurements and there is a lack of studies regarding shear toughness at elevated temperatures.

By elevating temperatures, the shear toughness decreases in both directions at all mixes used, regardless types or amount of the fibres contents. The relative decrease of the shear toughness related to crack slip due to elevated temperature, i.e., at 700 °C is found to be 13.1, 16.9, 29.9, 20.7 and 10.8 % for the mixes SFRC-0, SFRC-40, SFRC-80, P4 and SP, respectively. The relative decrease of the shear toughness related to crack width due to elevated temperature, i.e., at 700 °C is found to be 14.1, 24.2, 37.6, 19.8 and 19.3 % for the mixes SFRC-0, SFRC-40, SFRC-80, P4 and SP, respectively. Furthermore, the relative shear toughness for the SP kept the highest values at high temperature levels, i.e., 700 °C for both directions. This could be due to the advantages obtained by using steel fibres (SF) and polypropylene fibres (PP), in which SF has high strength and stiffness; thus, the fibres were highly effective in terms of bridging instantaneously over the cracks at a very small deformation or crack opening once the crack started to form (Horiguchi et al., 2004). In addition, the melted fibres could enhance some properties of concrete, similarly as the case in spalling (Wille and Schneider, 2002; Dehn and Werther, 2006; Balázs and Lublóy, 2012). Moreover, the post-peak response is clear using pp fibres specially at larger deformation or crack opening (Sukontasukku, 2004), thus some studies suggested for the content of pp fibres to be 8-12%, in order to increase the energy absorption capacity after exposure to the elevated (Guo et al., 2014).

Figure 4.31: Shear toughness related to crack slip and width at 20 and 700 °C temperatures

Comparing between toughness at the parallel direction to load (slip-toughness) and perpendicular to load (width-toughness), the results shown in *Table 4.10* demonstrate that shear toughness related to crack width have higher values than shear toughness related to crack slip. This result is valid regardless the type of the fibres used or the degree of the maximum temperatures. A possible interpretation for the previous result could be attributed to the fact

that loading has direct influence on the crack slip deformation, since they are at the same direction, whereas the influence of loading is less at the perpendicular direction (crack width deformation) in addition to the influence of the fibres in bridging the opening of the cracks. Therefore, the toughness keeps higher values at the perpendicular direction compared to the parallel one. *Figure 4.31* shows the difference between the shear toughness related to crack slip and crack width at 20 and 700 °C temperatures.

4.3 Failure modes

When a crack initiates, major propagation follows to result in splitting the specimen across the shear plane into two parts. In general, the mode of the failure in plain concrete is significantly different from mixes containing fibres at both ambient and elevated temperatures. The first observation reported in the plain concrete specimens was that once the crack occurs, it continuously propagates across the shear plane, completely splitting the specimens into two parts. Notwithstanding, the failure modes are different in case of presence of the fibres.

At the presence of the steel fibres, the first crack occurs near the shear plane, called in some studies "secondary tensile crack" (Barragan, 2006). However, the first crack does not control the failure to the end. Another crack follows at the shear plane to control the failure of the specimen spalling it to a completely two parts, as shown in *Figures 4.32 and 4.33*. In some cases, especially in higher amounts of steel fibres, spalling at the surface of the specimens is noticed near the shear plane due to the existence of the steel fibres in which thin tiny layers of the concrete covers are spalled. Finally, regarding the mixes that contain pp fibres, failure at ambient temperature has similar mode to the mixes containing steel fibres, yet once the temperature exceeds the melting point (approximately 150 ºC), the specimens are noticed to fall apart similarly to the mixes cast from plain concrete (*Figures 4.32 and 4.33*).

Furthermore, the influence of increasing temperatures on failure mode is also clear. Due to elevated temperatures up to 500 and 700 ºC, the effect of steel fibres decreases allowing crack opening to occur. Finally, there are no obvious differences between 28-day specimens and one-year old specimens in terms of failure mode. All specimens contain steel fibres remain without splitting even at high temperatures. No significant difference is noticed regarding the amount of steel or cocktail fibres. However, crack opening, after failure, is slightly increased in SFRC-40, SFRC-80 and SP by increasing temperatures up to 700 °C compared to the counterpart specimens at ambient temperature. This is clear by the fact of decreasing of yield tensile strength of the fibres.

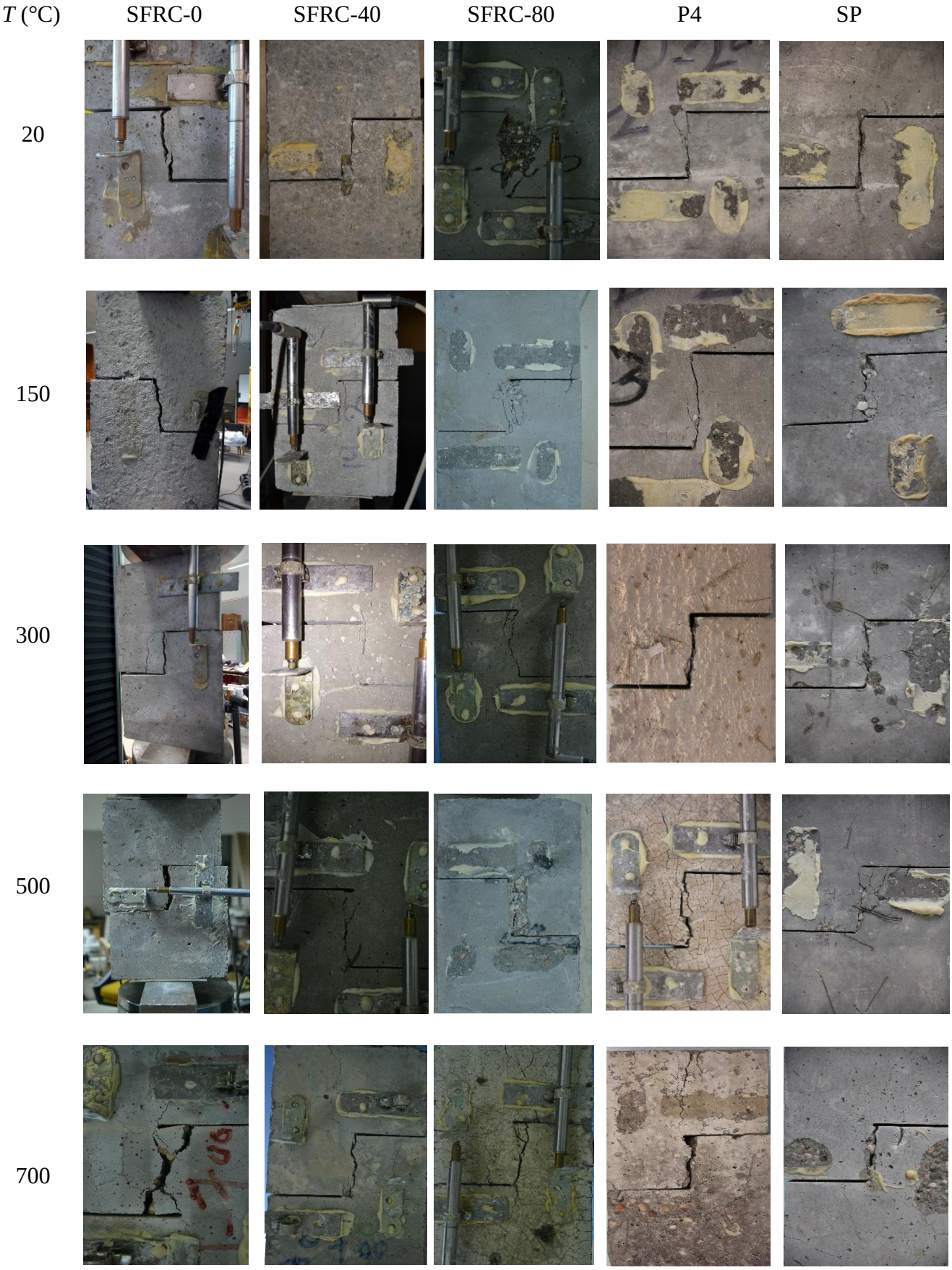

Figure 4.32: Different failure modes of the 28-days old specimens after push-off loading tests

Figure 4.33: Different failure modes of the one-year old specimens after push-off loading tests

5. Summary and New Scientific Results

5.1 Summary

Shear failure is considered as one of the most critical topics in reinforced concrete structures. In general, shear failure happens with little warning signs and is characterized by brittle nature. Comprehensive understanding of the shear behaviour of concrete structures is of great importance at room temperature. This question is even more complex at high temperatures.

Push-off is one of the most typical models that is used to test shear capacity. The push-off model is a non-standard and even in this case widely used test. Fibre-Reinforced Concrete (FRC) is widely used material as well. Numerous researches showed that deformation capacity and toughness of FRC are increased as a consequence of the bridging effect of the fibres, helping to resist the opening of cracks. Therefore, using FRC to enhance the shear behaviour of concrete could have promising results. In addition, incorporating the parameter of high temperatures on the study was of great importance.

I have chosen four main parameters to be investigated in the current study, namely*: type of fibres, amount of fibres, maximum temperature, and age of concrete at testing time*. Accordingly, five concrete mixes, depending on fibres content, were chosen as well as five maximum temperatures. In addition to, concrete is tested at two different ages; (I) 28-days and (II) one-year age. Push-off test setup is designed to measure the deformations occurred at the shear surface plane using means of Linear Variable Differential Transformers (LVDTs). LVDTs were used to measure two different deformations, i.e., relative displacement parallel to the load considered as *crack slip* , and relative displacement perpendicular to the load considered as *crack width*.

An extensive experimental study has been carried out to investigate the shear performance according to above parameters. The tests include compressive and flexural-tensile tests as well. Moreover, several approaches have been used to identify different properties of shear such as shear toughness, shear stiffness and shear failure modes. Finally, the current study could be considered as a major study for several future studies regarding the relevant topics, in which some parameters have not been included herein such as size-effect of the push-off specimens, further types of fibres used, and different models for shear testing.

Finally, the overall aim of the current study is to evaluate the shear performance of concrete using different types and amounts of fibres in the case of elevated temperatures. To fulfil the targeted aim, the following objectives were performed:

1. To evaluate the influence of fibres with different types and ratios on shear strength at different maximum levels of temperatures.

2. To evaluate the influence of fibres with different types and ratios on shear toughness at different maximum levels of temperatures.

3. To evaluate the influence of fibres with different types and ratios on shear stiffness at different maximum levels of temperatures.

4. To specify the different shear failure modes of the push-off specimens at elevated temperatures regarding FRC.

5.2 New Scientific Results (NSR)

NSR 1: Influence of fibres on shear strength at elevated temperatures

1.1 I have experimentally proved that *steel fibres* have significant influence on increasing the shear strength of concrete. The higher is the fibre content the more is the increase of shear strength. Increase of the shear strength due to steel fibres is more pronounced at specimens of age 28-days compared to specimens of 365-days old, and more pronounce at ambient temperature compared to elevated temperatures as well.

Related to publications NA11 and NA13, as well as NA1-10

Presence of steel fibres generally develops the strength of concrete mixes in shear. Results showed significant increase of shear strength due to steel fibres at ambient temperature by about 131.4 and 128.9 % for mixes SFRC-40-28 and SFRC-80-28 whereas developments were about 31.2 and 54.3 % for SFRC-40-365 and SFRC-80-365, respectively.

(*See Tables 4.1, 4.2, 4.3 and 4.4; Figures 4.12, 4.14, 4.16 and 4.18)*

1.2 I have demonstrated that adding *polymeric fibres (pp)* increases the shear strength at ambient temperature. The increase is higher at specimens of 28-days than specimens of 365-days old. However, by elevating temperatures up to 700 °C, significant decrease is noticed for specimens containing pp fibres compared to no-fibre specimens, for both ages.

Related to publications NA12 and NA15, as well as NA1-10

Although presence of pp fibres contributes to increase the shear strength at ambient temperature to reach 22.4% at age 28-day, a negligible influence is noticed for specimens of age 365-days old to reach 0.6%. This could be attributed to concrete enhancement obtained by reducing water content by time in addition to the possible degradations that could occur to the pp fibres by time. By increasing temperatures up to 700 °C, where pp fibres are totally vanished, a reduction in shear strength is noticed for the specimens that contain pp fibres to reach 44.0 and 31.7% for both ages 28-days and 365-days old, respectively.

(*See Tables 4.1 and 4.5; Figures 4.12 and 4.19)*

1.3 I have demonstrated that adding *cocktail fibres* significantly increases the shear strength at ambient temperature for specimens of both ages 28-days and 365-days old. However, insignificant increase is observed when temperatures are elevated up to 700 °C for specimens of both ages as well.

Related to publications NA12 and NA15, as well as NA1-10

Mixing pp fibres with the steel fibres in order to produce hybrid or cocktail fibres has found to increase shear strength of concrete at ambient temperature. The increase of the shear strength compared to the plain concrete is measured to be 71.6 and 58.9% for specimens of 28-days and 365-days old, respectively. However, increasing temperatures up to 700 °C, the increase in shear strength for specimens containing cocktail fibres is found to be 16.5 and 27.3% for specimens of both ages 28-days and 365-days old, respectively.

(*See Tables 4.1 and 4.5; Figures 4.12 and 4.19)*

NSR 2: Enhancement of shear toughness

2.1 I have experimentally demonstrated that existence of fibres increases the shear toughness at both directions, parallel and perpendicular to the load.

Related to publications NA14, NA16 and NA17

Shear toughness, indicated by toughness Index I_5, is generally increased at concrete mixes containing fibres, regardless the type of fibres [ASTM C 1018-89. 1990]. Results show that mixes containing 80 kg/m^3 of steel fibres have the highest shear toughness values among other mixes at both directions of loading. The relative increases of the shear toughness related to the crack slip due to existence of fibres at the ambient temperatures are 3.1, 23.1, 16.9 and 14.3 % for the mixes SFRC-40, SFRC-80, P4 and SP, respectively.

The relative increases of the shear toughness related to the crack width due to existence of fibres at the ambient temperatures are found to be 15.1, 32.3, 29.9 and 30.7 % for the mixes SFRC-40, SFRC-80, P4 and SP, respectively.

(*See Table 4.10 and Figure 4.28)*

2.2 I have experimentally demonstrated that shear toughness related to crack width have higher values than shear toughness related to crack slip. This result is valid regardless the type of the fibres used or the degree of the maximum temperatures.

Related to publications NA14, NA16 and NA17

This result could be attributed to the fact that loading has direct influence on the crack slip deformation since they are both at the same direction, whereas the influence of loading is less at the perpendicular direction (crack width deformation). In addition, fibres have direct influence on bridging the opening of the cracks. Consequently, shear toughness keeps higher values at the perpendicular direction compared to the parallel one.

(*See Table 4.10 and Figure 4.31)*

2.3 I have experimentally demonstrated that by elevating temperatures, the shear toughness decreases in both directions at all mixes, regardless types or amount of the fibres contents.

Related to publications NA14, NA16 and NA17

The decrease of the shear toughness related to crack slip due to elevated temperatures, i.e., at 700 °C is found to be 13.1, 16.9, 29.9, 20.7 and 10.8 % for the mixes SFRC-0, SFRC-40, SFRC-80, P4 and SP, respectively. The decrease of the shear toughness related to crack width due to elevated temperature, i.e., at 700 °C is found to be 14.1, 24.2, 37.6, 19.8 and 19.3 % for the mixes SFRC-0, SFRC-40, SFRC-80, P4 and SP, respectively. Furthermore, the highest value of the relative shear toughness, compared to the shear toughness of the plain concrete, was belong to the cocktail mix (SP) at high temperature levels, i.e., 700 °C for both directions. This could be the result of the influence of the presence of the steel fibres as well as the enhancement obtained by presence of polymeric fibres after melted, similarly to the case of spalling (Balázs and Lublóy, 2012). Similar results were confirmed regarding using hybrid fibres to increase toughness after elevating temperatures, but on compressive strength (Horiguchi et al., 2004). In addition, adding steel fibres in high amounts, i.e., 80 kg/m3 will result in

decreasing the cross-section of the shear plane and increasing the entrained air, thus decreasing the stress intensity factor in shear (Fehérvári et al., 2010). Simultaneously, elevating temperatures will result in decrease the mechanical properties of steel fibres. Therefore, results of the SFRC-80 mix show the highest decrease among other mixes.

(*See Table 4.10 and Figures 4.29 and 4.30)*

NSR 3: Enhancement of shear stiffness

3.1 I have experimentally demonstrated that the shear stiffness related to crack width has higher values than shear stiffness values related to the crack slip. This result is valid for all mixes and at more pronounce at elevated temperatures than at ambient temperature.

Related to publications NA14, NA16 and NA17

Results show that crack width is nearly zero before first crack initiates whereas crack slip is slightly more than zero, indicating that the shear stiffness of the perpendicular-to-load direction is higher than shear stiffness of the parallel-to-load direction (Mattock and Hawkins, 1972). This observation was confirmed for all types of mixes at all levels of elevated temperatures.

Furthermore, at high maximum temperatures, i.e., 500 or 700 °C, both crack width and crack slip have higher values, relating to the shear strength, than values of crack width and crack slip, relating to shear strength, at ambient temperature. A possible interpretation for the previous result could be due to the fact that load on specimens was vertical and the loading was in parallel to the shear plane, thus values of the crack deformation were more influenced (higher) in the vertical direction compared to the horizontal one, resulting in less stiffness. Moreover, ratios of the increase of the shear stiffness related to the crack width, to shear stiffness related to the crack slip at ambient temperature were 177, 45, 167, 1128 and 256% for the mixes SFRC-0, SFRC-40, SFRC-80, P4 and SP, respectively. From another hand, ratios of the increase of the shear stiffness related to the crack width, to shear stiffness related to the crack slip at elevated temperatures, i.e., 700 °C were 917, 554, 734, 1666 and 766% for the mixes SFRC-0, SFRC-40, SFRC-80, P4 and SP, respectively.

(*See Tables 4.6, 4.7, 4.8 and 4.9; Figures 4.23, 4.24, 4.25 and 4.26)*

3.2 I have experimentally demonstrated that elevating temperatures significantly decreases the shear stiffness of all mixes tested. This result is valid for both directions-to-load, i.e., parallelly or perpendicularly. By elevating temperatures up to 700 °C, the highest residual shear stiffness, at both directions, was measured for the cocktail fibres mixes.

Related to publications NA14, NA16 and NA17

Shear stiffness is significantly decreased by increasing temperatures. This notice is valid for all mixes at both crack deformations as well. Previous studies reported stiffness degradations for compression in case of FRC due to elevated temperatures (Poon et al., 2004). I have measured the crack deformations at all levels of temperatures. I calculated the relative residual shear stiffness through dividing the shear stiffness value at 700 °C by the shear stiffness value at 20

°C. The results show significant decline of the shear stiffness at both directions by increasing temperatures, in which values of decrease are higher than 95% for all mixes. The results show also that the residual shear stiffness has higher values for the cocktail fibres mixes.

(*See Figure 4.27)*

NSR 4: Influence of fibres on shear failure modes at elevated temperatures

I have demonstrated that presence of fibres has significant influence on controlling the cracks occurred at the shear planes, thus affecting the shear failure modes at different levels of elevated temperatures.

Related to publications NA11, NA12, NA13 and NA15

In general, the mode of the failure in plain concrete is significantly different from mixes containing fibres at both ambient and elevated temperatures. First observations reported in the plain concrete specimens were the continuous propagations across the shear plane once the first crack initiates, completely splitting the specimen into two separate parts. However, at the presence of the fibres, the failure mode is different. Some specimens, particularly containing steel fibres, experienced the first crack to be occur near the shear plane, called in some studies *secondary tensile crack* (Barragan et al., 2006). Moreover, the secondary tensile crack does not control the failure to the end, but another crack follows across the shear plane to control the failure of the specimen without complete separation. In some cases, especially in higher amounts of steel fibres, spalling at the surface of the specimens is noticed near the shear plane due to the existence of the steel fibres, in which thin tiny layers of the concrete covers are spalled.

Finally, regarding the mixes contain pp fibres (P4), failure at ambient temperature has similar mode to the mixes containing steel fibres, yet once the temperature exceeds the melting point, the specimens are noticed to fall apart similarly to the mixes cast from plain concrete.

(*See Figures 4.32 and 4.33)*

5.3 Applications of the New Scientific Results and future perspectives

The experimental data presented in this thesis provides a comprehensive understanding of the shear performance of fibre reinforced concrete exposed to elevated temperatures. Using fibres as a substitutional material for the conventional reinforcement, partially or totally, has only been accepted recently in construction codes. Therefore, investigating the fibre reinforced concrete regarding the shear is of great importance.

The adopted methodology includes using push-off model as the main model to represent the shear performance, in addition to several specimens of prisms and cubes for the other mechanical properties. Moreover, using LVDTs enables the research to cover several measurements for the shear performance, i.e., shear strength, shear toughness and shear stiffness that provided a better understanding for the targeted mechanical properties.

The current study establishes for further studies to be carried out using several parameters not used at the current study, such as investigating different types of fibres, investigating the size effect of the push-off model, investigating the difference between using uncracked or pre-cracked push-off model, investigating elevated temperatures above 700 °C, and investigating the difference between testing at the cold or hot state. Additionally, there was a lack of study in the research regarding shear toughness and shear stiffness at elevated temperatures, thus presenting the shear toughness and shear stiffness at the current study could be useful for the future studies regarding similar investigations. Finally, analytical model is necessary for future studies for the standardization process for the shear performance at elevated temperatures in FRC to be used in modelling or codes.

6. References

AASHTO. 1993. Guide for Design of Pavement Structures. *American Association of State Highway and Transportation Officals*.

Accion, F., Gobantes, J., Blanco, M.T. 1990. Cements Reinforced by Acrylic Fibers. Infrared Studies. I. Hydration and Hydrolysis Processes In Fibers. *Cement and Concrete Research, Vol. 20, pp. 702-710*

ACI Committee 318. 2008. Building code and commentary, Report ACI 318-08/318R-08. *American Concrete Institute*, Farmington Hills

ACI Committee 318. 318-11. Building code requirements for structural concrete and commentary. ACI; 2011. p 503

ACI Committee 544. 1973. Revision of State-of-the-Art Report (ACI 544 TR-73) on Fiber Reinforced Concrete, *ACI Journal, Proceedings*, Nov. 1973, Vol. 70, No. 11, pp. 727-744

ACI Committee 544. 2002. Report on Fiber Reinforced Concrete. (ACI Committee 544. 1R-96)

ACI-ASCE Committee 426. 1973. The shear strength of reinforced concrete members. *ACI Journal Proceedings*, 70(7), pp 471-473

Acker, V. 2003. Shear resistance of prestressed hollow core floors exposed to fire. *Structure Concrete Journal of fib*, Vol. 4 issue 2, pp 65-74

Adams DF, Walrath DE. 1987. Further developments of the Iosipescu sheartest method. *Exp Mech 27(2)*, pp 113 – 119

Ahmed O.A.Q., Abdullah, S. 2019. High Temperatures Effect on Shear Transfer Strength of Steel Fiber Reinforced Self-Compacted Concrete, *J. Eng. Applied Sci*., pp 3158-3174

Alani, A., Aboutalebi, M. 2013. Mechanical properties of fibre reinforced concrete-a comparative experimental study. *International Journal of Civil, Environmental, Structural, Construction and Architectural Engineering*, Vol. 7(9), pp 646-651

Ali, M., Liu, A., Sou, H., Chouw, N. 2012. Mechanical and dynamic properties of coconut fibre reinforced concrete. *Construction and Building Materials*, 30, pp 814-825

Ali, M., Majumdar, A., Rayment, D. 1972. Carbon fibre reinforcement of cement. *Cement and Concrete Research.* Vol. 2, Iss. 2, pp 201-212

Ali, M., Oehlers, D., Griffith, M. 2008. Shear transfer across cracks in FRP strengthened RC members. *Journal of Composites for Construction*, 12(4), pp 416-424

Alonso, M.C., Rodriguez, C., Sánchez, M., Barragan, B. 2010. Respuesta al fuego de HAC con y sin refuerzo de fibras, in: bac2010. (in English: Fire response of HAC with and without fiber reinforcement)-2Congresso Ibérico sobre betão auto-compactável. 2Congreso Ibérico sobre Hormigón Autocompactant, Guimarães, 2010.

Al-Owaisy, S. 2007. Effect of High Temperatures on Shear Transfer Strength of Concrete. *Journal of Engineering and Development*. Vol. 11, No. 1, pp 92-103

Amin, A., Foster, S. 2016a. Shear strength of steel fibre reinforced concrete beams with stirrups. *Engineering Structures*, Vol. 111 (2016), pp 323–332

Amin, A., Foster, S. 2016b. Numerical modelling of large-scale steel fibre reinforced concrete beams failing in shear. *Fibre-reinforced concrete: From design to structural applications. ACI-fib International Workshop, Joint 2014*. *fib*, bulletin 79, pp 161-170

Anderson A. R. 1960. Composite designs in precast and cast-in-place concrete. *Progressive Architecture.* Vol. 41(9), pp 172–179

Anderson, W.E. 1978. Proposed Testing of Steel-Fibre Concrete to Minimize Unexpected Service Failures, *Proceedings, RILEM Symposium of Testing and Test Methods of Fibre Cement Composites* (Sheffield, 1978), Construction Press, Lancaster, pp 223-232

Appa Rao G., Sreenivasa Rao A. 2009. Toughness indices of steel fiber reinforced concrete under mode II loading. *Materials and Structures* (2009) 42, pp 1173–1184

ASTM C 1018-89. 1990. Standard Test Methods for Flexural Toughness and First Crack Strength of Fiber Reinforced Concrete (Using Beam with Third Point Loading), ASTM, V 4.02, pp 637-644

Bakhshi, M., Nasri, V. 2016. Developments in design for fibre-reinforced concrete tunnel segments. *Fibre-reinforced concrete: From design to structural applications. ACI-fib International Workshop*. *Joint 2014*. *fib*, bulletin 79, pp 341-352

Balaguru, P., Narahari, R., Patel, M. 1992. Flexural Toughness of Steel Fiber Reinforced Concrete. *ACI Materials Journal*, V. 89, No.6, November-December 1992. pp 541-546

Balaguru, P., Ramakrishnan, V. 1986. Freeze-Thaw Durability of Fiber Reinforced Concrete, *ACI Journal, Proceedings*, Vol. 83, No. 3, 1986, pp 374-382
Balázs, G.L. 2010. A historical review of shear. *fib*: Shear and punching shear in RC and FRC elements. Bulletin 57, 2010, pp 1-13
Balazs, G.L., Lubloy, E. 2012. Post-heating strength of fibre-reinforced concretes. *Fire Safety Journal* 49. pp 100-106
Balázs, G.L., Lublóy, É., 2016. Fire resistance for thin-webbed concrete and masonry elements. Applications of Structural Fire Engineering. DOI: https://doi.org/10.14311/asfe.2015.036
Balendran, R.V., Zhou, F.P., Nadeem, A., Leung, A.Y.T. 2002. Influence of steel fibres on strength and ductility of normal and lightweight high strength concrete. *Building and environment*, Vol. 37(12), pp 1361-1367
Balugaru, P., Shah, S.P. 1992. Fiber-Reinforced Cement, Composites, *McGraw-Hill*, 1992, pp 530
Banthia, N., Trottier, J.F. 1995. Test Methods for Flexural Toughness Characterization of Fiber Reinforced Concrete: Some Concerns and a Proposition", *ACI Material Journal*, Vol. 92, No. 1, January-February 1995, pp 48-57
Bao, C., Bi, J.H., Xu, D., Guan, J., Cheng, W.X. 2019. Numerical simulation of the distribution and orientation of steel fibres in SCC. *Magazine of Concrete Research*, https://doi.org/10.1680/jmacr.18.00432 Q16
Barragan B., Gettu R., Agullo L., Zerbino R. 2006. Shear failure of steel fibre-reinforced concrete based on push-off tests. *ACI Materials Journal.* Vol. 103, No. 4, pp 251-257
Barros, J.A., Cunha, V.M., Ribeiro, A.F., Antunes, J.A.B. 2005. Post-cracking behaviour of steel fibre reinforced concrete. *Materials and Structures*, 38(1), pp 47-56
Batson, G.B., 1977. Strength of Steel Fiber Concrete in Adverse Environments. Champaign, Illinois (US)
Batson, G.B., Jenkins, E., Spatney, R. 1972. Steel fibers as shear reinforcement in beams. *Journal of the American Concrete Institute*. Proceedings, Vol. 69, No. IO, October 1972. pp 640-644
Baumann, T., Rüsch, H. 1970. "Versuche zum Studium der Verdübelungswirkung der Biegezugbewehrung eines Stahlbetonbalkens." Deutscher Ausschuss für Stahlbeton (Heft 210). (in English: Attempts to study the dowelling effect of the flexural reinforcement of a reinforced concrete beam)
Bayramov, F., Tasdemir, C., Tasdemir, M.A. 2004. Optimisation of steel fibre reinforcedconcretes by means of statistical response surface method. *Cem Concr Compos*. 2004;26(6), pp 665–675
Bazant, Z.P., et al. 1982. Normal and Refractory Concretes for LMFBR Applications—Vol. 1, Review of Literature on High-Temperature Behavior of Portland Cement and Refractory Concretes, EPRI Report NP-2437, Northwestern University and Portland Cement Association, Chicago, Illinois, June 1982
Behnood, A., Ghandehari, M. 2009. Comparison of compressive and splitting tensile strength of high-strength concrete with and without polypropylene fibers heated to high temperatures. *Fire Safety J* 2009
Belletti B., Cerioni, R., Meda, A., Plizzari, G. 2008. Design aspects on steel fiber-reinforcedconcrete pavements. *J Mater Civ Eng* 2008;20(9), pp 599–607
Bentur, A., Mindess, S. 2007. Fibre Reinforced Cementitious Composites. 2nd ed. CRC Press. New York
Bentz, E.C., Vecchio, F.J., Collins, M.P. 2006. Simplified modified compression field theory for calculating shear strength of reinforced concrete elements. *ACI Struct J*, 103 (4) (2006), pp 614-624
Bernard E. Correlations in the behaviour of fibre reinforced shotcrete beam and panel specimens. *Mater Struct* 2002;35(3), pp 156–164
Bernard, E.S. 2004. Durability of cracked fibre reinforced shotcrete. In: Bernard, E.S. (Ed.), Shotcrete: More Engineering Developments: *Proceedings of the Second International Conference on Engineering Developments in Shotcrete.* A.A. Balkema Publishers, Sydney, Australia, pp 59–66
Bilodeau, A., Malhotra, V.M., Hoff, G.C. 1998. Hydrocarbon Fire Resistance of High Strength Normal Weight and Light Weight Concrete Incorporating Polypropylene Fibres, *International Symposium on High Performance and Reactive Powder Concrete, Sherbrooke, QC*, pp 271-296
Birkeland, P.W., Birkeland H.W. 1966. Connections in precast concrete construction. *Journal of the American Concrete Institute*. Vol. 63(3), pp 345–468
Bisby, L.A., 2003. Fire behaviour of fibre-reinforced polymer (FRP) reinforced or confined concrete (pp. 2520-2520). Kingston (Kanada): Queen's University.
Buratti, N. Mazzotti, C., Savoia, M. 2011. Post-cracking behaviour of steel and macro-synthetic fibre-reinforced concretes. *Construction and Building Materials* Vol. 25, Issue 5, May 2011, pp 2713-2722 Bologna, Italy

Caetano, H., Ferreira, G., Rodrigues, J.P.C., Pimienta, P. 2019. Effect of the high temperatures on the microstructure and compressive strength of high strength fibre concretes. *Construction and Building Materials*, 199, pp 717-736

Carvel, R. 2005. Fire protection in Concrete Tunnels, in The Handbook of Tunnel Fire Safety (Eds. Beard, A. & Carvel, R.) Thomas Telford, London, UK.

Casanova, P., Rossi, P. 1997. Analysis and design of steel fiber reinforced concrete beams. *ACI Struct J*, 94 (5) (1997), pp 595-602

Casanova, P., Rossi, P., Schaller, I., 1997. Can steel fibers replace transverse reinforcement in reinforced concrete beams? *ACI Mater J* 94(5), pp 341–354

CECS Publication No. 38. 2004. Technical specification for Fibre-reinforced concrete structures. China Association for Engineering Construction Standardization

Chan, Y.N., Peng, G.F., Anson, M. 1999. Residual strength and pore structure of high-strength concrete and normal strength concrete after exposure to high temperatures. *Cement and concrete composites*, Vol. 21(1), pp 23-27

Chana, P.S. 1987. Investigation of the mechanism of shear failure of reinforced concrete beams. *Magazine of Concrete Research* 39(141), pp 196-204

Chanh, N.V. 2004. Steel fiber reinforced concrete. 8 Joint Vietnam Joint Seminars. pp 108-116

Choi, K.K., Park, H.G., Wight, J. 2007. Shear strength of steel fiber-reinforced concrete beams without web reinforcement. *ACI Struct J* 104(1), pp 12–22

Chu, T.Y. 1978. Radiant Heat Evolution of Concrete—A Study of the Erosion of Concrete Due to Surface Heating," Research Paper SAND 77-0922, Sandia National Laboratories, New Mexico, 1978.

Collet, Y. 1975. Conductive thermique du materiau beton (in English: thermal conductivity of concrete). Group de travail "Beton leger de structure" et "Compartment du Materiau Beton on Fonction de la Temperature", 1975.

Colombo, M., Di Prisco, M., Felicetti, R. 2010. Mechanical properties of steel fibre reinforced concrete exposed at high temperatures. *Materials and Structures*, Vol. 43(4), pp 475-491

Contec Fiber AG, fibre supply company (Switzerland). https://www.contecfiber.com/en/products/concrix/ (accessed October, 2018)

Contec Fiber AG. https://www.contecfiber.com/en/products/concrix/

Cook, D.J., Uher, C. 1974. The Thermal Conductivity of Fibre Reinforced Concrete, *Cement and Concrete Research*, Vol. 4, No. 4, July 1974, pp 497-509

Cook, J.G. 1984. Handbook of Textile Fibers. *Morrow Publishing Company, Ltd.*, Durham, England, 1984, pp 261-283

Cuenca, E., Echegaray-Oviedo J., Serna, P. 2015. Influence of concrete matrix and type of fibre on the shear behavior of self-compacting fibre reinforced concrete beams, *Composites Part B 75*, pp 135-147

Cuenca, E., Serna, P. 2010. Shear behavior of self-compacting Concrete and Fibre Reinforced concrete Push-Off Specimens: Design, Production and Placement of Self-Consolidating Concrete. RILEM Book-series Vol. 1, pp 429-438

Cuenca, E., Serna, P. 2013. Failure modes and shear design of prestressed hollow core slabs made of fiber-reinforced concrete. *Compos Part B-Eng* 45(1), pp 952–964

Cuenca, E., Serna, P. 2013b. Shear behaviour of prestressed precast beams made of felf-compacting fibre reinforced concrete. *Construction and Building Materials, Vol*. 45, pp 145-156

Czoboly, O., Lublóy, É., Hlavička, V., Balázs, G.L., Kéri, O., Szilágyi, I. 2017. Fibers and fiber cocktails to improve fire resistance of concrete. *J. of Thermal Analysis and Calorimetry*, 128(3), pp 1453-1461

De la Fuente, A., Pujadas, P., Blanco, A., Aguado, A. 2012. Experience in Barcelona with the use of fibres in segmental linings. Tunnelling and Underground Space Technology, 27 (1), pp 60-71

Dehn, F., Herrmann, A. 2017. Steel-fibre-reinforced concrete (SFRC) in fire: Normative and pre-normative requirements and code-type regulations. *Special Publication*, 310, pp 75-80

Dehn, F., Werther, N. 2006. Fire tests on tunnel elements for M 30 tunnel in Madrid(Brandversuche an Tunnelinnenschallenbetonen f¨ur den M 30-Nordtunnel in Madrid), Beton und Stahlbetonbau, 101/9, 2006, Berlin, ISSN 0005-9900 (in German)

Dehn, F., Wille, K. 2004. Micro analytical investigations on the effect of polypropylene fibres in fire exposed high-performance concrete (HPC)'', Proceedings of International RILEM Symposium on Fibre Reinforced Concretes,BEFIB,20–22 September 2004, Varrenna, Italy (Eds.: Prisco, M., Felicetti, R. Plizzari, G.A), pp 659–678

Destree, X. 2016. Steel-fibre-reinforced concrete elevated suspended slabs: Design cases in Europe and the USA. *Fibre-reinforced concrete: From design to structural applications. ACI-fib International Workshop*. *Joint 2014*. *fib*, bulletin 79, pp 409-418

di Prisco, M., Plizzari, G., Vandewalle, L. 2009. Fibre reinforced concrete: new design perspectives. *Mater Struct* 2009;42(9):1261–1281

di Prisco, R., Felicetti, R., Plizzari, G.A. 2004. Proceedings of the 6th RILEM Symposium on Fibre Reinforced Concretes (FRC), RILEM PRO 39, Bagneaux, France, pp 1514

Ding, Y., Azevedo, C., Aguiar, J.B., Jalali, S. 2012. Study on residual behaviour and flexural toughness of fibre cocktail reinforced self-compacting high-performance concrete after exposure to high temperature. *Construction and Building Materials*, 26(1), pp 21-31

Ding, Y., Zhang, C., Cao, M., Zhang, Y., Azevedo, C. 2016. Influence of different fibers on the change of pore pressure of self-consolidating concrete exposed to fire, Constr. *Build. Mater. 113*, pp 456–469

Dinh, H.H., 2009. Shear Behavior of Steel Fiber Reinforced Concrete Beams without Stirrup Reinforcement (Doctoral dissertation).

Dixon, J., Mayfield, B. 1971. Concrete Reinforced with Fibrous Wire, *Journal of the Concrete Society*, Concrete, Vol. 5, No. 3, Mar. 1971, pp 73-76

Dong, X., Ding, Y., Wang, T., 2008. Spalling and mechanical properties of fiber reinforced high-performance concrete subjected to fire. *Journal of Wuhan University of Technology-Mater. Sci*., 23(5), pp743-749

Dufour J., Trottier, J., Forgeron, D. 2006. Behaviour and performance of monofilament macro-synthetic fibres in dry-mix shotcrete. *Proc Shotcr Underground Support, X* 2006;215, pp 194–205

Dulacska, H., 1972, December. Dowel action of reinforcement crossing cracks in concrete. In Journal Proceedings. Vol. 69, No. 12, pp 754-757

Echegaray-Oviedo, J. 2014. Upgrading the push-off test to analyze the contribution of steel fibre on shear transfer mechanisms. PhD Thesis. Institute of Concrete Science and Technology (ICITECH), Universitat Politècnica de València. Spain.

Eleiott, A.F. 1974. An experimental investigation of shear transfer across cracks in reinforced concrete, M.S. Thesis, Cornell University, Ithaca, June 1974

EN 1992-1-1. 2004. CEN European Committee for Standardization. Eurocode 2. Design of concrete structures – general rules and rules for buildings., Brussels, Belgium; 2004. p 225

En 1994-1-2:2005. Eurocode 4-Design of Composite Steel And Concrete Structures-Part 1-2: General Rules-Structural Fire Design.

Ezeldin, S., Balaguru, P. 1992. Normal- And High-Strength Fiber-Reinforced Concrete Under Compression. Journal of Materials in Civil Engineering, Vol. 4, No. 4, pp 415-429

Fehérvári, S., Gálos, M., Nehme, S.G. 2010. Determination of K_{IIC} Stress Intensity Factor on new shape concrete specimens. Concrete Structures, Vol 11, 2010, pp 53-60

Fellinger, H. 2004. Shear and Anchorage Behavior of Fire Exposed Hollow Core Slabs. PhD. diss., Department of Civil Engineering, Delft University, Netherlands.

Fenwick, R.C., Paulay. T. 1968. Mechanisms of shear resistance of concrete beams. *Journal of the Structural Division*, ASCE 94(10), pp 2235-2350

Fernández Ruiz, M., Muttoni, A., Sagaseta, J. 2015. Shear strength of concrete members without transverse reinforcement:A mechanical approach to consistently account for size and strain effects. *Engineering Structures. 99*, pp 360-372

Ferrara, L, Meda, A. 2006. Relationships between fibre distribution, workability andthe mechanical properties of SFRC applied to precast roof elements. Mater Struct/Mat et Constr. 39(288), pp 411–20

Ferrara, L. Mobasher, B. 2016. Fibre-Reinforced Concrete – From fresh properties to structural design: New tools, Guides and Reports from ACI Technical Committee 544. *3rd FRC International Workshop Fibre Reinforced Concrete: from Design to Structural Applications*. ACI, *fib*, RILEM Joint Workshop. Italy

fib. 2007. Fire design of concrete structures, materials, structures and modelling, *fib* Bulletin 38, International Federation for Structural Concrete

fib. 2010. Model Code for Concrete Structures 2010. (2013). Ernst and Sohn. Lausanne, Switzerland

Fletcher, I.A., Welch, S., Torero, J.L., et al. 2007. Behaviour of Concrete Structures in Fire. *Thermal Science* 2007, 11, pp 37-52

Foster, S. 2016. FRC design according to the draft Australian bridge code. *Fibre-reinforced concrete: From design to structural applications. ACI-fib International Workshop*. *Joint 2014*. *bulletin 79*, pp 29-40

Foster, S.J. 2009. The application of steel-fibres as concrete reinforcement in Australia: From material to structure. *Mater. Struct*. 2009, 42, pp 1209–1220

Foster, S.J. 2010. Design of FRC beams for shear using the VEM and the Draft Model Code Approach. *fib Bulletin No. 57*, pp 195-210

Foster, S.J., Voo, Y.L., Chong, K.T. 2006. Analysis of steel fiber reinforced concrete beams failing in shear: variable engagement model. *Finite Element Analysis of Reinforced Concrete Structures, Eds. Lowes, L., and Filippou, F., ACI SP*-237

Gale, D.M., Riewald, P.G., Champion, A.R. 1986. Cement Reinforcement with Man-Made Fibers. *International Man-Made Fibres Congress*, E. I. Du Pont de Nemours and Co., Dornbirn, Austria

Garcés, P., Fraile, J., Vilaplana-Ortego, E., Cazorla-Amorós, D., Alcocel, E.G., Andión, L.G. 2005. Effect of carbon fibres on the mechanical properties and corrosion levels of reinforced portland cement mortars. *Cement and concrete research*, 35(2), pp 324-331

Gettu, R., Barragán, B., Garcia, T., Ortiz, J., Justa, R. 2006. Fiber concrete tunnel lining. *Concr Int* 2006; 28(8), pp 63–9

Goldfein, S. 1965. Fibrous Reinforcement for Portland Cement. *Modern Plastics*, Vol. 42, No. 8, pp 156-160

Golding. 1959. Polymers and Resins. *D. Van Nostrand Co*., 1959, pp 288- 289

Gopalaratnam, V.S., Shah, S.P., Batson, G., Criswell, M., Ramakrishnan, V., Wecharatana, M. 1991. Fracture Toughness of Fiber Reinforced Concrete, ACI Materials Journal, Vol. 88, No. 4, July-Aug. 1991, pp 339-353

Goto, Y. 1971. Cracks formed in concrete around deformed tension bars, *ACI-Journal, Proceedings*, Vol. 68, No. 4, April 1971, pp 244-251

Granju, J., Balouch, S. 2005. Corrosion of steel fibre reinforced concrete from the cracks. *Cement and Concrete Research*, Vol. 35, pp 573-577

Guo, Y.C., Zhang, J.H., Chen, G.M., Xie, Z.H. 2014. Compressive behaviour of concrete structures incorporating recycled concrete aggregates, rubber crumb and reinforced with steel fibre, subjected to elevated temperatures. *Journal of cleaner production*, 72, pp 193-203

Hager, I. 2013. Behaviour of Cement Concrete at High Temperature, Bulletin Of The Polish Academy Of Sciences Technical Sciences, vol. 61, no. 1, 2013.

Hamadi, Y.D., Regan, P.E. 1980. Behaviour in Shear of Beams with Flexural Cracks. *Magazine of Concrete Research* 32(111), pp 67-78

Hannant, D.J. 1978. Fiber Cements and Fiber Concretes, Book published by John Wiley & Sons, Ltd, 1978.

Hansel, D., Guirius, P., 2011. Steel fibre reinforced segmental linings: State of the art and complete projects. Tunnel, 30(1)

Hanson N.W. 1960. Precast-prestressed concrete bridges. 2. Horizontal shear connections. Development Department Bulletin D35. *Portland Cement Assoc*. Vol. 2(2), pp 38–58

Hertz, K. 1992. Danish Investigations on Silica Fume Concretes at Elevated Temperatures, ACI Materials Journal, July–August, 1992

Hofbeck, J.A., Ibrahim, I.O., Mattock, A.H. 1969. Shear transfer in reinforced concrete. *Journal of the American Concrete Institute*. Vol. 66(2), pp 119–128

Homma, D., Mihashi, H., Nishiwaki, T. 2009. Self-Healing Capability of Fibre Reinforced Cementitious Composites. *J. Adv. Concr. Technol*. 7, pp 217–228

Horiguchi, T., Sugawara, T. and Saeki, N., 2004. Fire resistance of hybrid fibre reinforced high strength concrete. RILEM Publications PRO, 39, pp 303-310

Houde, J., Mirza, M.S. 1974. A Finite Element Analysis of Shear Strength of Reinforced Concrete Beams. *ACI Special Publication* 42, pp 103-128

Iosipescu N. 1967. New accurate procedure for single shear testing of metals. *J Mater 2*(3), pp 537–566

Ismail, M.K., Hassan, A.A. 2019. Influence of fibre type on shear behavior of engineered cementitious composite. *Magazine of Concrete Research.* DOI:10.1680/jmacr.19.00172

Jansson, R., 2013. Fire spalling of concrete–A historical overview. In MATEC Web of Conferences (Vol. 6, p. 01001). EDP Sciences. DOI: 10.1051/matecconf/20130601001

Jindal, R. 1984. Shear and Moment Capacities of Steel Fiber Reinforced Concrete Beams. Fiber Reinforced Concrete—International Symposium, SP-81, *American Concrete Institute*, Detroit, 1984, pp 1-16

Jindal, R., Sharma, V. 1987. Behavior of Steel FRC Knee Type Connections. Fiber Reinforced Concrete Properties and Applications, SP-105, *American Concrete Institute*, Detroit, 1987, pp 475-491
Johnston, C.D. 1974. Steel Fibre Reinforced Mortar and Concrete—A Review of Mechanical Properties, Fiber Reinforced Concrete, SP-44, *American Concrete Institute*, Detroit, pp 127-142
Johnston, C.D. 1986. Toughness of Steel Fiber Reinforced Concrete. Steel Fiber Concrete, Elsevier Applied Science Publishers, Ltd., 1986, pp 333-360
Johnston, C.D. 1989. Effects on Flexural Performance of Sawing Plain Concrete and of Sawing and Other Methods of Altering Fiber Alignment in Fiber Reinforced Concrete. *Cement, Concrete and Aggregates, ASTM*, CCAGDP, Vol. 11, No. 1, Summer 1989, pp 23-29
Jongvivatsakul, P., Attachaiyawuth, A., Pansuk, W. 2016. A crack-shear slip model of high strength steel fiber-reinforced concrete based on a push-off test. Construction and Building Materials, vol 126 (2016), pp 924–935
Joseph, P.V., Rabello, M.S., Mattoso, L.H.C., Joseph, K., Thomas, S. 2002. Environmental effects on the degradation behaviour of sisal fibre reinforced polypropylene composites. *Composites Science and Technology*, 62(10-11), pp 1357-1372
JSCE (Japan Society of Civil Engineers). 1984. Recommendation for design and construction of steel fibre reinforced concrete. *Concrete Library International, JSCE*. no. 3, pp 41-69
JSCE Concrete Library International. 2008. Recommendations for design and construction of HPFRCC with multible fine cracks, Japan Society of Civil Engineers
JSCE Standard SF-4. 1984. Method of Test for Flexural Strength and Flexural Toughness of Fiber Reinforced Concrete, 1984, pp 58 – 66
Kani, G.N.J. 1964. The Riddle of Shear Failure and Its Solution. *ACI Journal.* Vol. 61 (28), pp 441-467
Katzer, J., Domski, J. 2012. Quality and mechanical properties of engineered steel fibres used as reinforcement for concrete. *Construction and Building Materials*, 34 (2012) pp 243-248
Kaufmann, J., Frech, K., Schuetz, P., Münch, B. 2013. Rebound and orientation of fibers in wet sprayed concrete applications. *Construction and Building Materials*. Vol. 49, pp 15–22
Khajuria, A. Bohra, K. and Balaguru, P. 1991. Long Term Durability of Synthetic Fibers in Concrete. *ACI Vol. 26. Pp 851-868*
Khaliq, W., Kodur, V. 2011. Effect of High Temperature on Tensile Strength of Different Types of High-Strength Concrete, *Mater. J., vol*. 108, pp 394-402
Khaliq, W., Kodur, V. 2011b. Thermal and mechanical properties of fiber reinforced high performance self-consolidating concrete at elevated temperatures, Cem. Concr. Res. 41 (11), pp 1112–1122
Khaloo, A.R., Kim, N. 1997. Influence of concrete and fiber characteristics on behavior of steel fiber reinforced concrete under direct shear. Materials Journal, *94(6), pp 592-601*
Khanlou, A., MacRae, G.A., Scott, A.N., Hicks, S.J., Clifton, G.C. 2012. Shear Performance of Steel Fibre-Reinforced Concrete. Australasian Structural Engineering Conference, Perth, Australia, 2012, p 8
Khomwan, N., Foster, S.J. 2005. FE Modelling of FRP-Strengthened RC Shear Walls Subjected to Reverse Cyclic Loading. *Proceedings of the International Symposium on Bond Behaviour of FRP in Structures (BBFS 2005)*, Chen and Teng (eds), pp 519-524
Khoury, G.A. 1983. Transient thermal creep of nuclear reactor concrete pressure vessel type concretes. PhD Thesis, University of London.
Khoury, G.A. 1992. Compressive strength of concrete at high temperatures: a reassessment. *Magazine of Concrete Research*, 44, No. 161, pp 291-309
Khoury, G.A. 2000. Effect of fire on concrete and concrete structures. *Progress in Structural Engineering and Materials*, 2 (2000), 4, pp 429-447
Khoury, G.A. 2008. Fire and Concrete. Encontro Nacional Betão Estrutural 2008, pp 21-34
Kim, Y.H., Hueste, M.B.D., Trejo, D., Cline, D.B. 2010. Shear characteristics and design for high-strength self-consolidating concrete. *Journal of structural engineering*, 136(8), pp 989-1000
Kobayashi, K. Cho, R., 1982. Flexural characteristics of steel fibre and polyethylene fibre hybrid-reinforced concrete. *Composites*, 13(2), pp 164-168
Kodur, V., Shakya, A. 2017. Factors governing the shear response of prestressed concrete hollow core slabs under fire conditions. *Fire Safety Journal* 88, pp 67–88
Kodur, V.K.R. 1998. Performance of High Strength Concrete-Filled Steel Columns Exposed to Fire. Canadian Journal of Civil Engineering, 25(6), pp 975-981

Kodur, V.K.R. 2000. Spalling in high strength concrete exposed to fire: concerns, causes, critical parameters and cures. *In Advanced Technology in Structural Engineering, pp 1-9*

Kodur, V.K.R., Cheng, F.P., Wang, T.C., Sultan, M.A. 2003. Effect of Strength and Fiber Reinforcement on Fire Resistance of High-Strength Concrete Columns, *J. Struct. Eng.*, vol. 129, no. 2, p. 253–259

Kodur, V.K.R., Lie, T.T. 1997. Fire Resistance of Fibre-Reinforced Concrete, Fibre Reinforced Concrete: Present and the Future, Canadian Society of Civil Engineers, *pp 189-213*

Koris, K., Kozma, A. and Bódi, I., 2018. Effect of the Shear Reinforcement Type on the Punching Resistance of Concrete Slabs. *Open Journal of Civil Engineering*, 8(1), pp 1-11

Kovacs, I, Balazs, G.L. 2004. Structural performance of steel fibre reinforced concrete. Budapest (Hungry): Publishing Company of Budapest University of Technology and Economics; BME

Kovács, I., Balázs, G.L. 2004. Structural performance of steel fibre reinforced concrete. Prepared for the *2nd International Conference on Fibre Reinforced Concrete − from research to practice −*, Budapest University of Technology and Economics, Budapest, Hungary 19 November 2004

Krefeld, W., Thurston, C.W. 1966. Contribution of longitudinal steel to shear resistance of reinforced concrete beams, *ACI-Journal, Proc.* Vol. 63, March 1966, pp 325-344

Kupfer, H. 1962. Extension of truss model by Mörsch by using the principle of minimal work of deformations (*Erweiterung der Mörsch' schen Fachwerkanalogie mit Hilfe des Prinzips vom Minimum der Formäderungarbeit*), Schear-Colloquium Stuttgart, Manuscript

Lankard, D.R., Birkimer, D.L., Fondriest, F.F., Snyder, M.J. 1971. Effect of Moisture Content on the Structural Properties of Portland Cement Concrete Exposed to Temperatures up to 500F, *ACI Special Publication SP-25*, Temperature and Concrete, Detroit, Michigan, USA, 1971, pp 59-102

Lau, A., Anson, M. 2006. Effect of high temperatures on high performance steel fibre reinforced concrete. *Cem Concr Res* 36, pp 1698–1707

Lea, F.M. 1960. Cement research: retrospect and prospect, Proc. 4th Int. Symp. 1960. On the Chemistry of Cement, 1960, pp 5–8

Lee, D, Han, S.J., Ju, H., Zhang, D., Kim, K.S. 2019. Shear strength model for prestressed concrete beams with steel fibers failed in shear. Magazine of Concrete Research. DOI:10.1680/jmacr.19.00391

Lee, M.K., Barr, B.I.G. 2004. An overview of the fatigue behaviour of plain and fibre reinforced concrete. *Cement and Concrete Composites*. Vol. 26, No. 4, pp 299-305

Leonhardt, F., Mönnig, E. 1973. Lectures about reinforced concrete (*Vorlesungen über Massivbau*), Part 2, Springer, pp 175-217

Leung, C.K.Y. 2016. An introduction to the Chinese guideline for fibre-reinforced concrete structures. *Fibre-reinforced concrete: From design to structural applications. ACI-fib International Workshop, Joint 2014. fib*, bulletin 79, pp 41-50

Li, H., Hao, X., Liu, Y., Wang, Q. 2019. Thermal effects of steel fibre-reinforced reactive powder concrete at elevated temperature. *Magazine of Concrete Research*, https://doi.org/10.1680/jmacr.19.00105

Li, V.C., Ward, R., Hamza, A.M. 1992. Steel and synthetic fibers as shear reinforcement. *Concr. Inst. Mater.* J. 89, pp 499-508

Lie, T.T., Kodur, V.K.R. 1995. Mechanical Properties of Fibre-Reinforced Concrete at Elevated Temperatures, NRC Publications Archive, 1995

Lim, D.H., Oh, B.H. 1999. Experimental and theoretical investigation on the shear of steelfibre reinforced concrete beams. Engineering Structures 21 (1999), pp 937–944

Lim, T.Y., Paramasivam, P., Lee, S.L. 1987. Shear and Moment Capacity of Reinforced Steel Fiber Concrete Beams, *Magazine of Concrete Research*, V. 39, No. 140, 1987, pp. 148-160

Liu, J.C., Tan, K.H., Yao, Y. 2018. A new perspective on nature of fire-induced spalling in concrete. *Construction and Building Materials*, 184, pp 581-590

Lublóy, É., Kopecskó, K., Balázs, G.L., Szilágyi, I.M., Madarász, J. 2016. Improved fire resistance by using slag cements. *Journal of thermal analysis and calorimetry*, 125(1), pp 271-279

Ma, Q., Guo, R., Zhao, Z., Lin, Z., He, K. 2015. Mechanical properties of concrete at high temperature — A review. *Construction and Building Materials*, 93, pp 371-383

MacGregor, J.G., Walters, A.R.V. 1967. Analysis of Inclined Cracking Shear in Slender Reinforced Concrete Beams. *ACI Journal* 64(10), pp 644-653

Mai, Y.W., Andonian, R., Cotterell, B. 1980. Thermal Degradation of Polypropylene Fibers in Cement Composites, *International Journal of Composites*, Vol. 3, No. 3, Aug. 1980, pp 149-155

Maidl, B.R. 1995. Steel fibre reinforced concrete. Berlin, Germany: Ernst & Sohn; 1995

Mansur, M.A., Vinayagam, T., Tan, K.H. 2008. Shear transfer across a crack in reinforced high-strength concrete. *Journal of Materials in Civil Engineering*, 20(4), pp 294-302
Mattock, A.H., Hawkins, N.M. 1972. Shear transfer in reinforced concrete—Recent research. *Pci Journal*, 17(2), pp 55-75
Mattock, A.H., Li, W.K., Wang, T.C. 1976. Shear transfer in lightweight reinforced concrete. *PCI J*, 21 (1) (1976), pp 20-39
Maya, L.F., Ruiz, M.F., Muttoni, A., Foster, S.J. 2012. Punching Shear Strength of Steel Fibre Reinforced Concrete Slabs, *Eng. Struct.*, Vol. 40, pp 83-94
Meda, A., Minelli, F., Plizzari, G.A., Riva, P. 2005. Shear behaviour of steel fibre reinforced concrete beams. *Materials and Structures*, Vol. 38(3), pp 343-351
Memon, S.A., Shah, S.F.A., Khushnood, R.A., Baloch, W.L. 2019. Durability of sustainable concrete subjected to elevated temperature–A review. *Construction and Building Materials*, 199, pp 435-455
Mindeguia, J.C., Pimienta, P. Carré, H., La Borderie, C. 2009. Experimental study on the contribution of pore vapour pressure to the thermal instability risk of concrete, *1st International Workshop on Concrete Spalling due to Fire Exposure.*
Minelli, F. 2005. Plain and Fibre reinforced concrete beams under shear loading: Structural Behaviour and Design Aspects. University of Brescia, Brescia, Italy
Minelli, F., Conforti, A., Cuenca, E., Plizzari, G. 2014. Are steel fibres able to mitigate or eliminate size effect in shear?. *Materials and structures*, 47(3), pp 459-473
Minelli, F., Plizzari, G.A. 2013. On the Effectiveness of Steel Fibers as Shear Reinforcement. *ACI Structural Journal*, 110 (3)
Mirsayah, A.A., Banthia, N. 2002. Shear strength of steel fiber-reinforced concrete, *ACI Mater. J.* 99 (5) (2002), pp 473-479
Mobasher, B. 2016. Design-baseded approaches for fibre-reinforced concrete: An overview of ACI Committee 544 activities. *Fibre-reinforced concrete: From design to structural applications. ACI-fib International Workshop*. *Joint 2014*. *fib*, bulletin 79, pp 17-28
Moghadam, M.A., Izadifard, R. 2019. Evaluation of shear strength of plain and steel fibrous concrete at high temperatures. *Construction and Building Materials*, Vol. 215, pp 207-216
Morgan, D.R., Mcaskill, N., Richardson, B.W., Zellers, R.C. 1989. A Comparative Evaluation of Plain, pp, Steel Fiber, and wire mesh reinforced shotcretes. *Transportation Research Record 1226,* pp 78-87
Mörsch, E. 1908. Reinforced concrete – Theory and application (*Der Eisenbetonbau – Seine Theorie und Anwendung), Verlag von Konrad Wittwer, Stuttgart*, pp 146-215
Mugume, R., Horiguchi, T. 2012. Effect of fibre type and geometry on max. pore pressures in fibre-reinforced high strength concrete at elevated temperatures. *Cement and Concrete Research*.Vol 42, pp 459-466
Muir, J.F. 1977. Response of Concrete Exposed to High Heat Flux on Surface, Research Paper SAND 77-1467, Sandia National Laboratories, Albuquerque, New Mexico.
Muttoni, A., Fernández Ruiz, M. 2008. Shear strength of members without transverse reinforcement as function of critical shear crack width. *ACI Struct J*, 105 (2) (2008), pp 163-172
Naaman, A.E. 2003. Engineered steel fibres with optimal properties for reinforcement of cement composites. *J Adv Concr Technol* 2003;1(3), pp 241–52
Naaman, A.E. Reinhardt, H.W. 1996. High performance fibre reinforced cement composites: HPFRCC 2. RILEM, No. 31, London, E. and FN Spon
Nanni, A. 1991. Ductility of Fiber Reinforced Concrete, *Journal of Materials in Civil Engineering, ASCE*, Vol. 3, No. 1, Feb. 1991, pp 78-90
Narayanan, M., Darwish, I.Y.S. 1987. Use of Steel Fibers as Shear Reinforcement, *ACI Structural Journal*, V. 84, No. 6, May-June 1987, pp 216-226
Naser, M.Z. 2019. Properties and material models for modern construction materials at elevated temperatures. Computational Materials Science, 160, pp 16-29
Natarajaa, M.C., Dhangb, N., Guptab, A.P. 2000. Toughness characterization of steel fiber-reinforced concrete by JSCE approach. *Cement and Concrete Research* 30 (2000), pp 593 – 597
Naus, D., Oland C., Robinson, G. 1976. Testing program for concrete at temperatures to 894oK. Oak Ridge National Laboratory, Tennessee 37830. USA
Naus, D.J. 2005. The Effect of Elevated Temperature on Concrete Materials and Structures—A Literature Review. Oak Ridge National Laboratory, USA

Nemegeer, D., Vanbrabant, J., Stang, H. 2000. Final report on Durability of Steel Fibre Reinforced Concrete. Copenhagen, Denmark
Neville, A.M. 1995. Properties of concrete, Longman Scientific and Technical, 1995
Neville, A.M., Brooks, J.J. 2010 Concrete Technology. Essex, England: Pearson Education Limited. 1987
Nordström, E., 2005. Durability of Sprayed Concrete Steel fibre corrosion in cracks. Lulea University of Technology.
Noumowe, A., 2005. Mechanical properties and microstructure of HSC containing polypropylene fibres exposed to temperatures up to 200 C. *Cement and concrete research*, 35(11), pp 2192-2198
Novák, J., Kohoutková, A. 2017. Fibre Reinforced Concrete Exposed to Elevated Temperature, *Mater. Sci. Eng*., 2017
Ozawa, M., Morimoto, H. 2014. Effects of various fibres on high-temperature spalling in high performance concrete. Construction and Building Materials. Vol 71, pp 83-92
Ozger, O.B., Girardi, F., Giannuzzi, G.M., Salomoni, V.A. 2013. Effect of nylon fibres on mechanical and thermal properties of hardened concrete for energy storage systems. *Mat. and Design*, 51, pp 989-997
Parra-Montesions, G.J. 2006. Shear strength of beams with deformed steel fibres. *Concrete International*, Vol. 28, No. 11, pp 57-61
Patel, J.K., Desai, N.B., Rana, J. C. 1989. Fibre Reinforced Cements and Concretes: Recent Developments (R. N. Swamy and B. Barr Eds.), *Elsevier Applied Science*, London, UK
Patel, P.A., Desai, A.K., Desai, J.A. 2012. Evaluation of Engineering Properties for Polypropylene Fibre Reinforced Concrete. *International Journal of Advanced Engineering Technology.* Vol. 3, Issue 1, January-March, pp 42-45
Paulay, T., Park, R., Phillips, M.H. 1974. Horizontal construction joints in cast in place reinforced concrete, *ACI-Special Publication SP-42*, "Shear in reinforced concrete", Vol. II, pp 599-616
Pliya, P., Beaucour, A.L., Noumowé, A. 2011. Contribution of cocktail of polypropylene and steel fibres in improving the behaviour of high strength concrete subjected to high temperature, *Constr. Build. Mater*. 25 (2011), pp 1926–1934
Poon, C.S., Shui, Z.H., Lam, L. 2004. Compressive behavior of fibre reinforced high-performance concrete subjected to elevated temperatures. Cem. Concr. Res. 34 (12), pp 2215-2222
Qasim, O.A., Ahmed, A.S. 2019. High temperature effect on shear transfer strength of steel fibre reinforced self-compacted concrete. Journal of Engineering and Applied Sciences, Vol. 14 (10), pp 3158-3174
Quon, D.H.H. 1980. Phase Changes in Concrete Exposed to Sustained High Temperatures, Division Report MRP/MSL 80-111(TR), Mineral Sciences Laboratories, CAANMET, Ottawa, Canada, August 1980.
Rahal, K.N., Khaleefi, A.L., Al-Sanee, A. 2016. An experimental investigation of shear-transfer strength of normal and high strength self-compacting concrete. *Engineering Structures*, Vol. 109, pp 16–25
Raheel, M. 1993. Manmade Fibers: Their Origin and Development (R. B. Seymour and R. S. Porter Eds.), *Elsevier Applied Science*, London, UK
Ramakrishnan, V., Brandshaug, T., Coyle, W.V., Schrader, E.K. 1980. A Comparative Evaluation of Concrete Reinforced with Straight Steel Fibers and Fibers with Deformed Ends Glued Together into Bundles. *ACI Journal* I May-June 1980, pp 135-143
Ramakrishnan, V., George, Y.W., Hosalli, G. 1989. Flexural Fatigue Strength, Endurance Limit, and Impact Strength of Fiber Reinforced Concretes. *Transportation Research Record 1226*, pp 17-24
Rasiah, S. 2012. High-strength Self-Compacting Concrete for Sustainable Construction. Centre for Built Infrastructure Research, University of Technology, Sydney, Australia, December 2012.
Regan, P.E. 1993. Research on shear: a benefit to humanity or a waste of time?. *The Structural Engineer*. Vol. 71, No 19/5 October
Rice, E., Vondran, G., Kunbargi, H. 1988. Bonding of Fibrillated Polypropylene Fibers to Cementitious Materials, *Materials Research Society Proceedings*, Pittsburgh, Vol. 114, 1988, pp 145-152
RILEM Technical Committee 19-FRC. 1977. Fibre Concrete Materials. *Materials and Structures, Test Res*., Vol. 10, No. 56, 1977, pp 103-120
Ritter, W. 1899. Construction method of Hennebique (Die Bauweise Hennebique), Schweizerische Bauzeitung, February 1899, pp 41-61
Rossi, P., Tailhan, J.L., Daviau-Desnoyers, D. 2017. Numerical models for designing steel-fibre-reinforced concrete structures: Why and which ones? *Special Publication*, 310, pp 289-300
Santos, P.M.D, Júlio, E.N.B.S. 2012. A state-of-the-art review on shear-friction. *Engineering Structure*. Vol. 45, pp 435-448

Savva, A., Manita, P., Sideris, K.K., 2005. Influence of elevated temperatures on the mechanical properties of blended cement concretes prepared with limestone and siliceous aggregates. *Cement and Concrete Composites*, Vol. 27(2), pp 239-248

Schneider, U. 1988. Concrete at High Temperatures -- A General Review. *Fire Safety Journal*, 13, pp 55–68

Schneider, U., Diererichs, C., Ehm, C. 1981. Effect of Temperature on Steel and Concrete for PCRV's, Nuclear Engineering and Design 67, pp 245–258

Schupack, M. 1986. Durability of SFRC Exposed to Severe Environments, *Steel Fiber Concrete, Elsevier Applied Science Publishers, Ltd*., 1986, pp 479-496

Serdar, M., Baričević, A., Jelčić Rukavina, M., Pezer, M., Bjegović, D. and Štirmer, N., 2015. Shrinkage behaviour of fibre reinforced concrete with recycled tyre polymer fibres. International Journal of Polymer Science, 2015

Serrano, R., Cobo, A., Prieto, M.I., de las Nieves González, M., 2016. Analysis of fire resistance of concrete with polypropylene or steel fibers. Construction and building materials, 122, pp 302-309

Shah, S.P. 1991. Do Fibers Increase the Tensile Strength of Cement-Based Matrixes? *ACI Materials Journal*, V. 88, No. 6, pp 595-602

Shah, S.P., Rangan, B.V. 1971. Fiber Reinforced Concrete Properties, *ACI Journal, Proceedings*, Vol. 68, No. 2, Feb. 1971, pp 126-135

Simon, T. 2003. Sand patch method for evaluation of concrete-to-concrete interaction. *Concrete Structures,* Vol. 4, pp 67-71

Sivakumar, A. Santhanam, M., 2007. Mechanical properties of high strength concrete reinforced with metallic and non-metallic fibres. *Cement and Concrete Composites*, 29(8), pp 603-608

Smith, H., Reid, E., Beatty, A., Stratford, T., Bisby, L. 2011. Shear strength of concrete at elevated temperatures. *Applications of Structural Fire Engineering.* Prague, pp 133-138

Snyder, M.L., Lankard, D.R. 1972. Factors Affecting the Strength of Steel Fibrous Concrete, *ACI Journal, Proceedings*, Vol. 69, No. 2, Feb. 1972, pp 96-100

Soetens, T. Matthys, S. 2017. Shear-stress transfer across a crack in steel fibre-reinforced concrete. *Cement and Concrete Composites* 82 (2017), pp 1-13

Soetens, T., Matthys, S. 2013. Evaluation of MC2010 models for prestressed SFRC beams subjected to shear. *7th International Conference: Fibre Concrete 2013: Technology, Design, Application, A. Kohoutkova (Ed.)*, Prague, Czech Republic

Solgaard, A., Kuter, A., Edvardsen, C., Stang, H., Geiker, M. 2010. Durability aspect of steel fibre reinforced concrete in civil infrastructures. *Proc. 2nd International Symposium on Service Life Design for Infrastructure, 4th - 6th October* 2010, Delft, The Netherlands

Sorelli, L. Meda, A. Plizzari, G.A. 2006. Steel fibre concrete slabs on grade: a structural matter. *ACI Structural Journal,* 103(4), pp 551-558

Sorelli, L.G., Meda, A., Plizzari, G.A. 2006. Steel fiber concrete slabs on ground: A structural matter. *ACI Struct J* 2006;103(4), pp 551–8

Soroushian, P., Lee, C.D. 1990. Distribution and orientation of fibres in steel fibre reinforced concrete. *Materials Journal*, Vol. 87(5), pp 433-439

Soutsos, M.N., Le, T.T., Lampropoulos, A.P. 2012. Flexural performance of fibre reinforced concrete made with steel and synthetic fibres. *Construction and Building Materials* Vol. 36, pp 704-710

Spinella, N. 2013. Shear strength of full-scale steel fibre-reinforced concrete beams without stirrups. *Computers and Concrete*, Vol. 11, No. 5 (2013), pp 365-382

Stanton, J.F. 1977. An investigation of dowel action of the reinforcement of nuclear containment vessels and their non-linear dynamic response to earthquake loads, M.S. Thesis, Cornell University

Suhaendi, S.L., Horiguchi, T., 2006. Effect of short fibers on residual permeability and mechanical properties of hybrid fibre reinforced high strength concrete after heat exposition. *Cement and Concrete Research*, 36(9), pp 1672-1678

Sukontasukkul, P. 2004. Toughness Evaluation of Steel and Polypropylene Fibre Reinforced Concrete Beams under Bending. *Thammasat Int. J. Sc. Tech.*, Vol. 9, No. 3, pp 35-41

Swamy, R.N., Jones, R., Chiam, T. Influence of Steel Fibers on the Shear Resistance of Lightweight Concrete I-Beams, *ACI Structural Journal*, V. 90, No. 1, Jan-Feb. 1993, pp 103-114

Tatnall, P.C. 2006. Fibre-Reinforced Concrete. *Significance of tests and properties of concrete, and concrete-making materials (Book)*, ch. 49. ASTM no. STP 169D. pp 578-590

Taylor, H.P.J. 1971. Fundamental behaviour in bending and shear of reinforced concrete, PhD thesis. University of London

Taylor, H.P.J. 1974. The Fundamental Behaviour of Reinforced Concrete Beams in Bending and Shear. *ACI Special Publication* 42, pp 43-77

The Condensed Chemical Dictionary. 1981. Van Nostrand, Rheinhold Company, New York, 8th ed., p. 635.

Tighiouart, B., Benmokrane, B. and Gao, D., 1998. Investigation of bond in concrete member with fibre reinforced polymer (FRP) bars. Construction and building materials, 12(8), pp 453-462

Toutanji, H.A., El-Korchi, T., Katz, R.N., Leatherman, G.L. 1993. Behaviour of carbon fiber reinforced cement composites in direct tension. *Cement and Concrete Research,* Vol. 23, Issue 3, pp 618-626

Trottier, J.F. Banthia, N. 1994. Toughness Characterization of Steel-Fiber Reinforced Concrete. *Journal of Materials in Civil Engineering*, Vol. 6, pp 264-289

Uchida, Y., Kunieda, M., Rokugo, K. 2016. FRCC: design and application in Japan. *Fibre-reinforced concrete: From design to structural applications. ACI-fib International Workshop*. *Joint 2014*. *fib*, bulletin 79, pp 51-60

Valle, M., Buyukozturk, O. 1993. Behaviour of fiber reinforced high-strength concrete under direct shear. *Materials Journal*, 90(2), pp 122-133

Vandewalle, L. 2000. Cracking behaviour of concrete beams reinforced with a combination of ordinary reinforcement and steel fibers. *Materials and structures*, 33(3), pp 164-170

Vecchio, F.J., Collins, M.P. 1986. The modified compression field theory for reinforced concrete elements subjected to shear. *ACI Journal*, Vol. 83, No. 22, pp 219-231

Victor, M.M., Alexander, M., Anders, S., Gregor, F., Carola, E., Torben Lund, S. 2016. Corrosion resistance of steel fibre reinforced concrete – a literature review. *fib Symposium 2016: Performance-based approaches for concrete structures*

Vintzeleou, E.N., T.P., Tassios. 1986. Mathematical Models for Dowel Action Under Monotonic and Cyclic Conditions. *Magazine of Concrete Research* 38(134), pp 13-22

Voo, Y.L., Foster, S.J., Gilbert, R.I. 2006. Shear strength of fiber reinforced reactive powder concrete prestressed girders without stirrups. *J. Adv. Concr. Technol*., 4(1), pp 123–132

Voo, Y.L., Poon, W.K., Foster, S.J. 2010. Shear Strength of Steel Fibre Reinforced Ultrahigh-Performance Concrete Beams without stirrups. *Journal of Structural Engineering*. DOI: 10.1061/ASCEST.1943-541X.0000234

Walrath, D.E., Adams, D.F., 1983. The Iosipescu shear test as applied to composite materials. *Exp Mech* 23(1), pp 105 – 110

Walraven, J. 1980. Aggregate Interlock: A theoretical and experimental analysis. PhD Dissertation, Delft University of Technology

Walraven, J. 1981. Fundamental analysis of aggregate interlock. *Journal of Structural Division*. Vol. 107, No. 11, pp 2245–2270

Walraven, J., Frenay, J., Pruijssers, A., 1987. Influence of concrete strength and load history on the shear friction capacity of concrete members. *PCI journal*, 32(1), pp 66-84

Walraven, J., MERCX, W.M. 1983. The bearing capacity for prestressed hollow core slabs. Heron (Delft), 28(3), pp 1-46

Walther, R. 1965. About the calculation of shear capacity of reinforced and prestressed concrete beams (*Über die Berechnung der Schubtragfaehigkeit von Stahl- und Spannbetonbalken -Schubtheorie*), Beton- und Stahlbetonbau, 11/1965, pp 261-268

Wang, Z.L., Wu, J., Wang, J.G. 2010. Experimental and numerical analysis on effect of fibre aspect ratio on mechanical properties of SRFC. *Construction and Building Materials*, 24(4), pp 559-565

Wille, K., Schneider, H. 2002. Investigation of fibre reinforced high strength concrete(HSC) under fire, particularly with regard to the real behaviour of poly-propylene fibres, Lacer 7 (2002), pp 61–70

Williamson, G.R. 1966. Response of Fibrous Reinforced Concrete to Explosive Loading. Technical Report No. 2-48. *Department of the Army, Ohio River Division Laboratory, U. S. Corp of Engineers, Cincinnati, Ohio*, Jan. 1966.

Xavier, J.C., Garrido, N.M., Oliveira, M., Morais, J.L., Camanho, P.P., Pierron, F. 2004. A comparison between the Iosipescu and off-axis shear test methods forthe characterization of Pinus Pinaster Ait. *Composites:* Part A 35 (2004), pp 827–840

Xiao, J., Falkner, H. 2006. On residual strength of high-performance concrete with and without polypropylene fibres at elevates temperatures. *Fire Safety J* 2006; 41, pp 115–21

Xiao, J., Li, Z., Li, J. 2014. Shear transfer across a crack in high-strength concrete after elevated temperatures. *Construction and Building Materials*, Vol. 71, pp 472–483
Yang, H., Qin, Y., Liao, Y., Chen, W. 2016. Shear behavior of recycled aggregate concrete after exposure to high temperatures. Construction and Building Materials 106 (2016), pp 374–381
Yang, H.H. 1993. Manmade Fibers: Their Origin and Development (R. B. Seymour and R. S. Porter Eds.), *Elsevier Applied Science*, London, UK
Yang, Y. 2014. Shear behavior of reinforced concrete members without shear reinforcement: a new look at an old problem. PhD Thesis. Delft University of Technology, Netherlands.
Yap, S.P., Alengaram, U.J., Jumaat, M.Z. 2013. Enhancement of mechanical properties in polypropylene– and nylon–fibre reinforced oil palm shell concrete. *Materials and Design*, 49, pp 1034-1041
Yermak, N., Pliya, P., Beaucour, A., Simon, A., Noumowé, A. 2017. Influence of Steel and/or Polypropylene Fibres on the Behaviour of Concrete at High Temperature: Spalling, Transfer and Mechanical Properties, *Constr. Build. Mater*., pp 240–250
Yuan, C., Chen, W., Pham, T.M. and Hao, H., 2018. Bond behavior between basalt fibres reinforced polymer sheets and steel fibres reinforced concrete. Engineering Structures, 176, pp 812-824
Zheng, Q., Chung, D.D.L. 1989. Carbon fiber reinforced cement composites improved by using chemical agents. *Cement and Concrete Research*, 19(1), pp 25-41
Zheng, Z., Feldman, D. 1995. Synthetic fibre-reinforced concrete. Prog. Polym. Sci., Vol. 20, 185-210, 1995. Centre for Building Studies, Concordia University, Montreal, Canada

List of own publications related to the PhD research

[NA1] **Alimrani, N**., Abdelmelek, N., Balázs, G.L. Lublóy, É, "Fire behaviour of concrete – influencing parameters", *Journal Concrete Structures*, 2017, Vol 18, pp. 36-44. http://fib.bme.hu/folyoirat/cs/cs2017.pdf

[NA2] Balázs L. Gy., Lublóy É., Kopecskó K. , Nehme S.G, Nemes R., Kausay T., Józsa Zsuzsanna, Hlavička V., Kakasy G., Tóth P., Nyíri Sz., Lizakovszky G., Molnár T., Czirják J., Földes T., Abdelmelek N., Abed M., **Alimrani N**., „Influence of fire on the structure of concrete – State-of-the-Art Report" („Tűz hatásai a beton szerkezetére – helyzetfelmérő jelentés"), *Journal VASBETONÉPÍTÉS*, 2017. Vol (2), pp. 26-32. (*in Hungarian*) http://fib.bme.hu/folyoirat/vb/vb2017_2.pdf

[NA3] Balázs, G.L., Kopecskó, K., **Alimrani, N.,** Abdelmelek, N., Lublóy, É., "Fire Resistance of Concretes with Blended Cements", *Proceedings*, "High Tech Concrete: Where Technology and Engineering Meet". *fib Symposium* 12-14 June 2017 Maastricht, The Netherlands, pp. 1420-1427.

[NA4] **Alimrani, N.,** Balázs, G.L., "Structural consequences of fire on concrete structures – Review article", *Proceedings*, "Innovative materials and technologies for concrete structures". *CCC2017 Congress Tokaj*, 31 Aug.-1 Sept. 2017, pp. 665-673. http://fib.bme.hu/konyvek/ccc2017.pdf

[NA5] **Alimrani, N.,** Balázs, G.L., "Precast Concrete Hollow Core Slabs exposed to elevated temperatures in terms of shear deteriorations–Review Article", *Journal Concrete Structures*, Vol (19), pp 14-21 2018. http://www.fib.bme.hu/folyoirat/cs/cs2018/cs2018-3.pdf

[NA6] **Alimrani, N.**, Balázs, G.L., "Behaviour of concrete at elevated temperatures with respect to shear failure". *Proceeding of 12th fib International PhD Symposium*, 2018, pp 27-35, Prague, Czech Republic.

[NA7] **Alimrani, N**.,Balázs, G.L.,"Behavior of concrete at elevated temperatures in terms of shear failure using push-off model" *fib Symposium* 2019, pp 171-172 Krakow, Poland.

[NA8] **Alimrani, N**.,Balázs, G.L.,"Steel fibers on shear strength of concrete at room and elevated temperatures", *Third International Fire Safety Symposium* 2019, pp 331-339. Ottawa, Canada.

[NA9] Abdelmelek N., **Alimrani, N**., Krelias, N., Lublóy, É, "Metakaolin-based High Strength Concrete Exposed to Elevated Temperatures". Submitted to *Journal of Building Engineering,* 2020.

[NA10] Boumaza, R., **Alimrani, N**., Abdelmelek N., Hlavicka-Laczák, LE ., Lublóy, É, "Effect of fibers on the fire resistance of concrete structures". Submitted to *Journal of Advanced Concrete Technology*, 2020.

[NA11] **Alimrani, N.,** Balázs, G.L., "Effect of steel fibres on concrete at different temperatures in terms of shear failure. *Magazine of Concrete Research*, 2020. https://doi.org/10.1680/jmacr.19.00479. **IF: 2.088**

[NA12] **Alimrani, N**., Balázs, G.L., "Synthetic fibres or fibre cocktail in terms of shear capacity of concrete after elevated temperatures". *Mechanics of Materials*, 2020. https://doi.org/10.1016/j.mechmat.2020.103504. **IF: 2.993**

[NA13] **Alimrani, N.S**. and Balazs, G.L., "Investigations of direct shear of one-year old SFRC after exposed to elevated temperatures". *Construction and Building Materials*, 2020. https://doi.org/10.1016/j.conbuildmat.2020.119308. **IF: 4.419**

[NA14] **Alimrani, N**., Balázs, G.L.,"Investigations of shear capacity and toughness in FRC at elevated temperatures *", Proceedings of the fib Symposium 2020 Shanghai, China*. -24 Nov. 2020.

[NA15] **Alimrani, N**., Balázs, G.L.,"One-year old push-off specimens using cocktail and polymeric fibres at elevated temperatures", Submitted to the *Periodica Polytechnica Civil Engineering.* 2020.

[NA16] **Alimrani, N**., Balázs, G.L.,"Toughness and stiffness of shear behavior in FCR exposed to elevated temperatures". Under preparation

[NA17] **Alimrani, N**., Balázs, G.L.,"A comprehensive study investigating shear behavior in FRC after exposed to elevated temperatures". Under preparation